NASA CR-172055

[redacted]

Axiomatix

(NASA-CR-172055) SPACECRAFT APPLICATIONS OF ADVANCED GLOBAL POSITIONING SYSTEM TECHNOLOGY Final Report (Axiomatix) 147 p CSCL 17G

N88-27180

Unclas G3/04 0154657

SPACECRAFT APPLICATIONS OF ADVANCED GLOBAL POSITIONING SYSTEM TECHNOLOGY

Final Report

Contract No. NAS9-17681

Prepared for

NASA Lyndon B. Johnson Space Center
Houston, Texas

Prepared by

Axiomatix
Tau Corporation
Motorola, Inc.

Contributors

Axiomatix	Gaylord Huth James Dodds Sergei Udalov Richard Austin
Tau Corporation	Peter Loomis
Motorola, Inc.	I. Newton Duboraw, III

Axiomatix Report No. R8805-5
May 31, 1988

TABLE OF CONTENTS

LIST OF FIGURES

LIST OF TABLES

1.0 INTRODUCTION AND OVERVIEW

This report summarizes the results of a study performed by a joint effort of Axiomatix, Tau Corporation and Motorola, Inc. The purpose of this study was to evaluate potential uses of GPS in spacecraft applications in the following areas:

1. Attitude Control and Tracking
2. Structural Control
3. Traffic Control
4. Time Base Definition (Synchronization)

Each of these functions are addressed in the sections that follow. Section 2 deals with GPS application to attitude control. This issue was examined by Axiomatix. Another issue examined by Axiomatix was the structure control. Section 3 deals with this topic. Section 4 examines the traffic control issue. Tau Corporation is the contributor in this area. The subject of time base definition was examined jointly by Motorola and Axiomatix. Section 5 deals with the time transfer technology.

Motorola also addressed the hardware related issues concerning the application of GPS technology and provided comparisons with alternative instrumentation methods for specific functions required for an advanced low earth orbit spacecraft. Appendix A summarizes Motorola's findings in these areas. Appendix B contains analysis pertaining to attitude determination.

20 ATTITUDE CONTROL

21 Problem Statement

One potential application of GPS is to perform space vehicle control and pointing by use of radio-interferometry.

The attitude of a spacecraft is its orientation in space. Attitude determination is the process of computing the orientation of the spacecraft relative to either an inertial reference or some object of interest such as the Earth. Attitude control and pointing is the process of orienting the spacecraft in a specified, predetermined direction. We address attitude determination since that is necessary before attitude control can be done.

Current techniques to obtain attitude determination include Sun Sensors, Horizon Sensors, Magnetometers, Star Sensors and Gyroscopes (Rate Gyros, Rate Integrating Gyros, and Control Moment Gyros).

The motivation for the task described in this section is to develop the possibility of using GPS-based interferometric techniques to determine and control the attitude of a large spacecraft.

GPS signals from a particular Navstar satellite can be simultaneously received by three (or more) antennas aboard the host vehicle. Phase comparison of two received signals can yield the angle of the baseline between the two antennas and the transmitting Navstar. If the angles are measured with respect to different Navstars, the absolute orientation of the spacecraft can be determined. Through observation of the attitude or attitude rates (or some combination thereof) experienced by the baselines between antennas, the vehicle can be stabilized or re-oriented. Two orthogonal baselines, one along the attitude and one perpendicular to it, can be used to determine the attitude and rotational position. Attitude without regard to rotational position can be obtained by using only one baseline with two antennas, in principle.

In subsections which follow, we provide the technical details pertaining to the use of GPS for attitude determination.

2.2 GPS Attitude Measurement Performance

2.2.1 Background

This section describes the simulation developed to assess the performance of GPS in measuring spacecraft attitude. To determine the attitude of a spacecraft using GPS requires the position vector of the spacecraft and 3 appropriate GPS satellites. These data were obtained from two programs written by William Lear of TRW, Inc. The positions generated by these programs are referenced to the Earth Centered Inertial (ECI) coordinate system. The first program, Traj2, computes the orbit (state vector as a function of time) for a spacecraft given the state vector at some initial time. The second program called GPSNAV generates GPS measurements and processes these data in a Kalman filter. The initial part of this program contains the ephemerides for the full constellation of 18 GPS satellites and given the position of the GPS receiver, picks the 4 GPS satellites that will minimize position dilution of precision, PDOP. This portion of GPSNAV forms the initial part of the GPS attitude simulation. The rest of the program was written at Axiomatix and is described in this section.

2.2.2 Concept

The basic concept of how GPS can be used to determine Space Station attitude is illustrated in Figure 2.2-1. The figure shows two receivers separated by a distance B_L, the baseline. A line drawn between them defines the attitude vector, **A**. Using interferometry, the differential path, ΔR, between the GPS satellite and the two GPS receivers can be determined. This, in turn, allows α, the angle between the baseline and the line to the GPS satellite to be determined. This does not, however, uniquely determine **A**. As shown in Figure 2.2-2, the lack of any information describing the direction of α results in the possible solutions of **A** describing a cone with half angle α about **G**. If two GPS satellites are used, then the solution to **A** is narrowed to the two vectors formed by the intersection of the two resulting cones as shown in Figure 2.2-3. One intersection represents the true

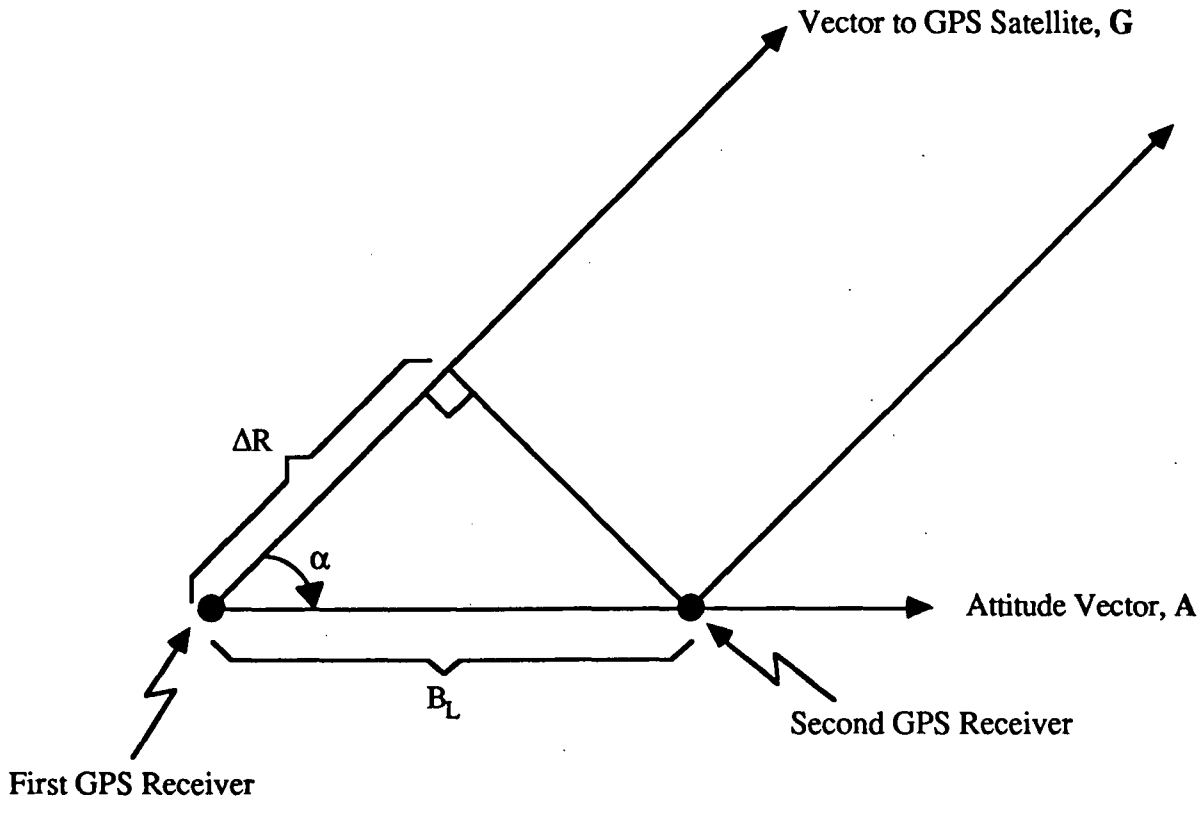

$$\alpha = \cos^{-1}(\Delta R / B_L)$$

Figure 2.2-1. Definition of Baseline Angle, α.

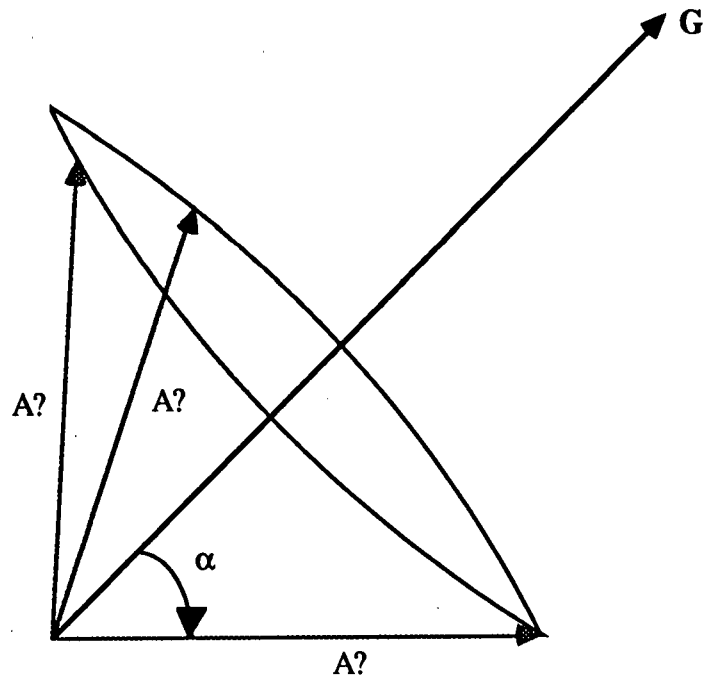

Figure 2.2-2. Solution to A is cone with half angle α.

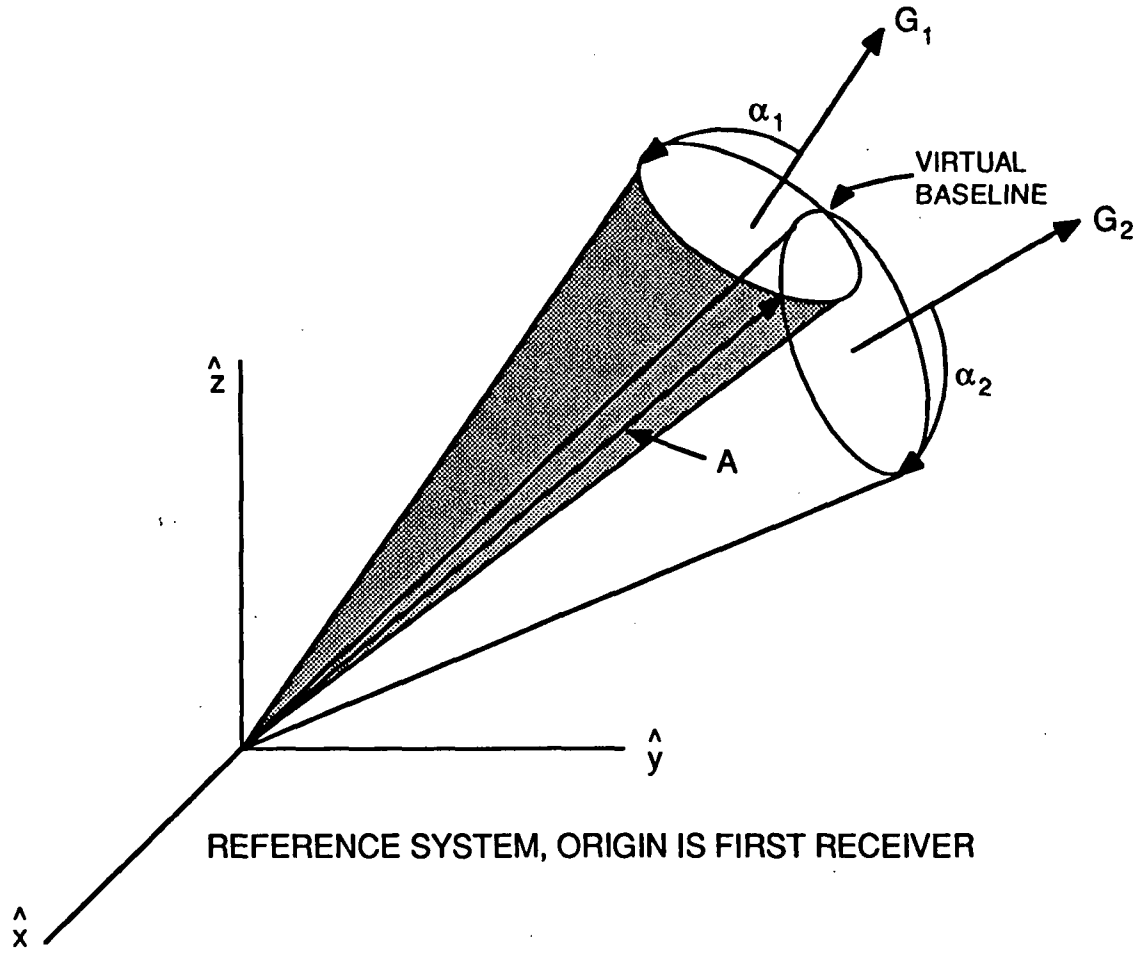

Figure 2.2-3. Use of Two GPS Satellites Narrows True Attitude Vector to One of Two Possible Solutions.

attitude vector, and the other is the virtual baseline. The resolution of this final ambiguity requires a third GPS satellite, the vector defined by the intersection of the three cones being the true attitude vector. This is illustrated in Figure 2.2-4 where the cones are viewed end on. The overall configuration showing the Space Station, the 3 GPS satellites and the three resulting angles α_1, α_2, and α_3 is shown in Figure 2.2-5.

2.2.3 Simulation Overview

We have shown that given the vectors to 3 GPS satellites (G_1, G_2 and G_3) and the resulting angles between them and the baseline α_1, α_2, and α_3 the attitude vector, A, defined by the coordinates of the baseline, can be determined. As shown in Figure 2-2-6, the vectors G_1, G_2 and G_3 which give the coordinates of the 3 GPS satellites in the Space Station centered frame of reference, are determined by the vectors defining the true position (in ECI coordinates) to the 3 GPS satellites and the Space Station. The simulation imparts no error into the value of G_1, G_2 and G_3. This is not unrealistic as the uncertainty in the position of the head and the tail of the vector (position of GPS satellite and Space Station receiver, respectively) is on the order of 10 of meters while the length of the vector is on the order of 25,000 km.

The main source of error is in the determination of the baseline angle α_1, α_2 and α_3. The angle α is determined from the path difference ΔR between the GPS satellite and the two receivers. The error in ΔR is related to the error in the phase of the received carrier as measured by the two receivers. Using a model of the receiver, the simulation introduces an error into the true values of α_1, α_2 and α_3. Using α_{e1}, α_{e2} and α_{e3} and G_1, G_2 and G_3, an estimate of the attitude vector, A_e, is determined by solving for the intersection of the 3 cones as previously described. The estimated attitude is then compared against the true attitude, A_T, the difference being the error in the attitude measurement.

Figure 2.2-7 shows a flow diagram of the simulation. The two inputs to the program are the baseline (distance between the two receivers) selected by the user, and the

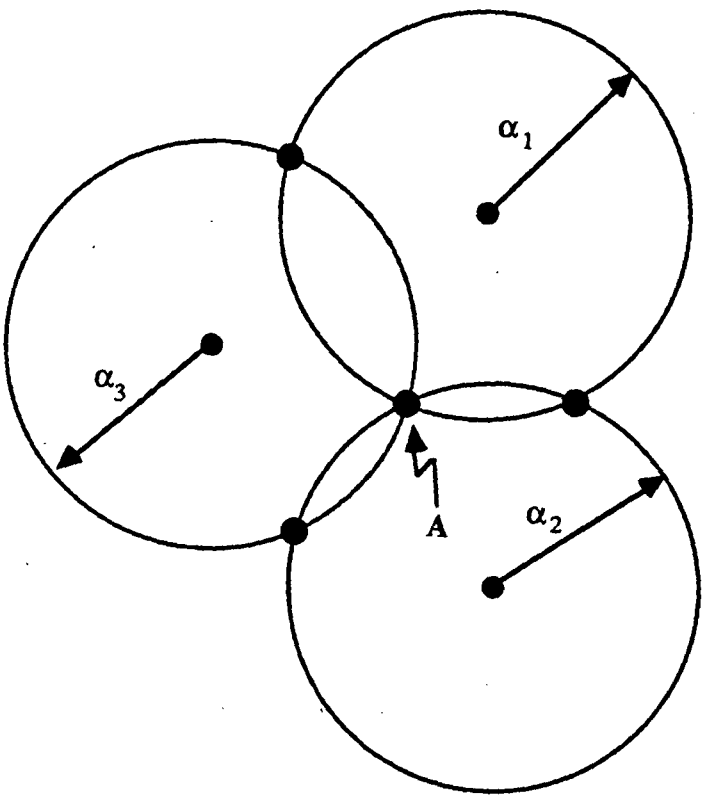

Figure 2.2-4. True Attitude, A , Is Intersection of 3 Cones.

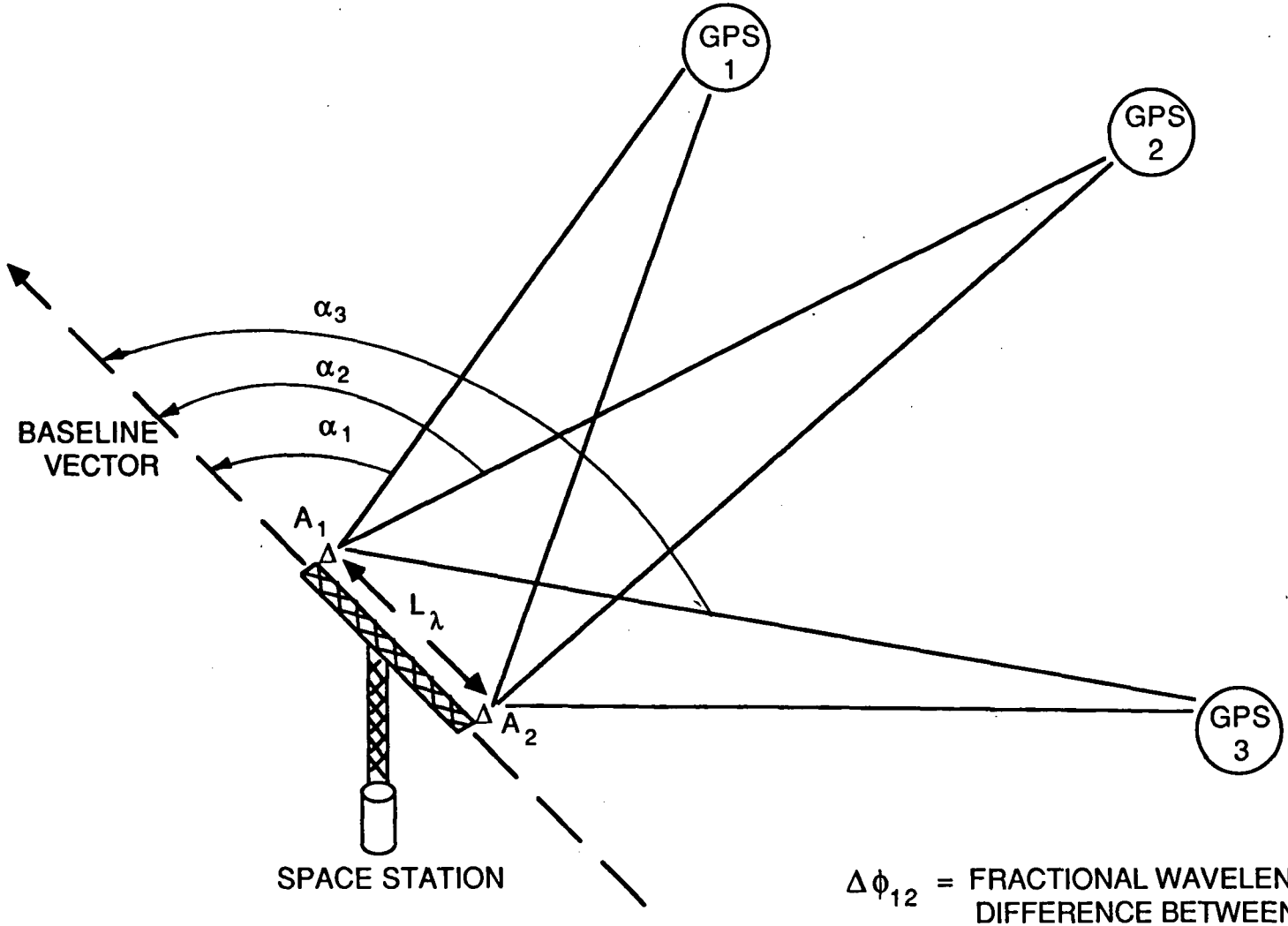

$$\cos(\alpha_1) = \frac{n_{12} + \Delta\phi_{12}}{B_L}$$

$\Delta\phi_{12}$ = FRACTIONAL WAVELENGTH PHASE DIFFERENCE BETWEEN ANTENNAE A_1, A_2

n_{12} = INTEGRAL WAVELENGTH DIFFERENCE BETWEEN ANTENNAE A_1, A_2

Figure 2.2-5. Overall Configuration of Space Station and GPS Satellite.

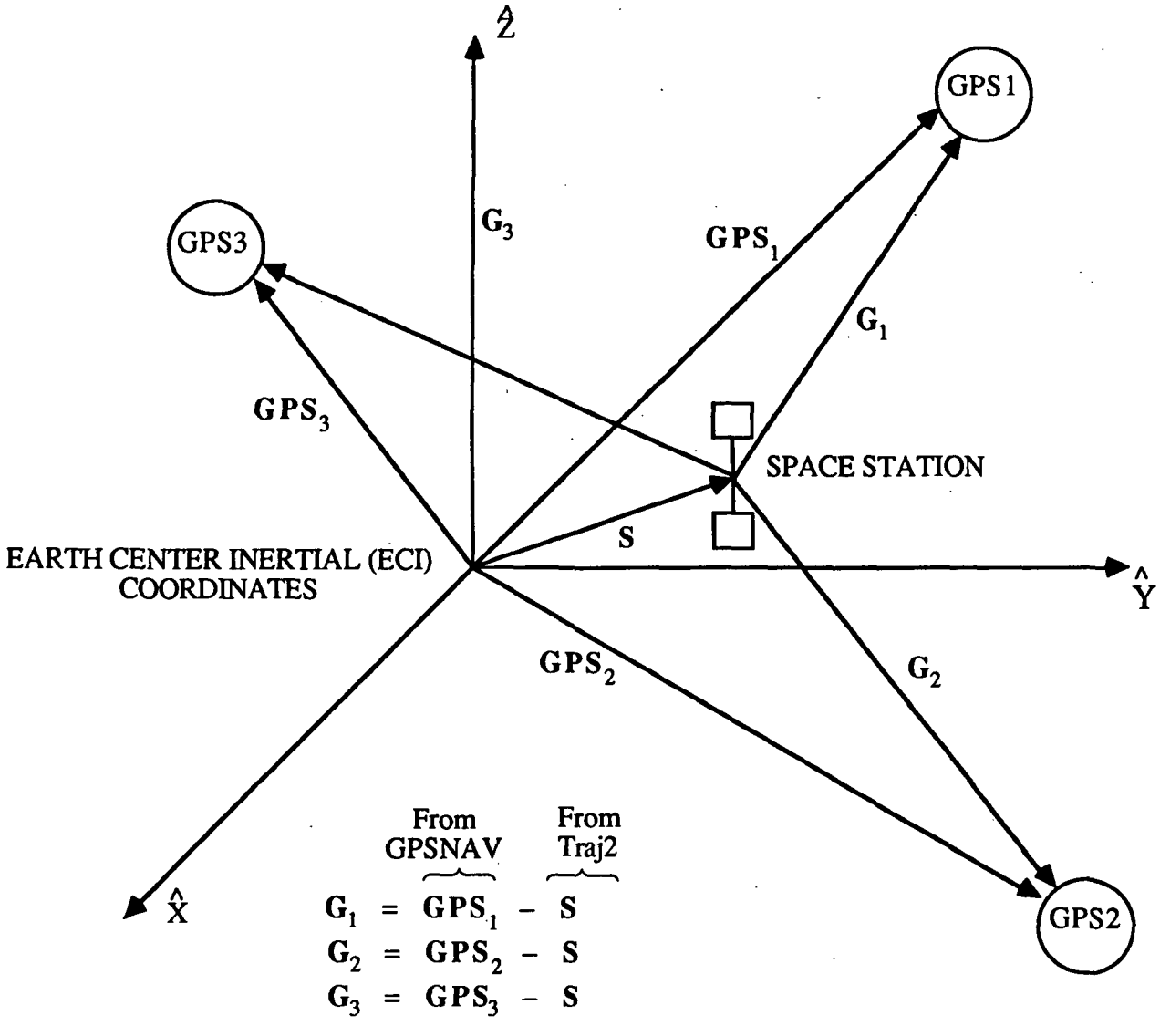

Figure 2.2-6. Definition of Coordinate System and G.

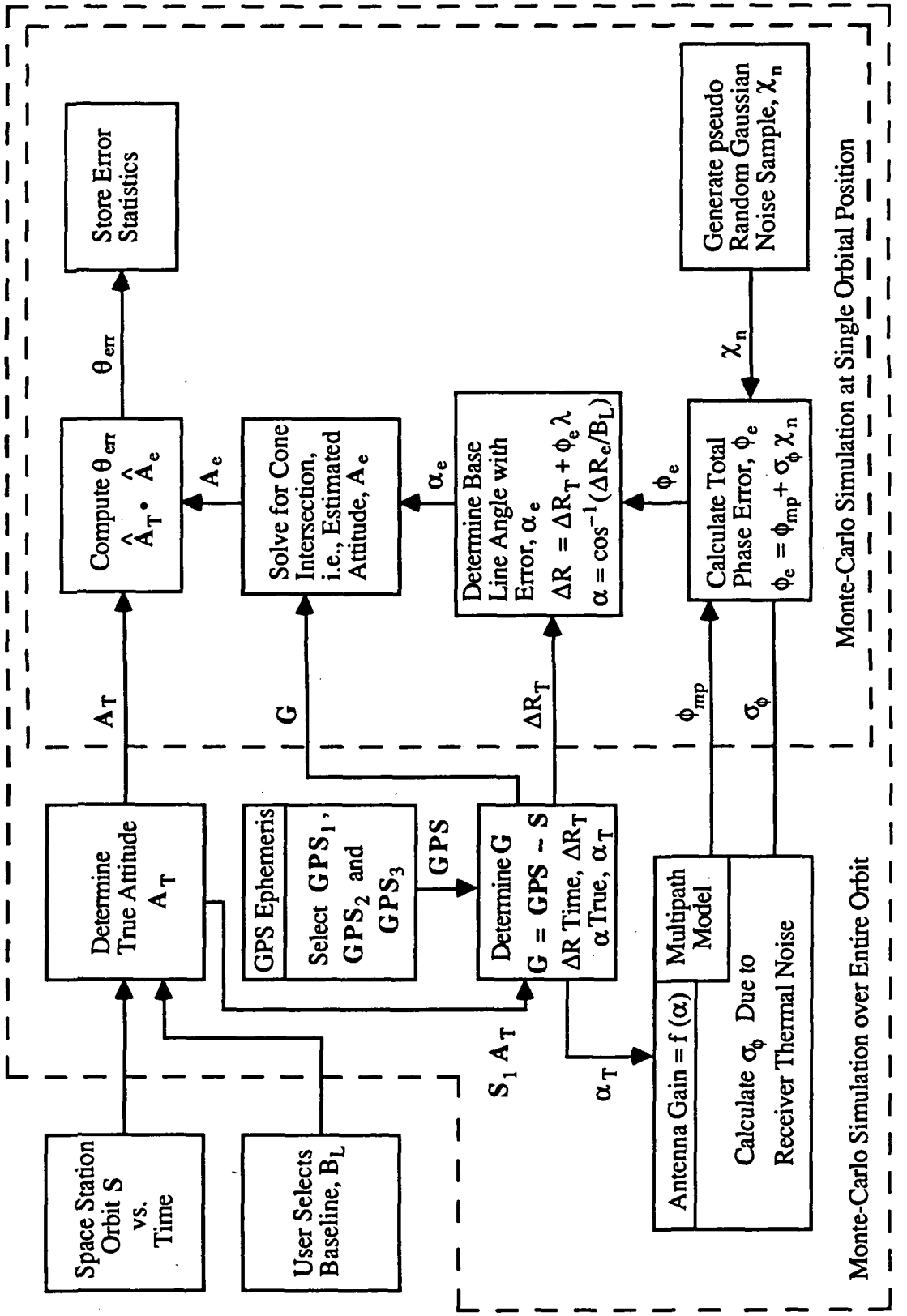

Figure 2.2-7. Simulation Block Diagram.

orbit (state vector vs. time) of the Space Station. These latter data were generated using Dr. Lear's Traj2 program and are stored in a data file which is read by the simulation. The program first establishes the true attitude vector $\mathbf{A_T}$. This vector is defined by the line drawn between the two receivers. The position of the first receiver is assumed to be the coordinates of the Space Station, S from the data file generated by Traj2. The position of the second receiver is established a distance B_L away from the first in a direction radially outward from the earth's center. Hence, $\mathbf{A_T}$ always points straight "up" simulating the orientation that will be maintained by the Space Station.

Given the position of the Space Station (first receiver), the program then selects the 3 GPS satellites that will minimize PDOP. Subtracting (vectorially) S from $\mathbf{GPS_1}$, $\mathbf{GPS_2}$ and $\mathbf{GPS_3}$ yields $\mathbf{G_1}$, $\mathbf{G_2}$ and $\mathbf{G_3}$ (see Figure 2.2-6). Using the position of the second receiver relative to the first, the 3 differential ranges, ΔR, are determined.

The model of the receiver generates two sources of phase error. The first, ϕ_{mp}, is an error in the phase measurement due to multipath. The second is an error due to receiver thermal noise. Here, the model generates the random error statistic, σ_ϕ, which is a function of the net C/N_o. The receiver model utilizes a model of the antenna gain pattern to modify the nominal C/N_o value of 42.75 dB based on the effective gain in the direction of the GPS satellite. Additionally, as will be explained in more detail later, multipathing also affects the net C/N_o.

The resulting value of σ is then converted into a pseudo-random carrier phase error by a Gaussian random number generator. The resulting phase error due to receiver thermal noise is then summed with the phase error due to multipath and the total converted into an error in ΔR by multiplying by the wavelength, λ. This error in the measurement of ΔR is then added to the true value of ΔR and the baseline angle (with error) α_e computed.

Using the three values of α_e and the three values of G, the program then solves for the attitude vector, $\mathbf{A_e}$. After converting $\mathbf{A_e}$ and $\mathbf{A_T}$ to unit vectors, the angular error

between the measured attitude and the true attitude is found by forming the dot product. We have:

$$\cos \theta_{err} = \mathbf{A_T} \cdot \mathbf{A_e}$$

A value of is θ_{err} determined for each value of ϕ from the random noise generator and stored in an accumulator. After the requisite number of trials have been run, the mean and standard deviation are determined. The program then reads in the next orbital position from the Space Station orbit data file and the process begins again. This is repeated until the error statistics for an entire orbit are obtained.

2.2.4 Detailed Simulation Description

The only significant inputs to the simulation made by the user are the baseline (distance between the two receivers) and the number of monte-carlo trials to be run. The first action taken by the simulation is to read in the state vector of the Space Station for the first orbital position (T = 0). The state vector is comprised of the position (x, y, z) and velocity ($\dot{x}$, $\dot{y}$, $\dot{z}$) of the Space Station. The position of the first GPS receiver, S, is defined to be at this location. Based upon these position data, it then selects the ID numbers (1 through 18) of the 4 GPS satellites that will minimize PDOP. Once identified, the state vectors of these four GPS satellites are then determined.

The next task is to determine the position of the second or what will be referred to here as the offset receiver, S_o. Refer to Figure 2.2-8 for the following discussion. It is to be located a distance B_L away from the first receiver radially outward from the earth. The position of the offset receiver X_o, with respect to the first is generated by forming a unit vector from the position vector S of the first receiver. Since the origin of S is the center of the earth, S points radially outward. Multiplying by B_L gives it the correct length. The position of the offset receiver in ECI coordinates is then given by:

$$\mathbf{S_o} = \mathbf{S} + \mathbf{X_o}$$

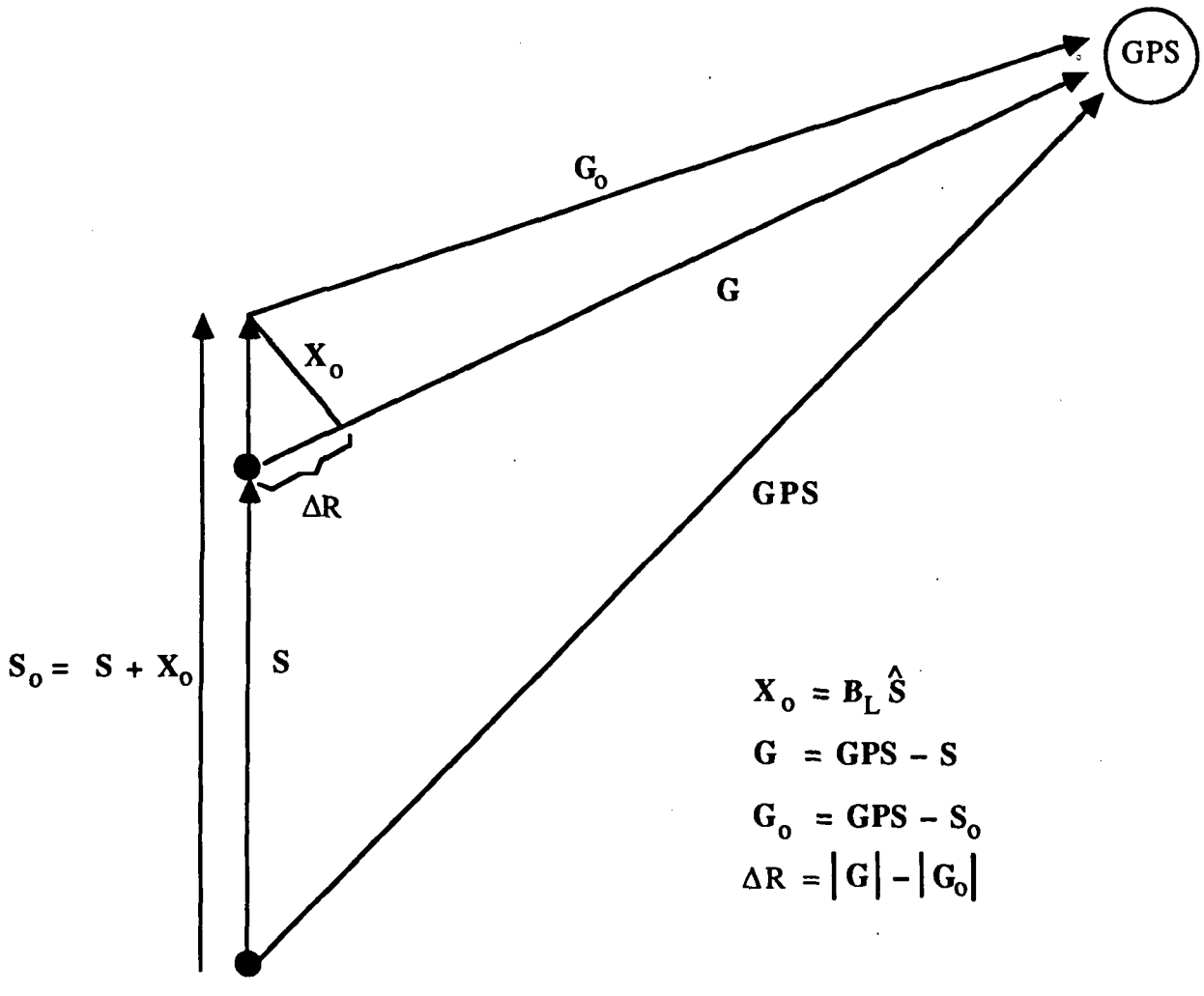

Figure 2.2-8. Definition of Required Vectors.

To determine the coordinates of the GPS satellites in an inertial coordinate system centered about the first receiver, the following vector subtraction is performed.

$$\mathbf{G} = \mathbf{GPS} - \mathbf{S}$$

The magnitude of G is the distance between the first receiver and the GPS satellite.

The position of the GPS satellite relative to the offset receiver is then given by

$$\mathbf{G_o} = \mathbf{GPS} - \mathbf{S_o}$$

The difference in the magnitudes of G and $\mathbf{G_o}$ then is the differential range, ΔR.

$$\Delta R = |G| - |G_o|$$

After calculating ΔR for each of the 4 GPS satellites, the 4 baseline angles α, are determined by:

$$\alpha = \cos^{-1} (\Delta R/B_L)$$

Dr. Lear's GPS NAV program required four GPS satellites in order to yield a GPS position measurement, however, we need only 3 to solve for attitude. The next task is to select the best 3 to suit our purpose. The greatest accuracy in the measurement of α (i.e, minimize $\Delta\alpha$ dependency on ΔR) is obtained when α is 90°. Hence, the program examines the four values of α and selects the three GPS satellites with the highest values of α.

We now have 3 values of G and resulting 3 error free half cone angles, α. The next task is to use a model of the receiver to generate an error in the values of α representative of a real system. This begins the monte-carlo portion of the simulation. As discussed earlier, the receiver model injects error due to thermal noise and multipath. The multipath model is complex and is described in detail in Section 2.6. A flow diagram of the receiver is given in Figure 2.2-9. As shown, the receiver first determines the gain of the

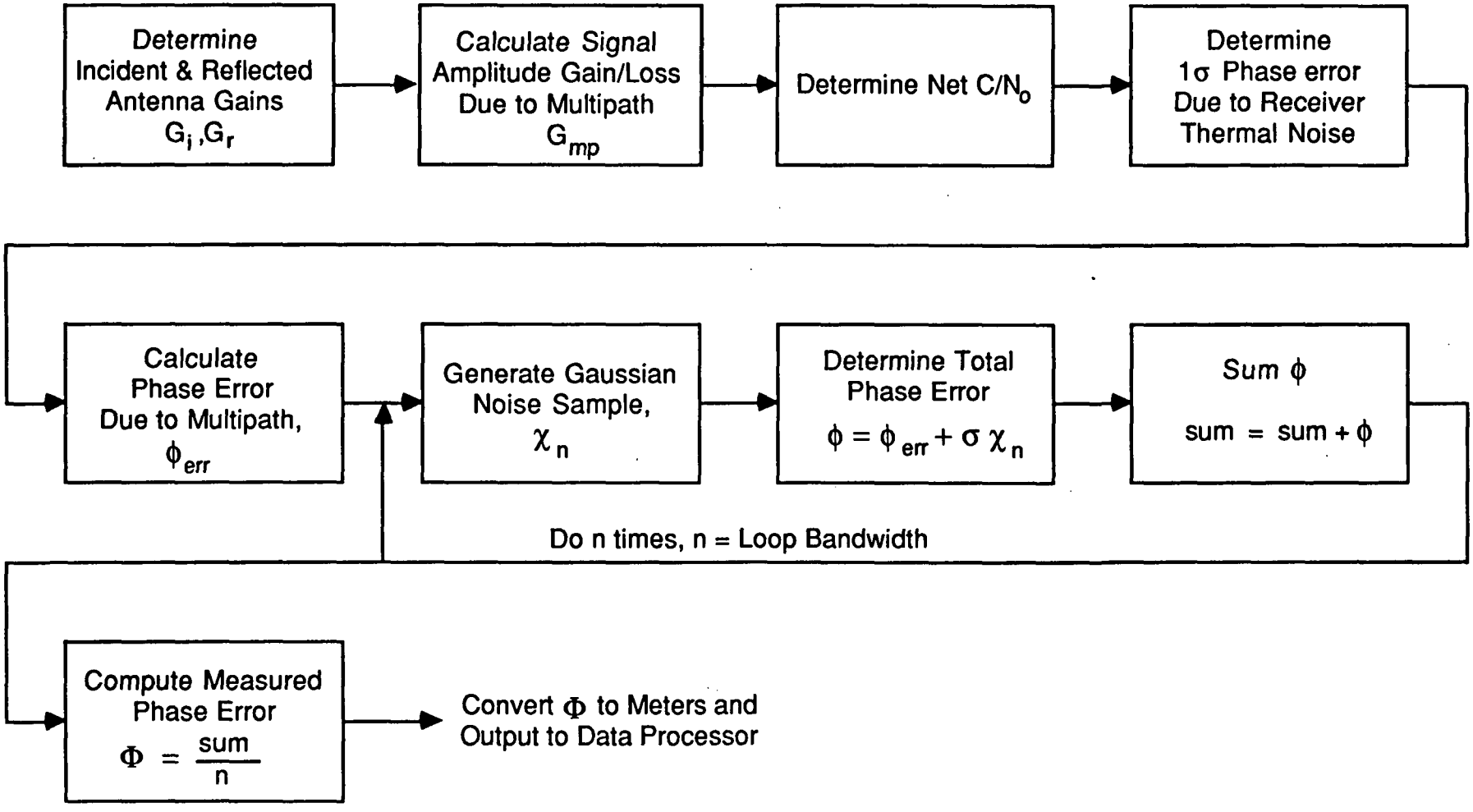

Figure 2.2-9. Receiver Model with Multipath.

antenna in the direction of the incident and reflected signal. These gains are used by the multipath model to determine the net C/N_o. From this, the $1-\sigma$ phase error due to receiver thermal noise is obtained. Next, the phase error due to multipath ϕ_{mp}, is determined. Now, we begin an integration over the loop bandwidth. For each pass through the loop, a Gaussian noise sample χ_n, is generated. The measured phase error for that trial is determined by

$$\phi_{err} = \phi_{mp} + \sigma\chi_n$$

The value of ϕ_{err} is summed to an accumulator and after the requisite number of trials (equal to the bandwidth in Hz) the mean value is determined by:

$$\Phi = \frac{\Sigma\phi}{B_L}$$

The value of Φ represents the error in a single phase measurement by the receiver. Three values of Φ are determined, one for each of the 3 GPS satellites.

The next task is convert the error in the phase measurement to an error in the baseline angle α. First, Φ is converted to meters by multiplying by the wavelength, λ. The product of Φ and λ is the error in ΔR. The value of ΔR with error, ΔR_{err} is given by

$$\Delta R_{err} = \Delta R + \Phi\lambda$$

where ΔR is the true differential range.

From this we determine the value of α with error, α_{err}

$$\alpha_{err} = \cos^{-1}\left(\frac{\Delta R_{err}}{B_L}\right)$$

At this point, the program has generated the three values of G; G_1, G_2 and G_3 and the accompanying three values of α_{err} ; α_{err1}, α_{err2} , α_{err3} . Using these six parameters, the simulation solves for the intersection of the three cones to determine the measured attitude

vector. This solution is complex and is described in detail in Appendix B. We note that due to the fact that the three values of α used in the solution are not error free, the three cones will not intesect at a single point. The result will actually be three pairs of intersections as shown in Figure 2.2-10. The simulation picks (pairwise) the three closest to the true attitude. The estimated attitude A_e, is formed by averaging these three solutions by summing them (vectorially). The result is then converted into a unit vector by dividing by the magnitude of the resulting vector.

Using the true attitude vector $\hat{A}_T$ defined at the beginning of the program and the estimated attitude $\hat{A}_e$, the simulation is now ready to determine the attitude error defined by the angle between them. This is done by forming the dot product of the two vectors. We have

$$\cos \theta_{err} = \hat{A}_T \cdot \hat{A}_e$$

The value of θ_{err} is stored in an accumulator. The simulation now returns to the receiver model and generates new values of the error in the phase measurement Φ, utilizing the Gaussian noise generator. This results in a new value of θ_{err}. After the selected number of Monte Carlo trials have been run, the mean value of θ_{err} is determined by dividing the summed value of θ_{err} by the number of trials. The result is the mean attitude, or pointing error for the particular orbital position of the Space Station. The simulation now returns to the beginning and reads the state vector for the next orbital position and the whole process repeats resulting in a mean value of the pointing error for the new orbital position. This process repeats until the error statistics for the entire orbit have been collected.

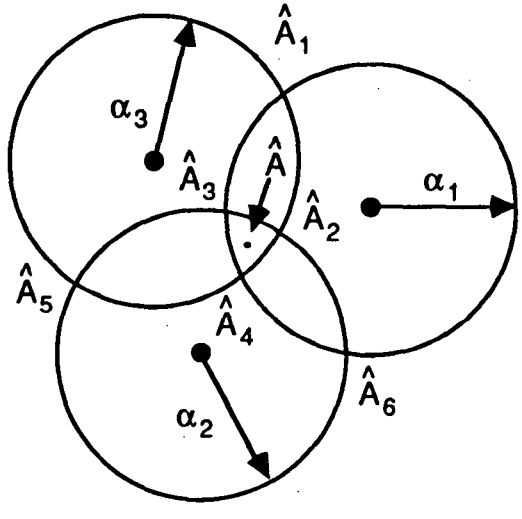

$$\hat{A} = \frac{\hat{A}_2 + \hat{A}_3 + \hat{A}_4}{\left|\hat{A}_2 + \hat{A}_3 + \hat{A}_4\right|}$$

Figure 2.2-10. Solution to Non-Ideal of 3 Cones.

2.3 Receiver Model

The receiver model plays a role in determining the random carrier phase error, which in turn, determines the attitude determination accuracy. In establishing the receiver model, we have assumed that a modern GPS receiver such as GPSDR which is being built by Motorola for the TOPEX satellite is used. This allows us to take into account various implementation losses which may occur in a modern, digitally implemented receiver.

Figure 2.3-1 shows an overall functional block diagram for the random carrier phase error. This model is quite general and not all of the capabilities of this model have to be utilized for our problem on hand.

The left portion of the model contains the block which represents the path loss/receiver RF portion of the model. The factors which determine the nominal C/N_0 value applied to the receiver are listed in this block and are taken into the account. Some of these factors are invariable with the satellite selection. Other factors depend on the angle to a particular GPS satellite. For example, the received signal level is a function of the antenna gain in the direction of a GPS satellite. Consequently, the C/N_0 value is affected.

The right portion of the receiver model represents the block which accounts for the signal losses contributed by the receiver processor/Costas loop demodulator. As the result of passing through this block, the C/N_0 is converted into an equivalent random phase measurement error. Another output of this model block is the mean slip time. For the purpose of attitude determination, the mean slip time may not be of concern because it usually is in hours, while the attitude measurement is required within minutes or even seconds. Thus, the main result of the output of the model is the random phase measurement error.

Another error which is developed in a GPS receiver is the systematic error. This error is typically caused by the effect of either the doppler or the doppler rate, or both, upon the receiver circuitry. Figure 2.3-2 shows the model for the systematic error. As shown , there may be two components of the systematic error. These components, however, can be

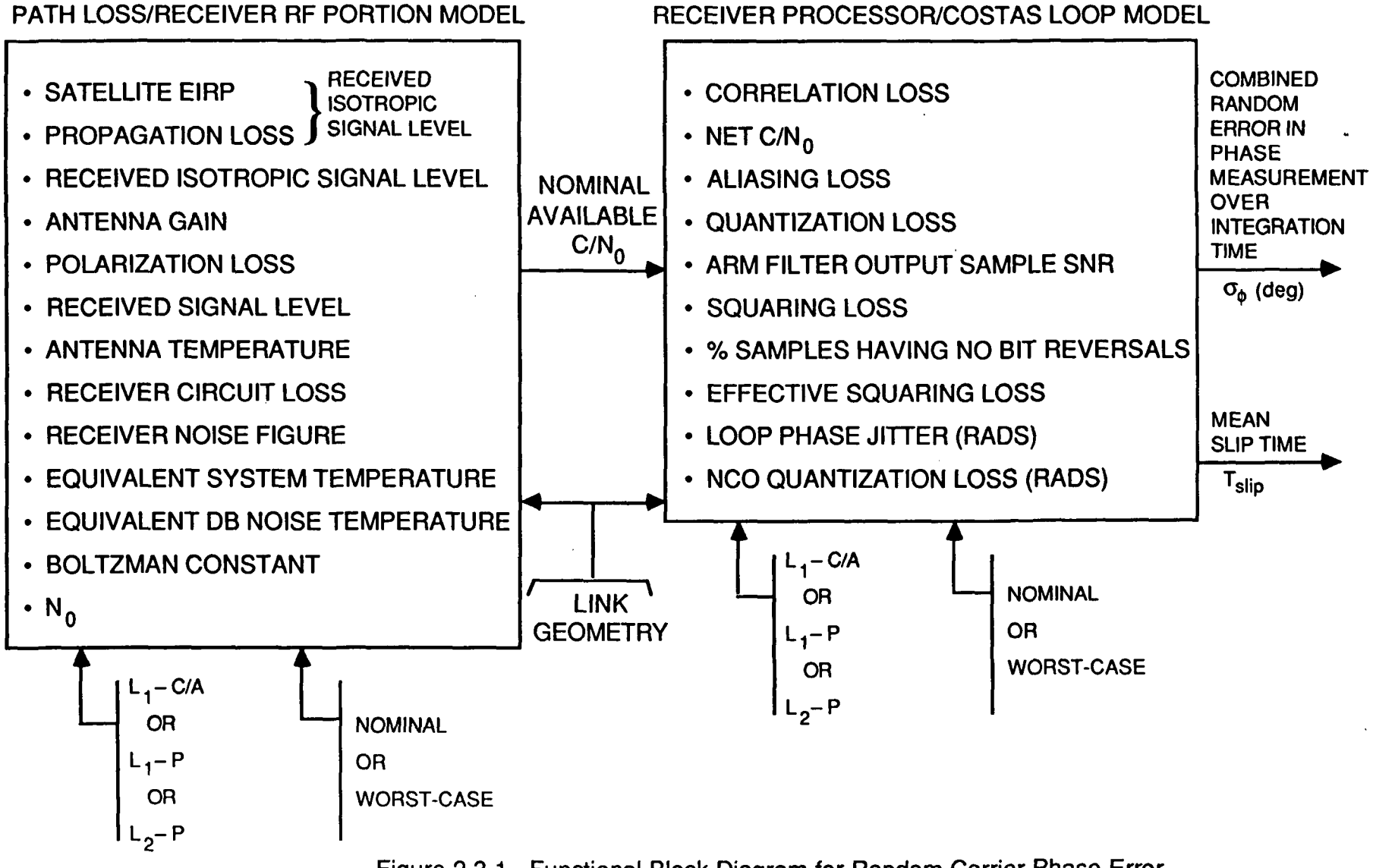

Figure 2.3-1. Functional Block Diagram for Random Carrier Phase Error.

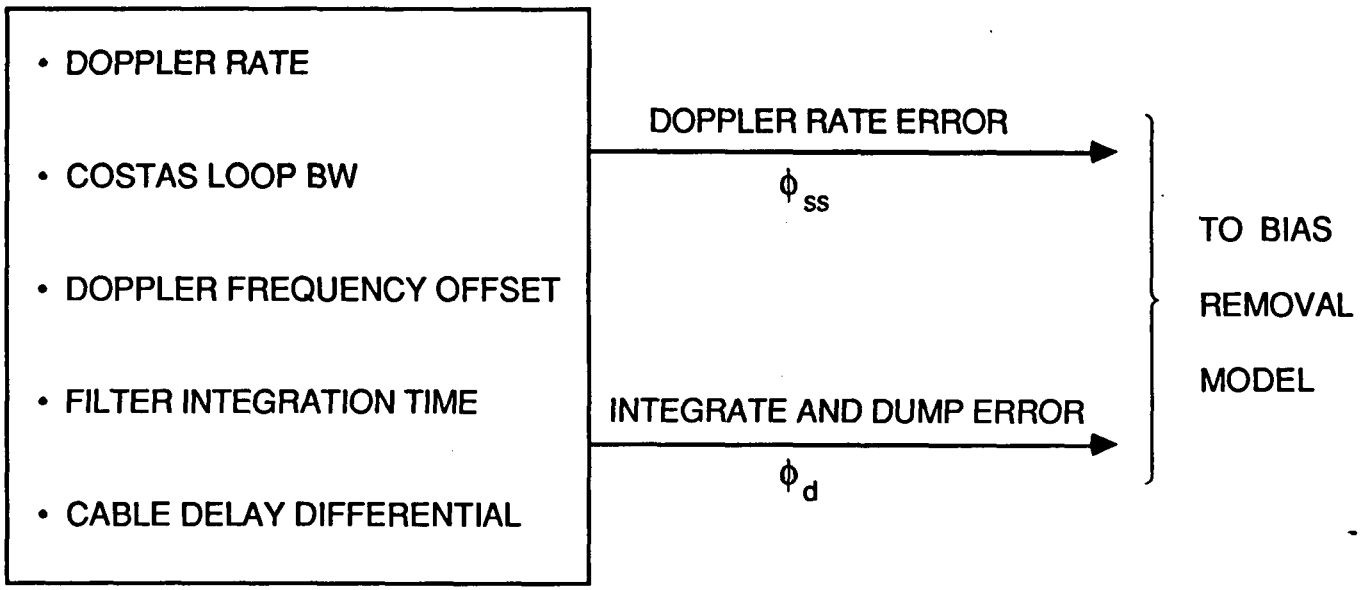

Figure 2.3-2. Systematic Carrier Error Model.

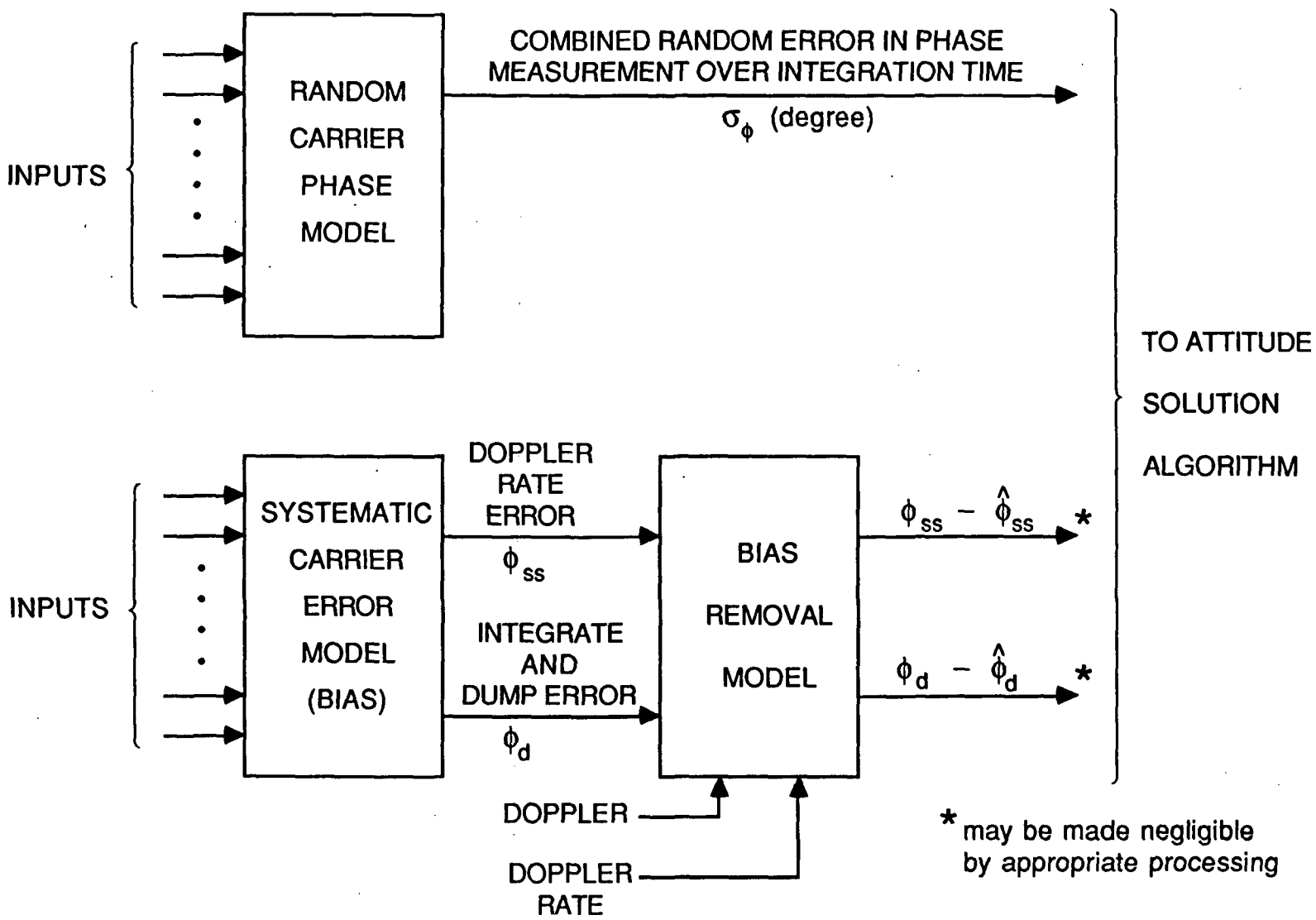

Figure 2.3-3. Functional Block Diagram for Random and Systematic Carrier Phase Error Models.

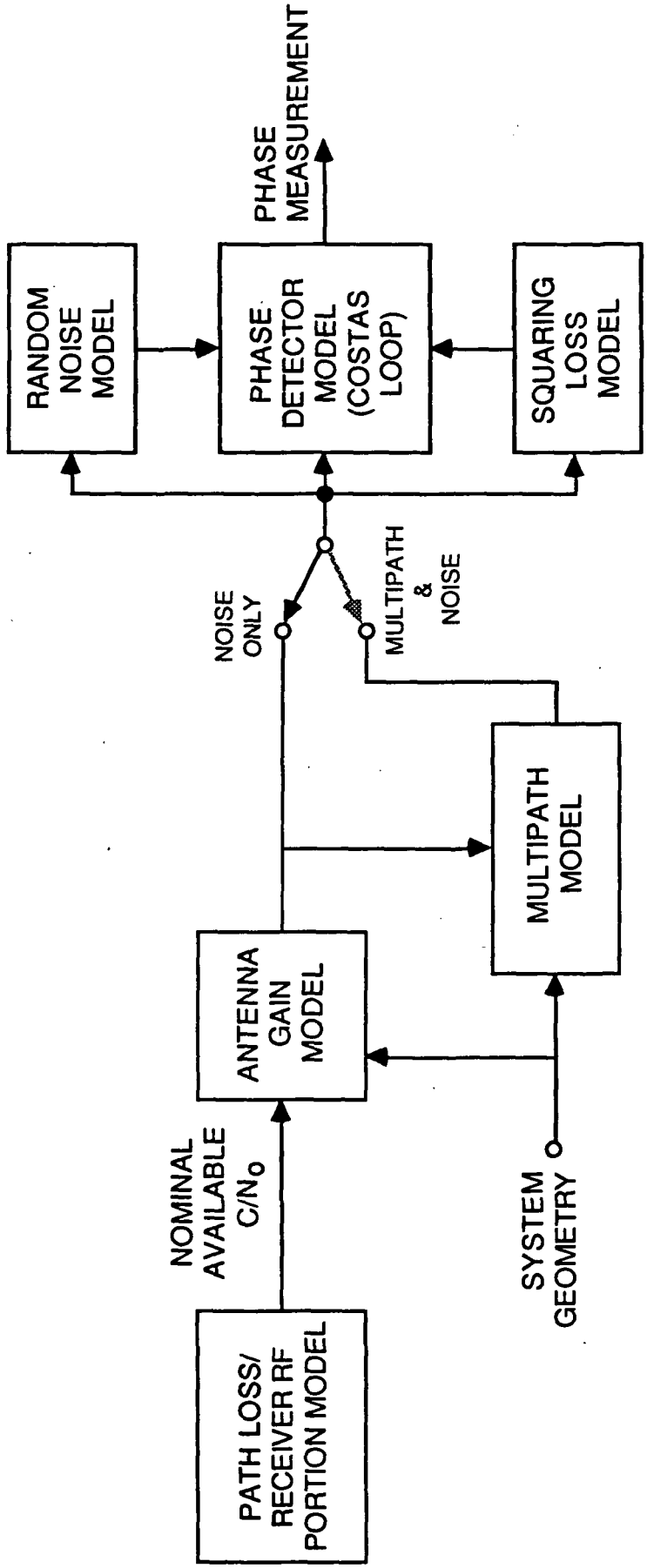

Figure 2.3-4. Simplified Model of Random Carrier Phase Error.

either removed or virtually eliminated by subsequent signal processing which utilizes good estimates of doppler and doppler rate.

Figure 2.3-3 shows a functionally reduced model for both the random and the systematic phase error (bias) models. As indicated in this figure, the doppler rate and the integrate and dump bias errors can be made negligible by appropriate processing. The information required for such processing can be obtained from almanac (doppler and doppler rate) as well as from inertial sensors (doppler rate). After considering all of the factors indicated in Figures 2.3-1 through Figure 2.3-3, we reduced the receiver model to being responsible only for elements contributing to the random carrier phase error. The functional diagram of this simplified model is shown in Figure 2.3-4. With this model, we assume a "nominal" C/N_0 which is based on fixed RF receiver losses and noise temperature. Based on system geometry, we then modify this C/N_0 value by the antenna gain in the direction of a particular satellite. Depending on the resulting C/N_0, we compute the Costas loop squaring loss and then use random noise model to develop noise corresponding to a particular resulting C/N_0. The output is then the required phase measurement error which subsequently is used for calculating the attitude accuracy. If a multipath case is selected, then the phase measurement is affected accordingly as described in Section 2.5 of this report.

2.4 Antenna Model

The antenna model assumes that the maximum gain of the antenna used for determining the attitude is always in the zenith direction.

The gain vs. direction relationship for the antenna model used for our simulations is shown in Figure 2.4-1. This pattern is modeled after GPSDR equipment to be used on TOPEX satellite.

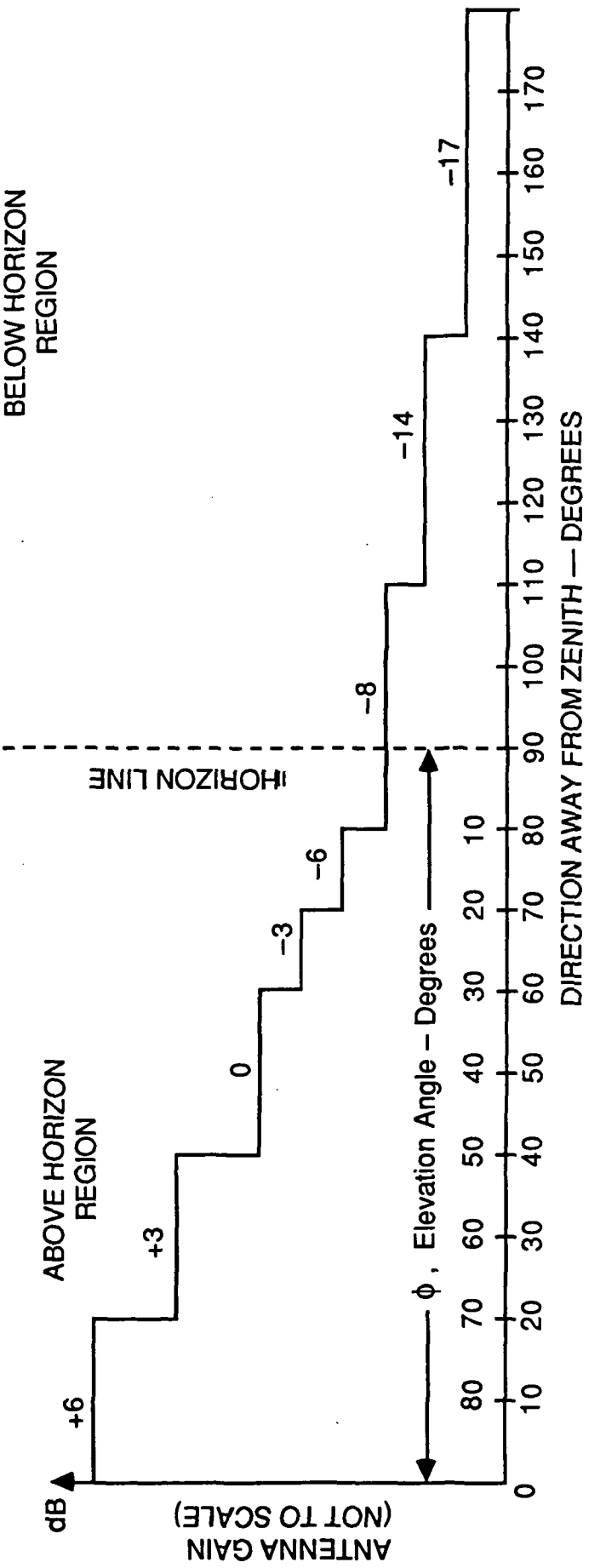

Figure 2.4-1. Antenna Gain Model.

2.5 Multipath Model

2.5.1 Background

Multipathing results when the incident wave is reflected off ancillary structures into the backlobe of the receiving antenna. The signal that arrives at the receiver then is actually a composite signal comprised of both incident and reflected energy. Since the reflected wave arrives at the antenna out of phase (in general) with the incident wave, the ability of the receiver to recover the phase of the incident wave is reduced.

The easiest way to understand this effect is through the use of a phasor diagram. Such a diagram is shown in Figure 2.5-1 where **I** is the incident voltage vector with phase ϕ, **R**, the reflected wave voltage vector and **C**, the resulting composite voltage vector seen by the receiver. We note that there are two effects. First, depending upon the relative phase of **I** and **R**, the magnitude of **C** will be either larger or smaller than the magnitude of **I** (constructive or destructive interference). This, in turn, affects the net C/N_0. Second, a phase error, ϕ_{err}, is introduced. The measured phase is now $\phi + \phi_{err}$.

2.5.2 Derivation of Model

The difficulty in developing a multipath model is that the actual effects are highly dependent on the specific geometry of the structures involved and the relative placement of the antenna. A general model is described in this report which can be used as a basis for a more detailed accurate model as specifics of the the structure become finalized. This section deals with the derivation of the interaction between a primary incident wave and a secondary reflected wave of arbitrary phase and reduced amplitude. The approximation involved assumes that the reflected wave is significantly smaller than the primary wave so that small angle approximations can be used.

If the primary incident wave is $\cos(\omega t)$, then the secondary reflected wave will be $\beta \cos(\omega t + \delta)$, with β the ratio of the amplitude of the secondary and primary waves, and δ the relative phase of the two. Thus,

I = INCIDENT WAVE

R = REFLECTED (MULTIPATH) WAVE

C = COMPOSITE (RECEIVED) SIGNAL

ϕ_{err} = PHASE ERROR

G_{mp} = MULTIPATH GAIN/LOSS

$$= \left[\frac{|C|}{|I|}\right]^2$$

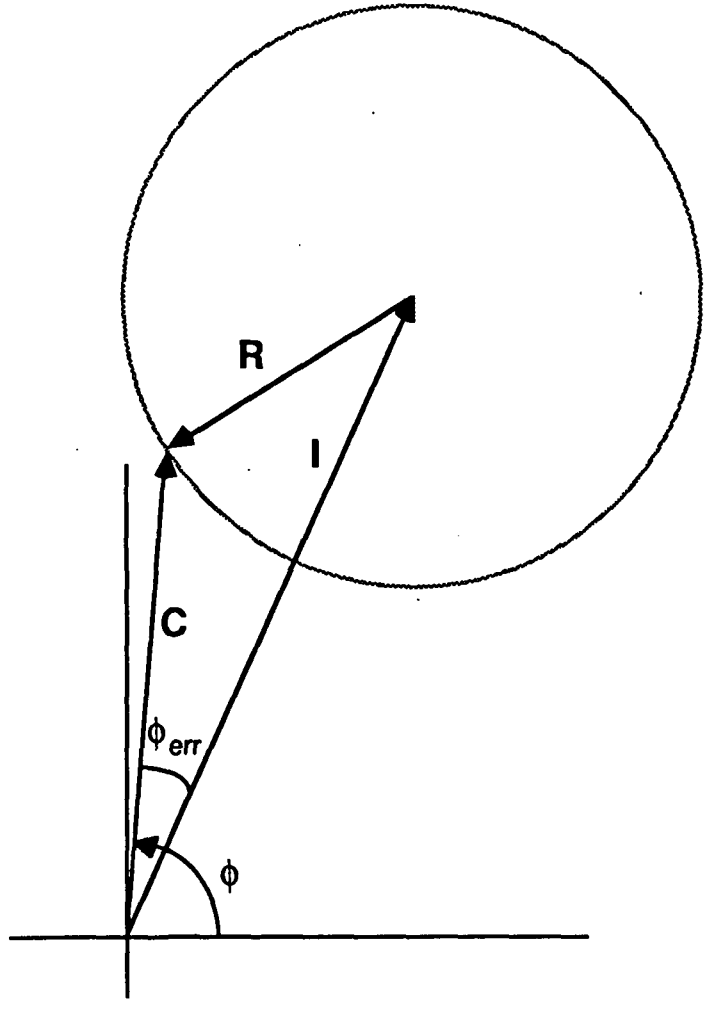

Figure 2.5-1. Multipath Vector Representation.

$$C(t) = \cos(\omega t) + \beta \cos(\omega t + \delta),$$
$$= \cos(\omega t) + \beta \cos(\omega t)\cos(\delta) - \beta \sin(\omega t)\sin(\delta)$$
$$= \{1 + \beta \cos(\delta)\} \cos(\omega t) - \beta \sin(\delta) \sin(\omega t)$$

These are the I and Q components of the signal. The magnitude is then

$$|C| = \left\{(1 + \beta \cos(\delta))^2 + (\beta \sin(\delta))^2\right\}^{1/2}, \text{ and the phase is}$$

$$\Phi = \tan^{-1}\left\{\frac{\beta \sin(\delta)}{1 + \beta \cos(\delta)}\right\}$$

If $\beta << 1$, i.e., the reflected energy is much less than the direct energy, then

$$|C| = \left\{1 + 2\beta \cos(\delta) + \beta^2 \cos^2(\delta) + \beta^2 \cos^2(\delta)\right\}^{1/2}$$

$$= \left\{1 + 2\beta \cos(\delta) + \beta^2\right\}^{1/2} \approx 1 + \beta \cos(\delta)$$

and $$\phi = \tan^{-1}\left\{\frac{\beta \sin(\delta)}{1 + \beta \cos(\delta)}\right\} \approx \tan^{-1}\left\{\beta \sin(\delta)\right\} \approx \beta \sin(\delta),$$

and $$C(t) = (1 + \beta \cos(\delta)) \cos(wt + \beta \sin(\delta)), \beta << 1.$$

We are now left to solve for β, the ratio of the amplitude of the secondary or reflected wave to the primary or incident wave. After much consideration it was decided to model the reflected wave as a radar problem. This is illustrated in Figure 2.5-2. Specifically, the reflected wave results from a portion of the incident wave being reflected by some ancillary part of the structure assumed to have a radar cross section, σ. By the definition of sigma, this energy is spread isotropically into space and arrives at the antenna a distance r away. To solve for β, we must compute the received power of both the incident and received signal.

Let us assume that the signal from the GPS satellite arrives with power flux density (watts/m^2) S_i. The total power received due to the incident wave, P_i, is then

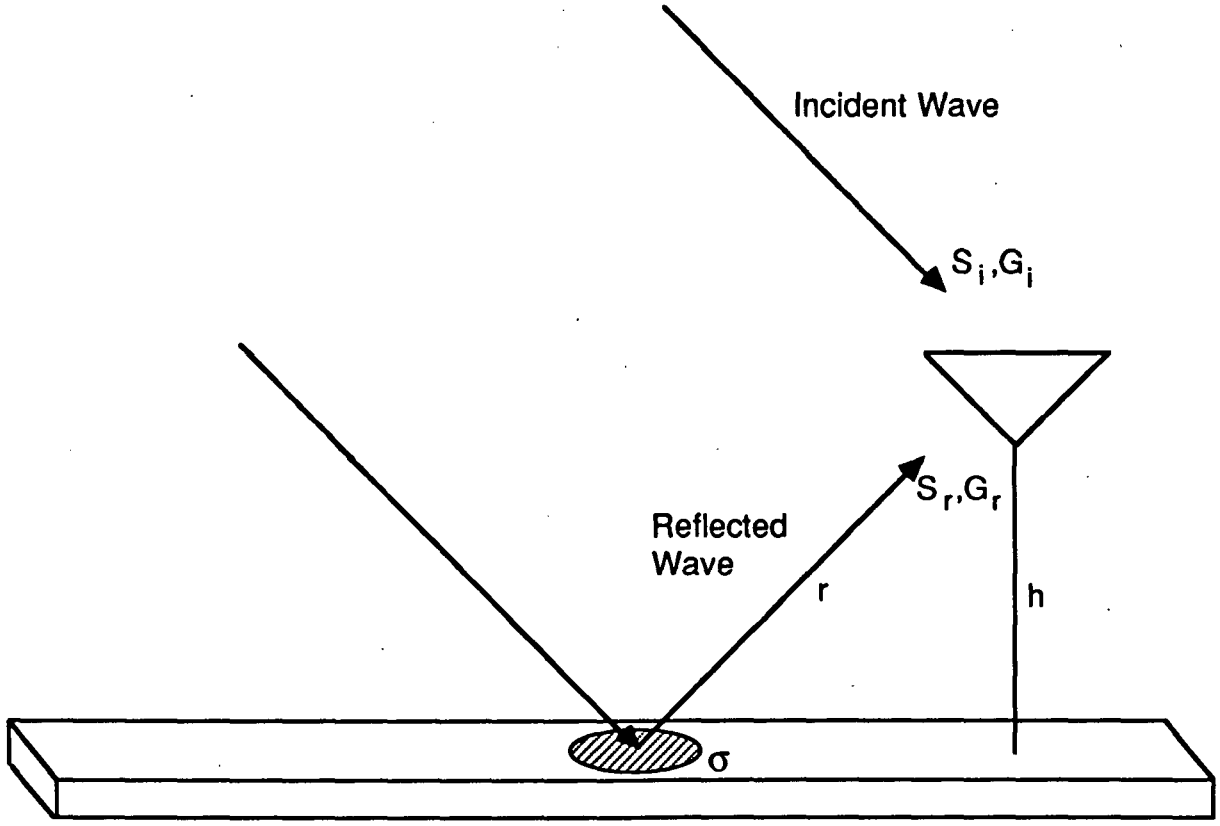

ANTENNA HEIGHT, h (ARBITRARY) = 0.3 m

"RADAR" CROSS SECTION, σ (ARBITRARY) = 1 m^2

Figure 2.5-2. Reflected Wave Relative Strength.

$$P_i = S_i A_i$$

where A_i is the effective aperture of the antenna in the direction of the received signal. We normally characterize antenna by their gain so making the following substitution, we have

$$G\alpha \frac{A}{\lambda^2}$$

$$P_i = \frac{SG_i}{\lambda^2}$$

where G_i is the gain of the antenna in the direction of the received signal.

Now we solve for the total reflected power, P_i. The total power intercepted by the structure and reradiated back into space is

$$P = S_i \sigma$$

Upon arrival at the antenna, the power flux density of the signal is

$$S_r = \frac{S_i \sigma}{4\pi r^2}$$

The total power P_r, intercepted by the antenna is then

$$P_r = S_r A_r$$

$$= \frac{S_i \sigma A_r}{4\pi r^2}$$

where A_r is the effective aperture of the antenna in the direction of the reflected wave. Making the substitution for gain, we have

$$P_r = \frac{S_i \sigma G_r}{4\pi r^2 \lambda^2}$$

The ratio of the received reflected signal power to the received incident signal power is then

$$\frac{P_r}{P_i} = \frac{\frac{S_i \sigma G_r}{4\pi r^2 \lambda^2}}{\frac{S_i G_i}{\lambda^2}}$$

$$= \frac{\sigma G_r}{4\pi r^2 G_i}$$

Since β is in voltage and we have calculated a power ratio, we have for β

$$\beta = \left[\frac{\sigma G_r}{4\pi r^2 G_i} \right]^{1/2}$$

In order to calculate r, some height must be established for the antenna. A value of 0.3 m was chosen although it is completely arbitrary. A value of 1 m^2 was assigned for σ, the "radar" cross section.

Lastly, the relative phase of the two signals, δ, is shown in the derivation as a constant for simplification reasons. In reality, due to the orbital motions of the Space Station, δ is a time varying parameter and is equal to

$$\delta = 2\pi \sin(\gamma t)$$

where γ is the orbital rate of the Space Station in radians per second.

2.6 Results

2.6.1 Background and Definition of Mean Pointing Error

As described in Section 2.2, the simulation is configured to output a mean pointing error for each point of the orbit (based on Monte Carlo trials of receiver thermal noise). The Traj2 program computeS the orbital position of the Space Station at 120 sec intervals for T = 0 to T = 5520 sec (one orbit) resulting in a total of 46 points. At the end of the program, a mean pointing error for the entire orbit is computed by averaging these 46 individual pointing errors. Additionally, the 1σ standard deviation of the error is also computed. Two versions of the program were developed and run. The first assumes that receiver thermal noise is the only error source. The second includes error due to multipath. Comparison of the results of these two cases reveals much about the various error mechanism involved.

The definition of the pointing error requires some explanation. As was explained in Section 2.2, the pointing error is defined as the angle between the true attitude vector A_T and the measured attitude vector A_e. It is determined by taking the dot product of the two vectors:

$$\theta_{err} = \cos^{-1} [A_T \cdot A_e]$$

This method is in contrast to the more conventional method of describing the pointing error solely by the 1σ standard deviation of the attitude error. This latter method assumes that a scatter plot of the measured attitude error would form a 2-dimensional Gaussian with zero mean about the true attitude. This method was not adopted for two reasons. First, as we will see, the affect of multipath is to introduce a bias term into the attitude error. Hence, a scatter plot of the attitude error is not centered about zero error but is offset by the amount of the bias. Secondly, for each point in the orbit, the Space Station is assumed to be stationary so a large number of Monte Carlo trials can be run to determine the mean pointing error. In the real world, this is not the case. Orbital motion of the Space Station

will result in rotation of the attitude vector at a rate of 2π radians per orbital period. As a result, the receiver will only have the opportunity of integrating a few samples before smearing of the attitude vector due to its rotation exceeds the accuracy of the measurement process. Hence, for each point in the orbit, the output of the receiver would have some mean value.

The results indicate three sources of error the effects of which will be discussed in detail later in this section. The first is due to receiver thermal noise and acts to spread the pointing error values out in the familiar 2-dimensional Gaussian shape when viewed in a scatter plot. The second results from the solution to the intersection of the cones when the cones intersect at nonuniform error source angles and acts to skew the Gaussian distribution in one direction (i.e., nonuniform σ). The last error source is due to multipath effects and as already stated acts to introduce a bias term to the pointing error.

2.6.2 Results from Single Orbit

Figure 2.6-1 shows the mean pointing error vs. time for one complete Space Station orbit for a receiver baseline of 5 meters. The results from both the multipath (with noise) and the noise only program are plotted for comparison. Note that for some periods of time the multipath results "track" the noise only results, i.e., where there is a peak in the multipath results, there is a peak in the noise only results, etc. Examples of this are at T equal approximately 700 sec, 1800 sec and 3400 sec. Yet at other times, peaks in the multipath results are accompanied by valleys or regions of benign activity in the noise only case. Examples of this are at T equal 2800 sec and 5200 sec. For the noise only results, peaks (regions of large error) are due to shallow cone intersection angles that result from the relative geometry of the three GPS satellites and the Space Station. The effect of this error can be seen in a scatter plot of the pointing error. Here, individual values of θ_{err} (resolved into x and y coordinates) are plotted. Each is the result of one Monte-Carlo trial for a single orbital position. Figure 2.6-2 shows the results for T = 0, the first orbital

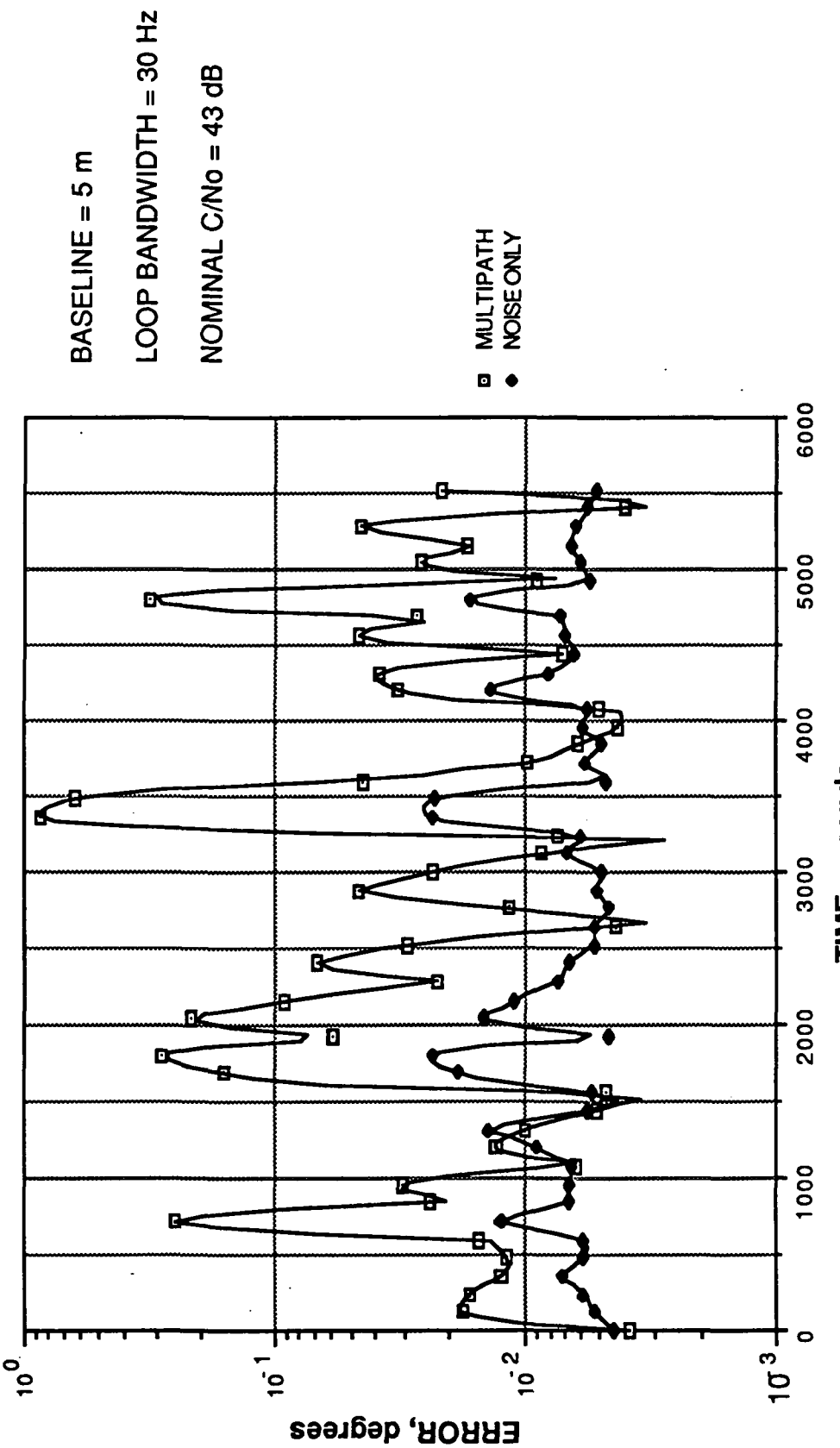

Figure 2.6-1. Mean Error vs. Time for Complete Orbit.

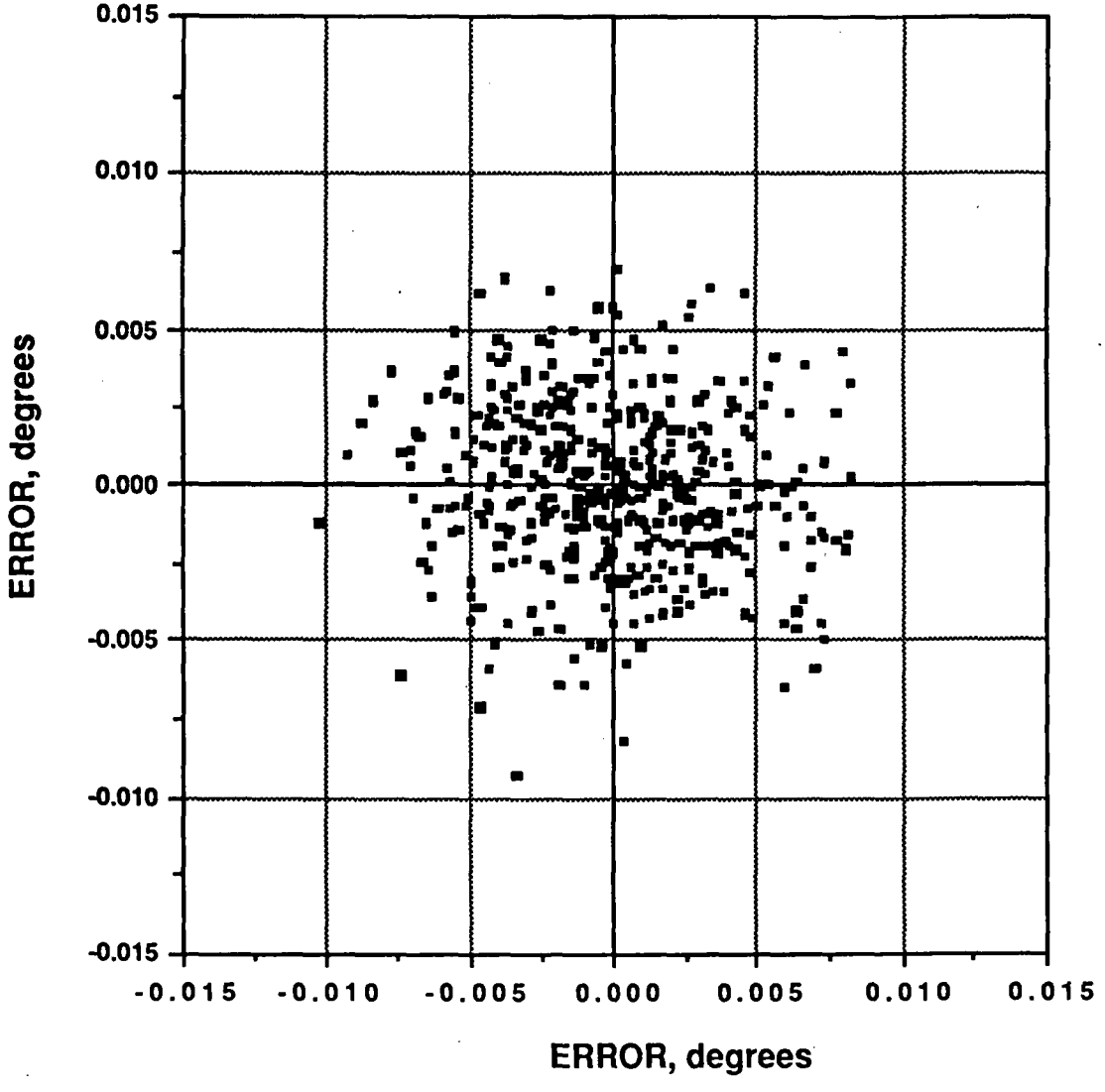

SINGLE ORBITAL POSITION , T = 0 sec

BASELINE = 5 m

LOOP BW = 30 Hz

NOMINAL C/No = 43 dB

NUMBER OF TRIALS = 500

MEAN ERROR = 3.77×10^{-3} degrees

STANDARD DEVIATION (1σ) = 2.03×10^{-3}

ERROR DUE TO SATELLITE GEOMETRY NEAR ZERO

ERROR DUE TO MULTIPATH ZERO

Figure 2.6-2. Scatter Plot of Pointing Error for T = 0.

position. Here, the mean pointing error is about as low as at any other point in the orbit. Note that the points are distributed in a nearby uniform 2-dimensional Gaussian pattern. Compare these results with those of T = 2880 presented in Figure 2.6-3. The mean error is only slightly larger, but we can see that the points are beginning to be stretched or skewed in one direction. Now lets examine a case where the mean pointing error is high. Figure 2.6-4 shows the data for T = 1800 sec where the mean pointing error is nearly an order of magnitude greater than it is in the previous two cases (T = 0 and T = 2800 sec). Here, the points are highly skewed along a single axis.

2.6.3 Error Due to Satellite Geometry

Section 2.2 and Appendix B describe how the simulation solves for the estimated attitude vector by finding the intersection of the three cones. The accuracy by which the point of intersection can be determined, however, is dependent on the relative geometry of the cones. The problem is easily understood by examining the solution for the intersection of two lines as shown in Figure 2.6-5. If the lines cross at right angles, then a disturbance in the position of one line by the amount Δx moves the intersection point an amount equal to Δx. If, however, the lines cross at a very shallow angle, then shifting one line an amount Δx will shift the intersection point much more.

Figure 2.6-6 illustrates this for two intersecting cones. When the cones intersect at a shallow angle, the intersection point is a strong function of the perturbation in the half cone angle α ($\Delta\alpha$) due to thermal noise. The result is that the points get spread out along a line formed by the two intersection points.

2.6.4 Error with Multipath

As mentioned before, multipath introduces a bias error term in the overall pointing error. Hence, instead of the points being spread out about 0,0 as was the situation for the noise only case, they will be shifted in a particular direction. Figure 2.6-7 shows a plot of the data from T = 1080 with multipath. Note the moderate error due to satellite geometry

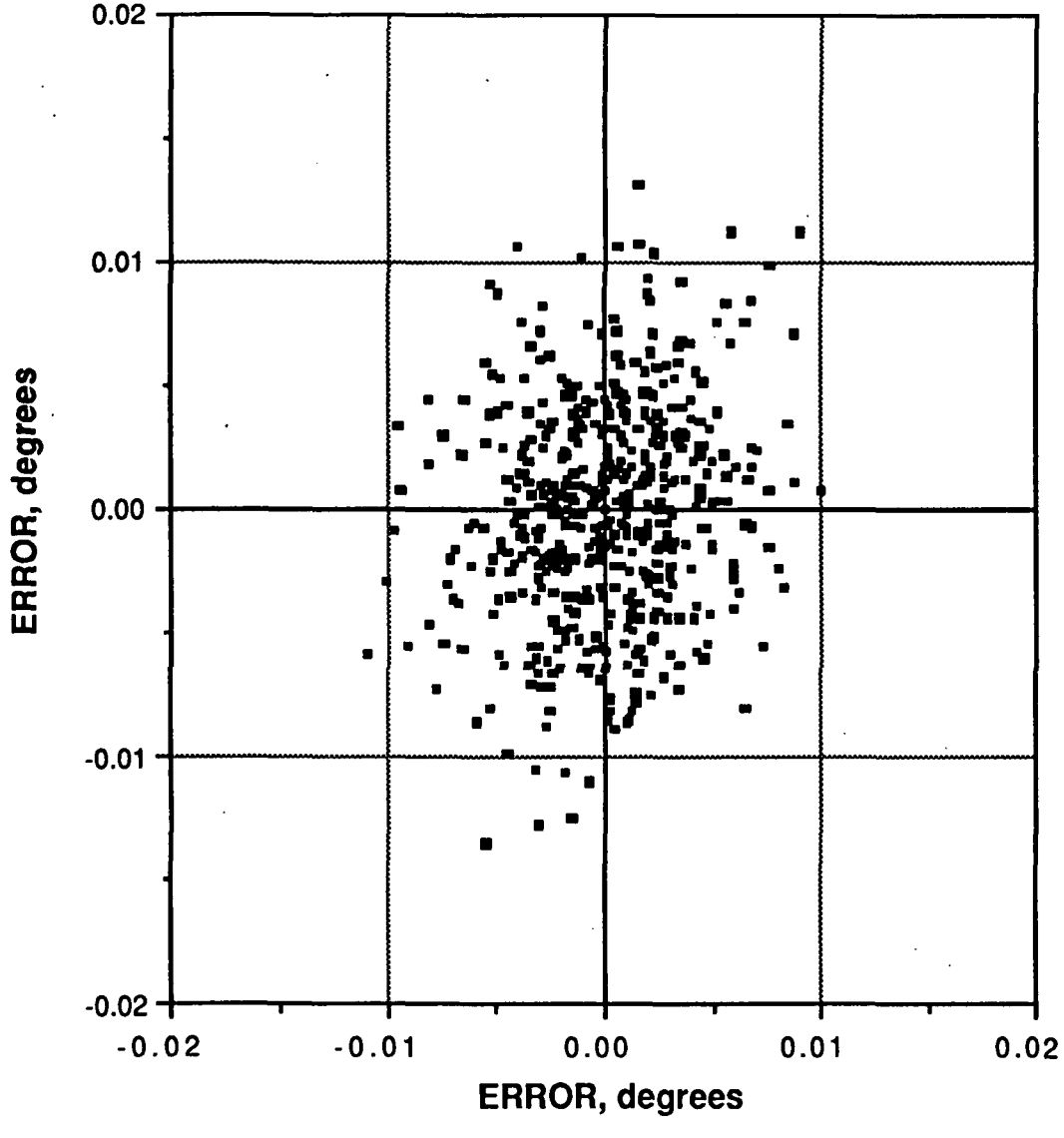

SINGLE ORBITAL POSITION , T = 2880 sec

BASELINE = 5 m

LOOP BW = 30 Hz

NOMINAL C/No = 43 dB

NUMBER OF TRIALS = 500

MEAN ERROR = 4.49×10^{-3} degrees

STANDARD DEVIATION (1σ) = 2.69×10^{-3}

ERROR DUE TO SATELLITE GEOMETRY LOW

Figure 2.6-3. Scatter Plot of Pointing Error for T = 2880 sec, Noise Only.

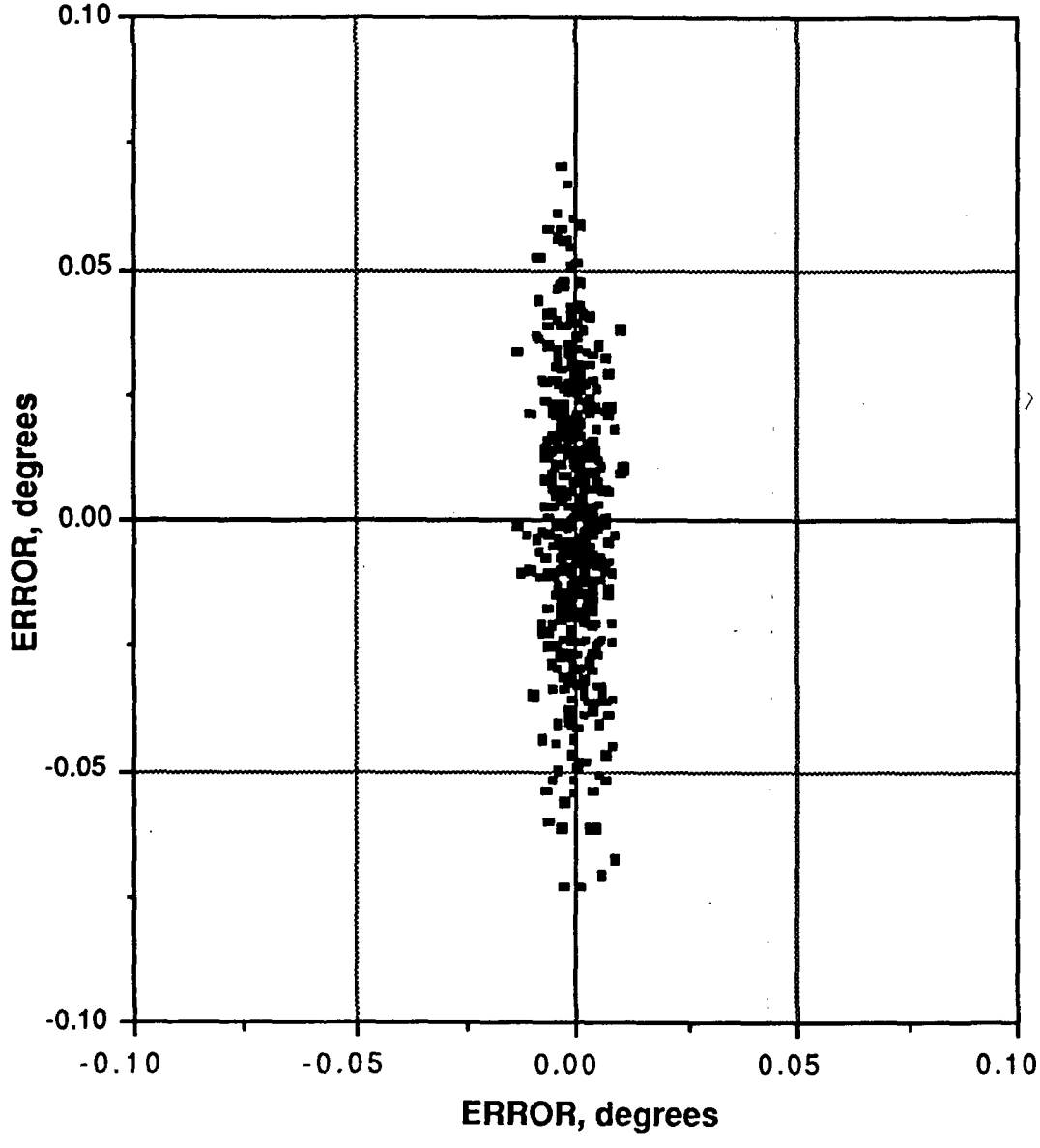

SINGLE ORBITAL POSITION, T = 1800 sec

BASELINE = 5 m

LOOP BW = 30 Hz

NOMINAL C/No = 43 dB

NUMBER OF TRIALS = 500

MEAN ERROR = 2.21 X 10^{-2} degrees

STANDARD DEVIATION (1σ) = 1.51 x 10^{-2}

ERROR DUE TO SATELLITE GEOMETRY HIGH

Figure 2.6.4. Scatter Plot of Pointing Error T = 1800 sec, Noise Only.

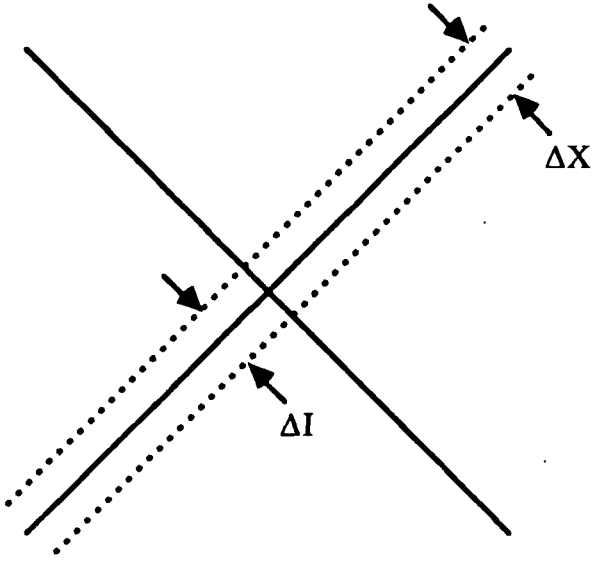

Steep Intersection on Angle

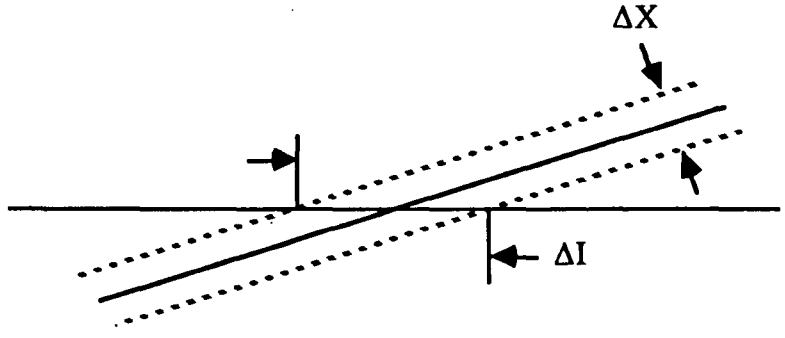

Shallow Intersection Angle

Figure 2.2-5. Accuracy.

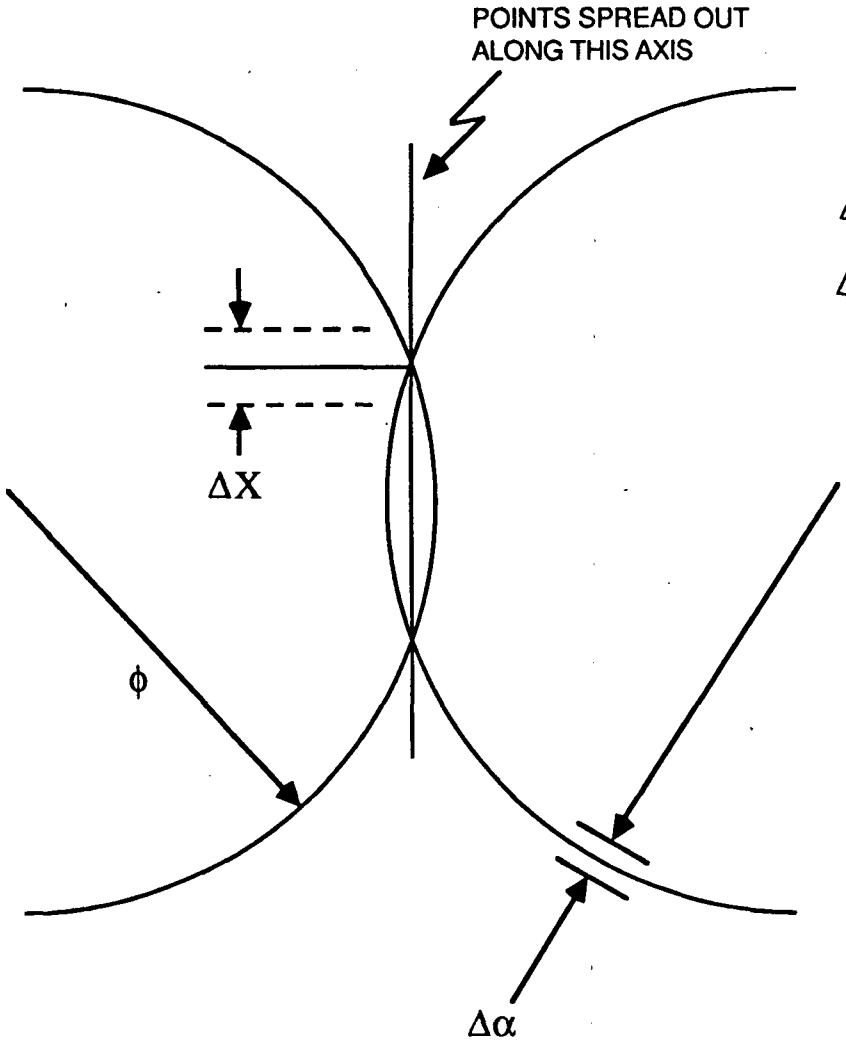

Δα = ERROR IN CONE ANGLE MEASUREMENT

ΔX = RESULTING ERROR IN INTERSECTION POINT

ΔX STRONG FUNCTION OF Δα FOR SHALLOW CONE INTERSECTION ANGLES

Figure 2.6-6. Intersection Point Estimate Error.

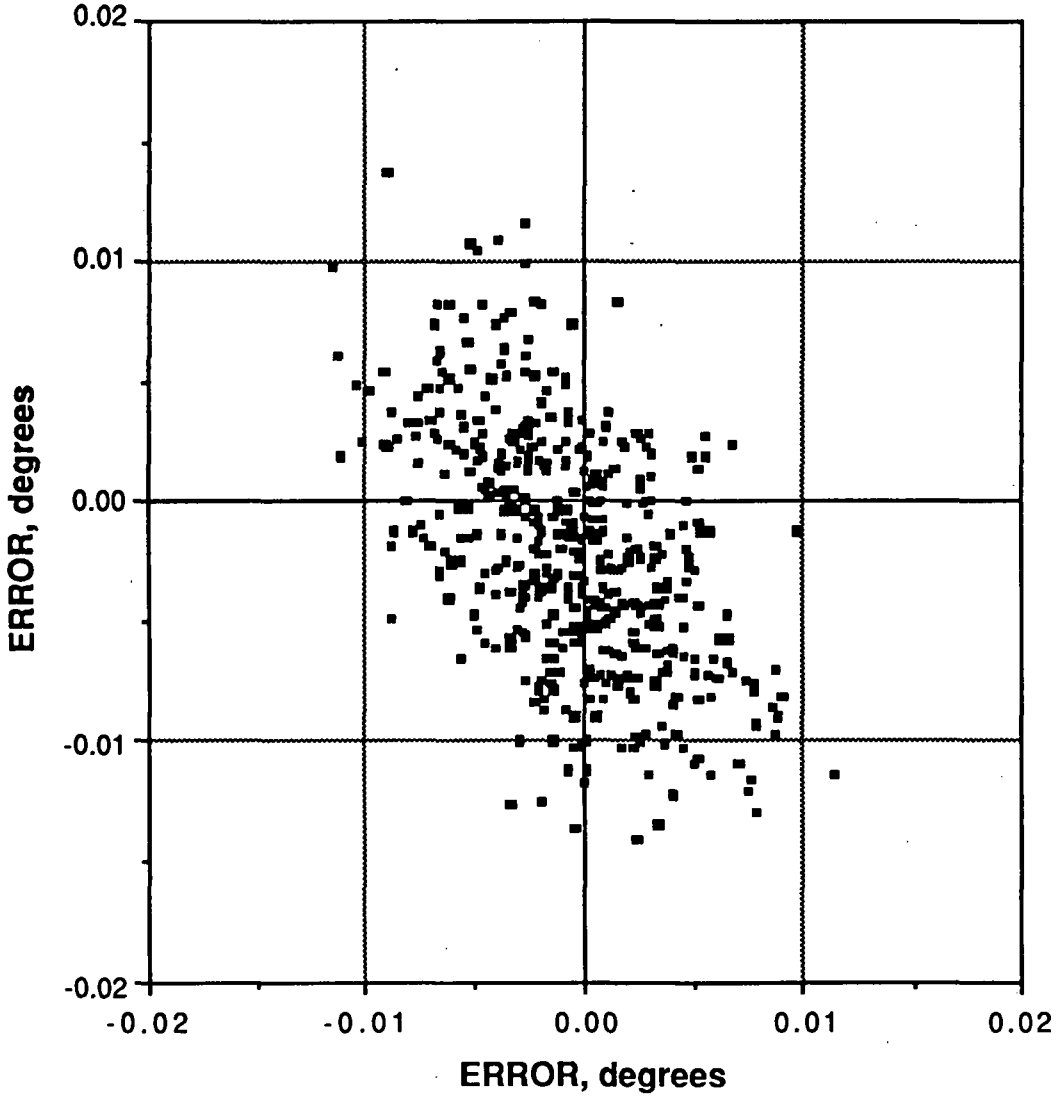

SINGLE ORBITAL POSITION , T = 1080 sec

BASELINE = 5 m

LOOP BW = 30 Hz

NOMINAL C/No = 43 dB

NUMBER OF TRIALS = 500

MEAN ERROR = 5.87×10^{-3} degrees

STANDARD DEVIATION (1σ) = 3.13×10^{-3}

ERROR DUE TO SATELLITE GEOMETRY MODERATE

ERROR DUE TO MULTIPATH MINIMAL

Figure 2.6-7. Scatter Plot of Pointing Error T = 1080 sec, Multipath.

which results in the skewing of the data points. A slight error due to multipath can also be seen evidenced by the slight offset from 0,0. Now lets examine the results with multipath for T = 2880 sec. The results for this time for noise only were shown in Figure 2.6-3. The results for this time with multipath are shown in Figure 2.6-8. Note that the basic pattern indicating a low error due to satellite geometry is maintained. But that the entire collection of points has been shifted from 0,0. Figure 2.6-9 shows the results with multipath for T = 1800 seconds. Again, compare it against the results from the same item for noise only in Figure 2.6-4. The shape of the pattern due to satellite geometry is maintained while the entire plot is shifted from 0,0 due to the bias error term introduced as a result of multipath.

2.6.5 Error Due to Multipath

As described briefly in Section 2.2.4 and in detail in 2.6, multipath introduces a phase error term, ϕ_{mp}, into the overall phase error term generated in the receiver model. The equation for ϕ_{mp} is given by

$$\phi_{mp} = \beta \sin (2\pi \sin (\gamma t))$$

where β is the ratio of the reflected (multipath) signal to the incident (primary) signal and γ is the rotation rate of the attitude vector due to orbital motion equal to 2π radians per orbital period. Hence, the value of ϕ_{mp} depends upon both the position in the orbit ($\sin (\gamma t)$) and the strength of the multipath signal (β). It results in a bias error term because for any point in the orbit, it is a constant where as the phase error term due to receiver thermal noise follows a Gaussian distribution, i.e., will have both positive and negative values of varying magnitude.

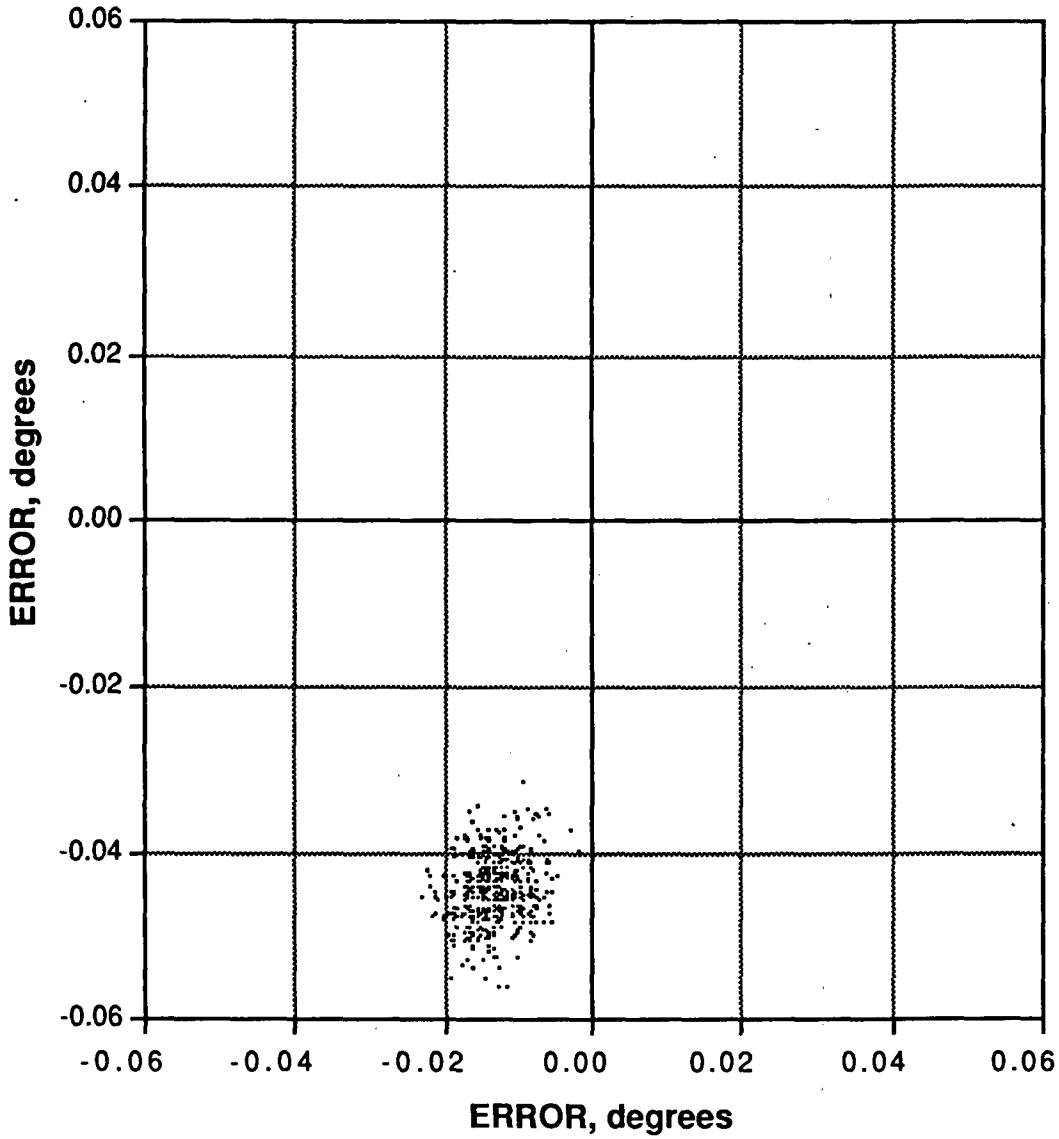

SINGLE ORBITAL POSITION , T = 2880 sec

BASELINE = 5 m

LOOP BW = 30 Hz

NOMINAL C/No = 43 dB

NUMBER OF TRIALS = 500

MEAN ERROR = 4.64×10^{-2} degrees

STANDARD DEVIATION (1σ) = 4.01×10^{-3}

ERROR DUE TO SATELLITE GEOMETRY LOW

ERROR DUE TO MULTIPATH MODERATE

Figure 2.6-8. Scatter Plot of Pointing Error – Multipath.

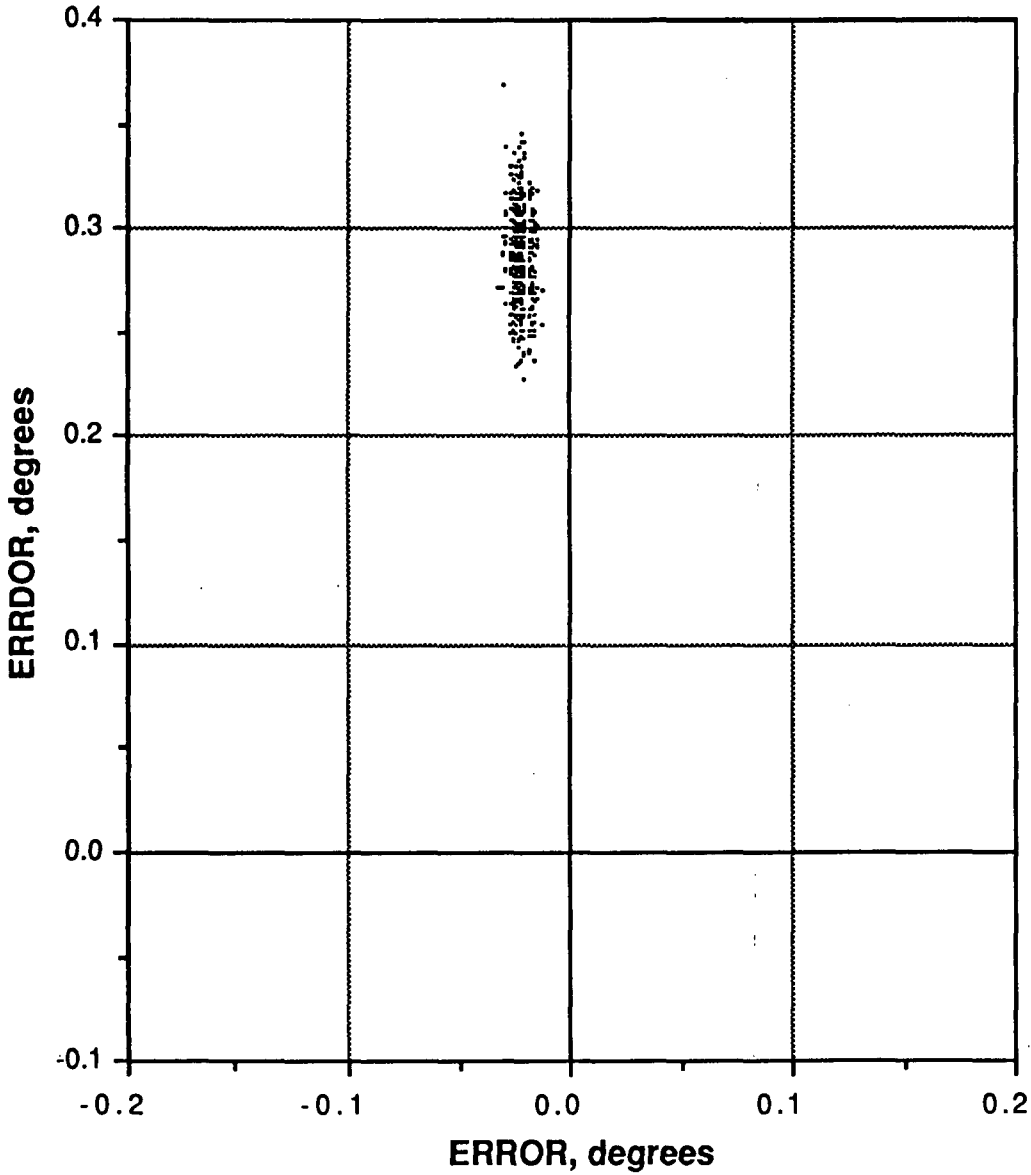

SINGLE ORBITAL POSITION , T=1800 sec

BASELINE = 5 m

LOOP BW = 30 Hz

NOMINAL C/No = 43 dB

NUMBER OF TRIALS = 500

MEAN ERROR = 2.87×10^{-1} degrees

STANDARD DEVIATION (1σ) = 2.17×10^{-2}

ERROR DUE TO SATELLITE GEOMETRY HIGH

ERROR DUE TO MULTIPATH HIGH

Figure 2.6-9. Scatter Plot of Pointing Error – Multipath.

2.6.6 Mean Error vs. Antenna Baseline

Figure 2.6-10 gives the mean pointing error (averaged over an entire orbit) as a function of antenna baseline for the multipath and noise only cases. As expected, the pointing error is inversely proportional to the baseline length.

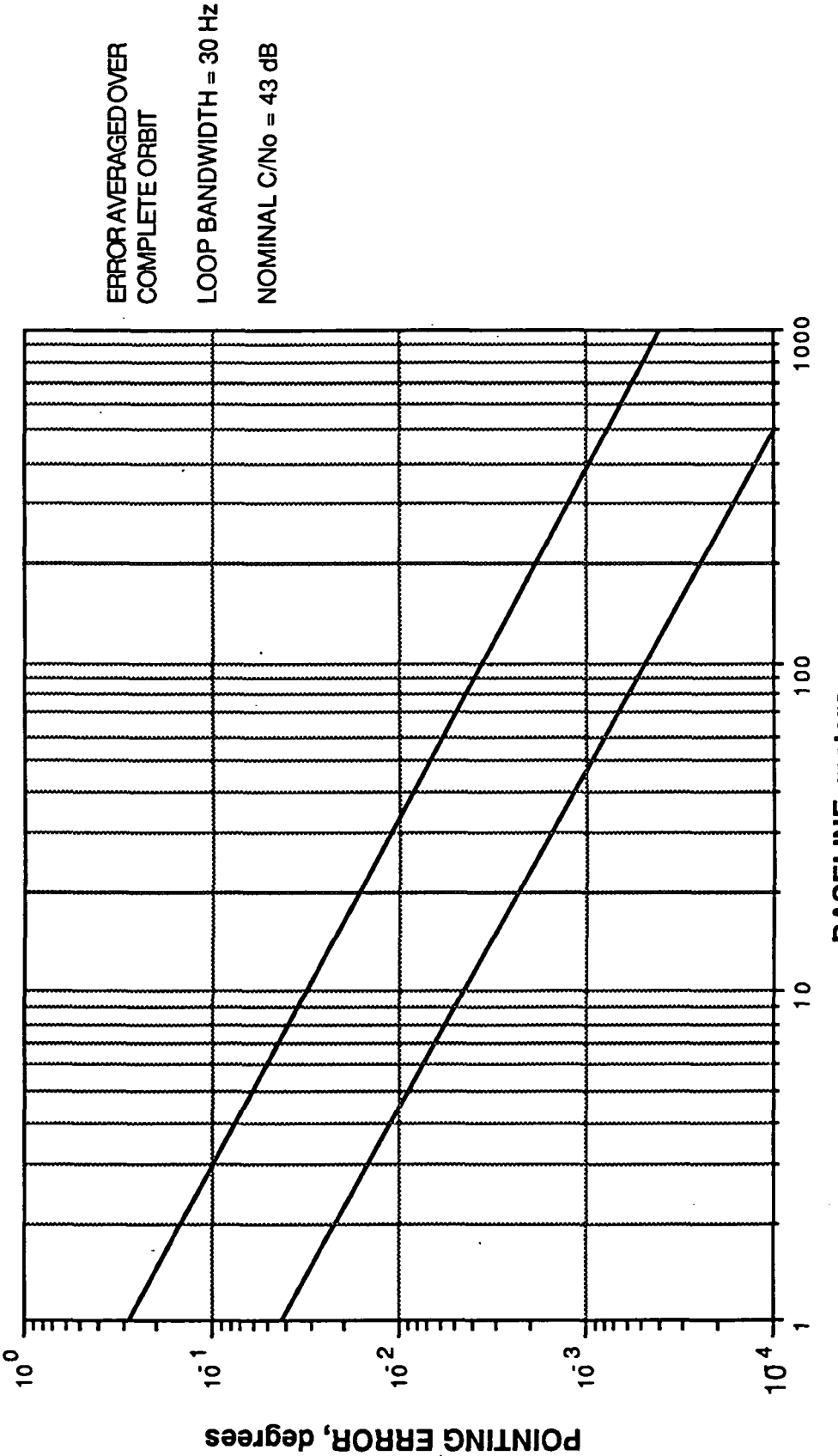

Figure 2.6-10. Mean Error vs. Antenna Baseline – Multipath.

2.7 Comparison with Alternate Approaches (Attitude)

The alternative method of attitude determination is to use a star tracker such as represented by Ref. [2.7-1]. Such instruments have been proven for space applications and can achieve accuracies that are 2 orders of magnitude better than those projected for schemes using the GPS signals. Cost of this star tracker is also competitive with projected costs for multiple space borne GPS receivers to observe attitude.

Table 2.7-1 summarizes the methods available for attitude control and tracking. Table 2.7-2 provides a comparison between these methods.

2.8 References

[2.7-1] Specification Sheet for Large Field of View Star Tracker – CT-411 Ball Aerospace Systems Division, Boulder, Colorado.

GPS → PRECISE RELATIVE PHASE – MULTIPLE ANTENNAS

a) RELATIVE PHASE BETWEEN ANTENNAS

b) RELATIVE BASELINE BETWEEN ANTENNAS

- MULTIPATH / PHASE CENTER STABILITY
- REFERENCE PHASE DELAY
- SATELLITE CLOCK VARIATIONS
- PHASE

STARTRACKERS → STAR FIELD TRACKING

a) ABSOLUTE ATTITUDE MEASUREMENT

b) PROVEN TECHNOLOGY

IFOG → INERTIAL ATTITUDE SENSING – NEEDS ABSOLUTE REFERENCE

a) RELATIVE ATTITUDE SENSING

b) MATURING TECHNOLOGY

Table 2.7-1. Attitude Control and Tracking Methods.

	PERFORMANCE	COST	RELIABILITY	COMPLEXITY
GPS	1 mrad	$3M	MED (3 – 5 YR LIFE)	MED 6 CHANNEL 1500 PARTS
STAR TRACKERS	.05 mrad	$1M	MED	MED
INTER-FEROMETRIC FIBEROPTIC GRYO	0.34 $\frac{\text{mrad}}{\text{hr}}$	\$0.35 $\frac{\text{M}}{\text{axis}}$	HIGH	LOW

Table 2.7-2. Technology for Spaceborn Attitude Control and Tracking.

3.0 LARGE SPACE STRUCTURE CONTROL

3.1 Problem Statement

Structure control involves the characterization and control of the possible modes of oscillation associated with the configuration. Position sensors must measure the vibrational displacements and periods, and this information is then analyzed to determine means to counteract the resultant oscillations. Corrective control mechanisms must then be activated which will counterbalance the vibrational forces.

The use of GPS for structure control can be implemented in a number of ways. The most obvious technique uses many GPS receivers located throughout the structure to make simultaneous absolute position measurements, which when correlated, characterizes the vibrational modes. GPS differential position measurements using interferometry, as discussed earlier for attitude control, is another possibility. This GPS differential carrier phase sensor can make continuous simultaneous measurements, an important feature for sensing relative vibrational displacements.

The GPS absolute position measurements are straightforward but slow due to processing time and costly due to the large number of receivers required. The GPS differential position measurements may not have enough accuracy to be useful. The GPS differential carrier measurements, however, show more promise for this particular application and will, therefore, be described in more detail in this section.

3.2 Literature Survey

As a part of this task, Axiomatix performed a literature survey. The references examined are listed in Table 3.2-1. The summary of this survey is given in Table 3.2-2.

Table 3.2-1. Large Space Structure Control Review of Literature.

AUTHOR(S) OR ORIGINATOR	TITLE
1)* G. S. NURRE, R. S. RYAN H. N. SCOFIELD, J. L. SIMS	DYNAMICS OF LARGE SPACE STRUCTURES
2)* R. H. CANNON, JR., D. E. RONSENTHAL	EXPERIMENTAL CONTROL OF FLEXIBLE STRUCTURES WITH NONCOLOCATED SENSORS AND ACTUATORS
3)* D. B. SCHAECHTER, D. B. ELDRED	EXPERIMENTAL DEMONSTRATION OF THE CONTROL OF FLEXIBLE STRUCTURES
4)* H. J. BUCHANAN, R. W. SCHOCK H. B. WAITES	AN ON-ORBIT EXPERIMENT FOR DYNAMICS AND CONTROL OF LARGE STRUCTURES
5) HUGHES	POTENTIAL APPLICATIONS OF THE GLOBAL POSITIONING SYSTEM (GPS) AS AN INPUT SENSOR FOR SPACECRAFT SYSTEM, FINAL REPORT, SECTION 5

*JOURNAL OF GUIDANCE, CONTROL, AND DYNAMICS, VOLUME 7, NO. 5, SEPTEMBER 1984.

Table 3.2-2. Literature Review Summary

TECHNICAL LITERATURE (REFERENCE 1, 2, 3, AND 4)

THE IDEAS PRESENTED ARE DIRECTED MAINLY TOWARDS A CLOSED LOOP CONTROL OF VARIOUS MECHANICAL STRUCTURES. ALTHOUGH PROVIDING GOOD GENERAL BACKGROUND, THE MATERIAL REVIEWED DOES NOT ADDRESS SPECIFICALLY THE PROBLEM OF GPS-BASED SENSOR EVALUATION.

HUGHES REPORT

STRUCTURAL VIBRATION SENSING IS DISCUSSED IN SECTION 5. THE STRUCTURE MODEL CONSIDERED IS OF A VIBRATING BOOM (ASTROMAST). IDEALIZED INTERFEROMETER DATA HAS BEEN SIMULATED IN ONE DIRECTION. THE EFFECT OF THE RF LINK/RECEIVER LOSSES MODEL WAS NOT INCLUDED IN THE SIMULATION.

3.3 GPS Differential Carrier Phase Measurement

The GPS differential carrier phase measurement scheme can be implemented in a number of ways, but the most straightforward method is shown in Figure 3.3-1, where the main features are that the PN code (C/A or P) is stripped from the carrier and the Costas loops are used to measure the carrier phase difference between relative positions. The differential carrier phase change (over time), corrected for the angular relationship to the GPS satellite, is a direct measure of the induced vibrational displacement. Specifically, this technique operates as follows:

- In absence of vibrational / displacement, both the "moving" and the "fixed"Costas receivers track the phase of the incoming GPS signal.
- When vibration and / or displacement takes place, the "moving" Costas receiver tracks the phase of the received carrier. Thus, a phase difference is generated between the VCO phases of the two Costas receivers.
- Comparison of phases of the two VCO's generates a relative phase difference signal which is proportional to the displacement of the structure.

An elaboration on the two-point differential measurement is shown in figure 3.3-2. With this scheme displacement of several structure points can be measured with respect to some long-term average phase. Specifically, this method operates as follows:

- Each receiver tracks its own phase by means of a Costas loop which includes a VCO.
- Phases of VCO's are compared and averaged over a period much longer than the vibration period.
- Thus, an average "reference" phase is established.
- Comparison of phases of different VCO's against the "reference" phase yields signals proportional to the displacement of each receiver.

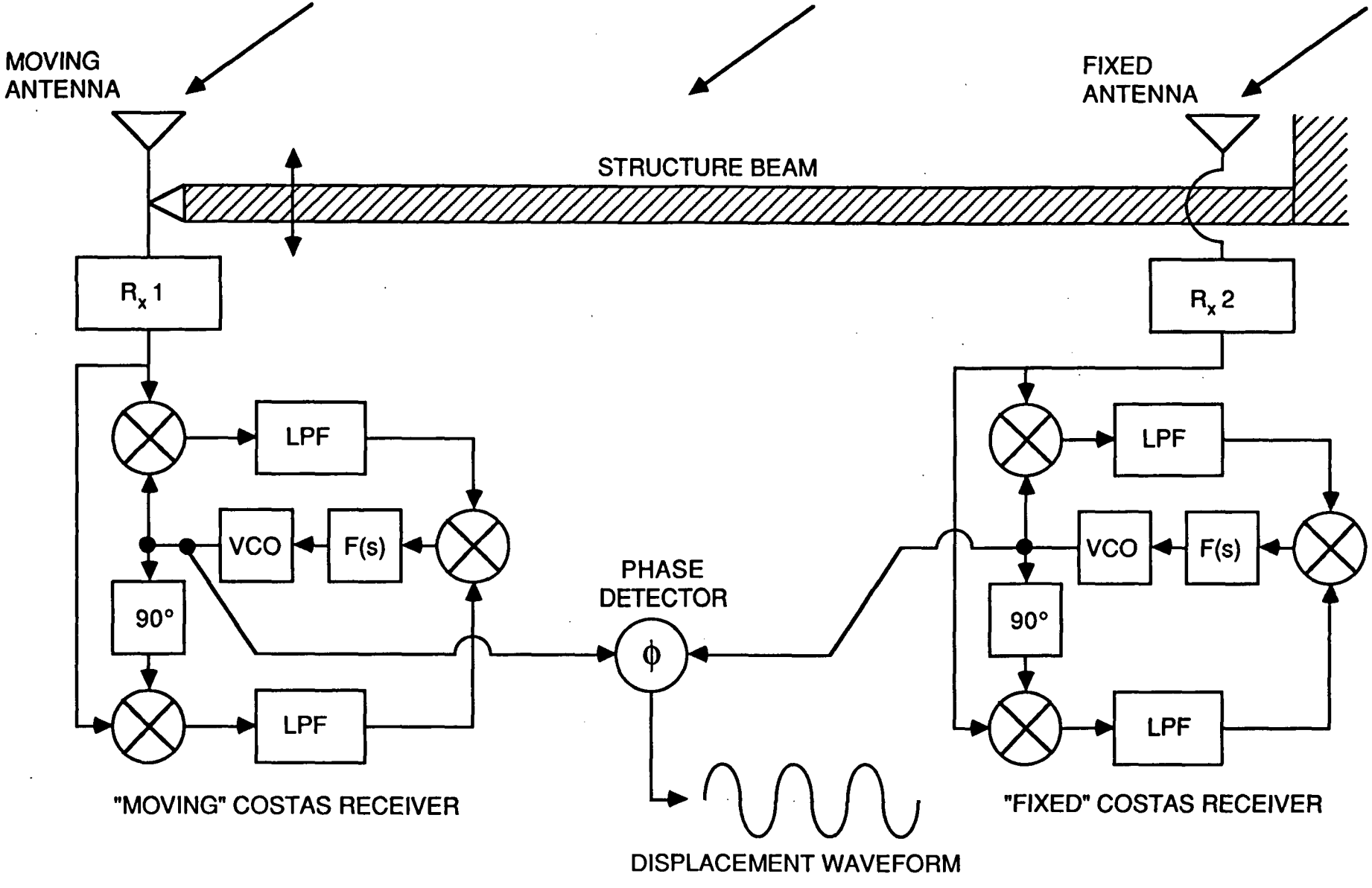

Figure 3.3-1. Structure Displacement Based on Relative Phase Difference.

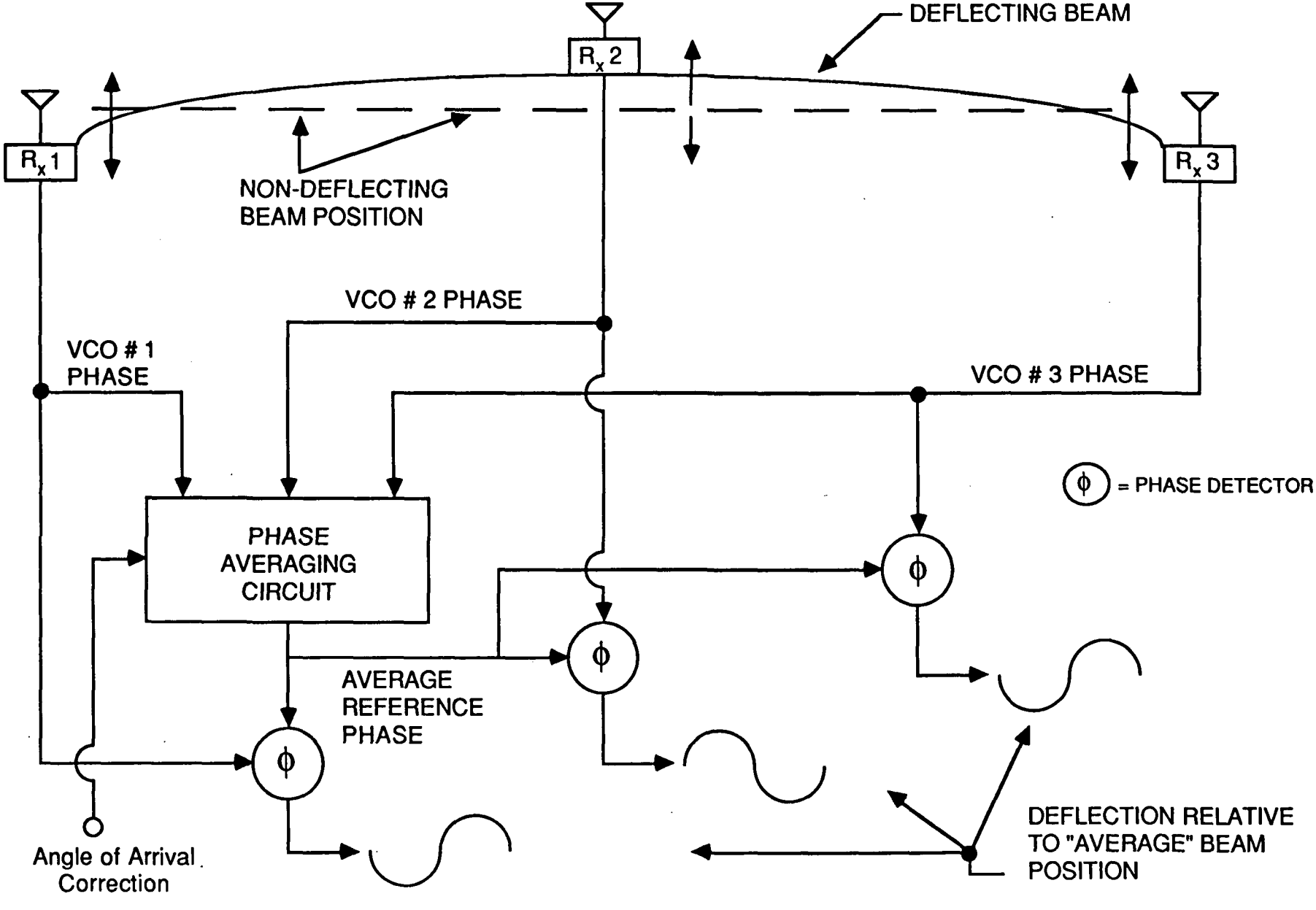

Figure 3.3-2. Phase Measurement W/R to Average Phase.

Because the relative phase of signals applied to the phase averaging circuit may change with time as the entire structure moves in its orbit with respect the GPS satellites an angle of arrival correction should be applied to remove the "bias" which is generated. The correction can be computed by determining the attitude of the structure or the beam with respect to a selected set of satellites in view.

The effectives of this scheme depends on good differentiation between the "average" phase and the relatively "fast" changes in the relative displacements. For example, for a structure in a near earth orbit, the average phase "bias" may change at the rate of one cycle in approximately 90 minutes. In comparison, the relative phases may change at the structure vibration frequencies which may be in the range of one cycle per ten seconds to one cycle per second.

3.4 Sensor Model

Figure 3.4-1 shows a functional diagram of the large space structure control sensor model developed by Axiomatix for the purpose of simulating relative displacement measurement.

As shown in this figure, the measurement error is the difference between (1) the true displacement of the space vehicle's (in this case a Space Station) points with respect to a GPS constellation and (2) a noisy estimate of the displacement. The true R and $\dot{R}$ relative displacements are computed and from these displacements, $\ddot{R}$ is generated. The true values of R, $\dot{R}$, and $\ddot{R}$ are then applied to a receiver model described in Section 2.3 and various aberrations associated with the receiver model are added. The resulting ϕ_B (bias) and σ_ϕ (random component) are then applied to a pseudorandom carrier phase generator. This generator provides a random perturbation to a true phase. The randomness is determined by a Monte-Carlo method under control of the output of the receiver model. The random perturbation is then summed with the true displacement resulting in a simulated "noisy" displacement. The latter is then differenced with the true displacement. The error

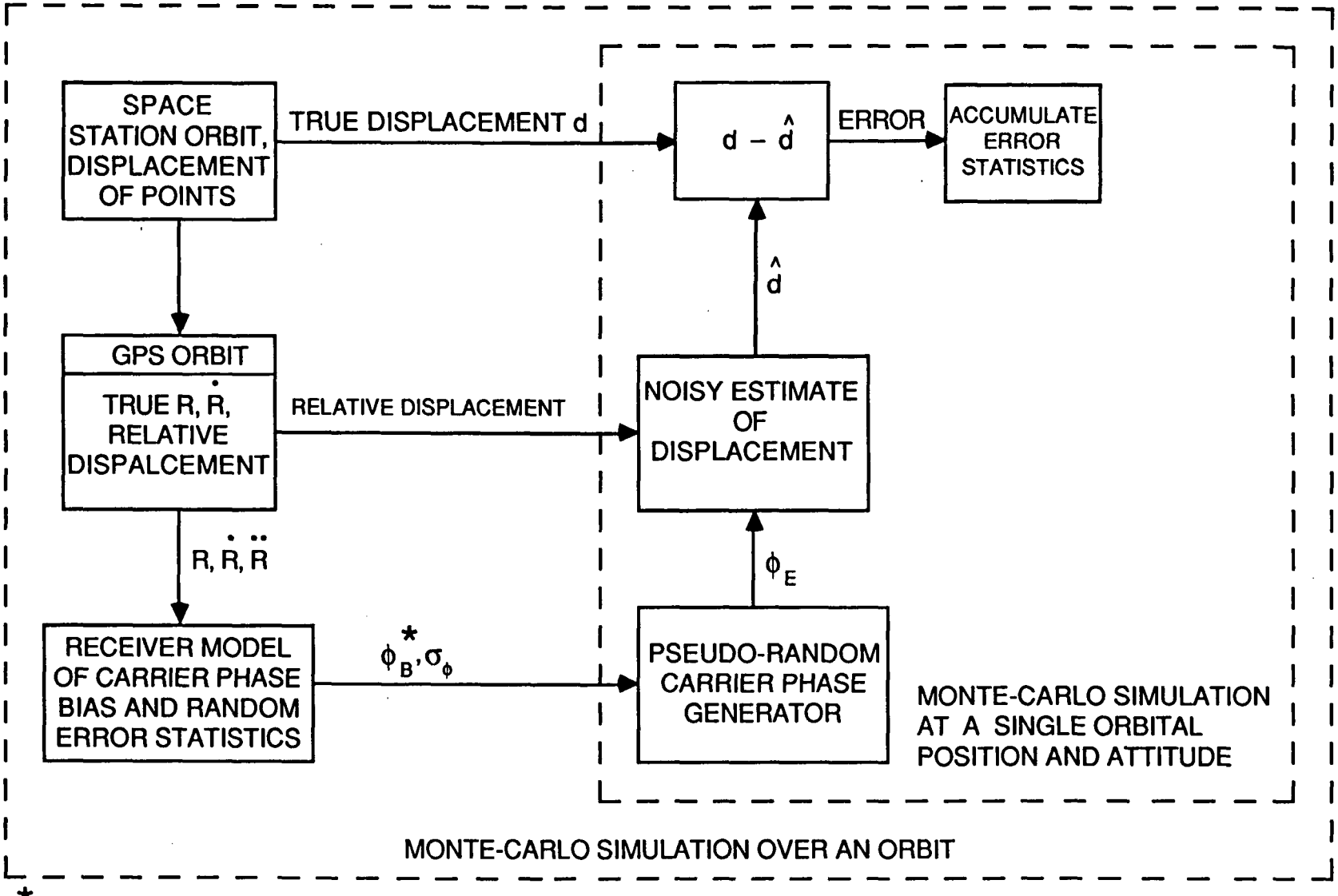

*Correctable bias error

Figure 3.4-1. Large Space Structure Control Sensor Model.

generated in this manner can be used for determining the statistical characteristics of the result error.

3.5 Sensor Dilution of Precision (SDOP) Considerations

In sensing the relative displacement of various points on a given structure, the best accuracy is obtained when the displacements are along a vector extending from the sensors to a given reference satellite. If the vector is deviating from this "optimum" position, then the measured displacement becomes smaller in magnitude and, therefore, noisier. To provide some quantitative definition of this phenomenon, we introduced a concept of SDOP which characterizes sensor dilution of precision. In general

$$\text{SDOP} \propto \frac{1}{\cos\theta}$$

where θ is the angle of deviation from the optimum direction.

Figure 3.5-1 illustrates this concept for a one-dimensional displacement measurement. Similarly, Figure 3.5-2 demonstrates this concept for a two dimensional displacement. The point being made here is that when the displacement measurement are made using a set of GPS satellites, only the best satellites for the displacement measurement along a given axis should be selected. It is important to note that this selection may not necessarily be compatible with the best GDOP selected for the conventional position measurement.

Figure 3.5-3 illustrates how best SDOP may be selected for space structures of different orientations in space.

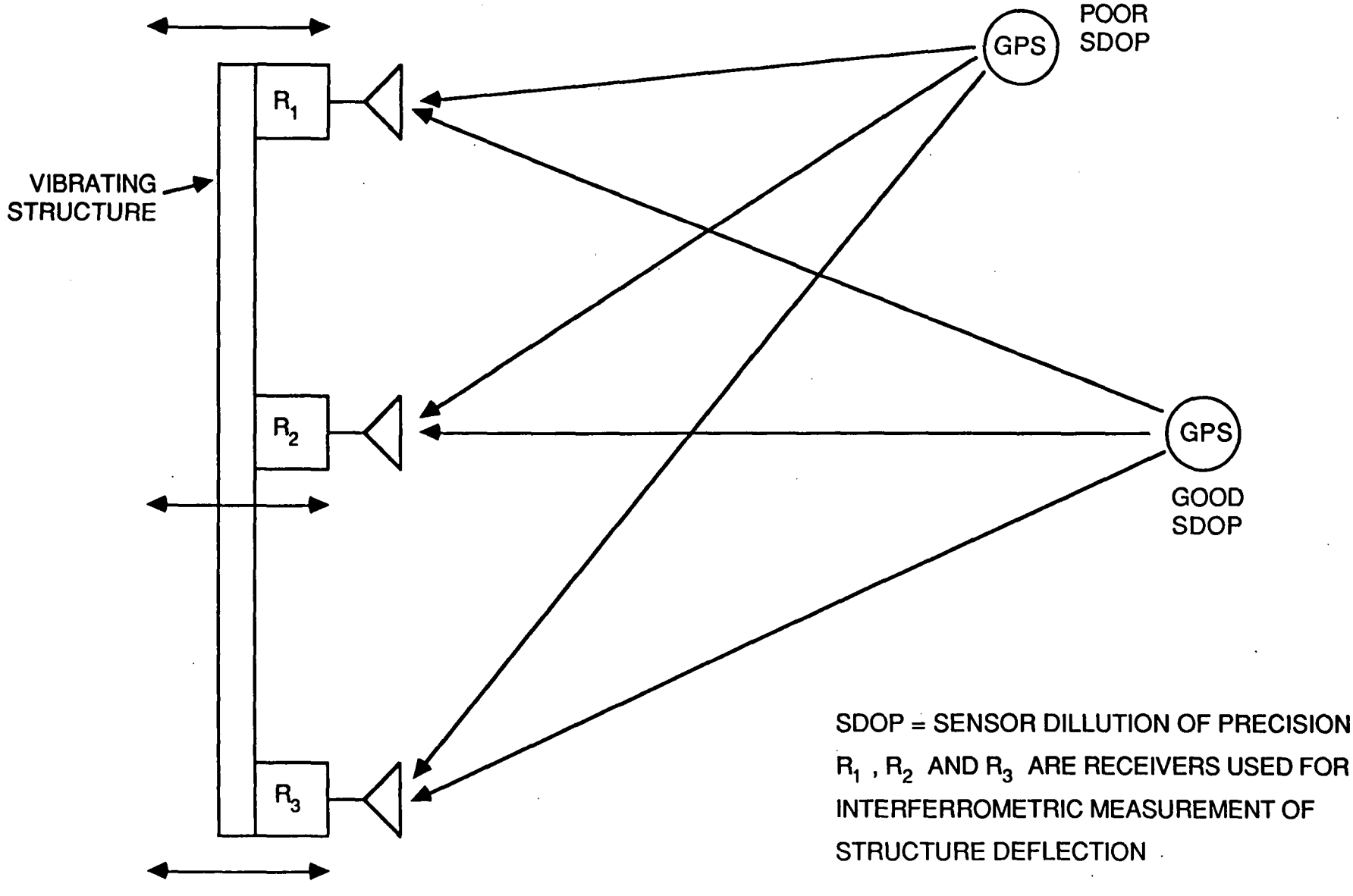

Figure 3.5-1. Good vs. Poor SDOP for One-Dimensional Displacement.

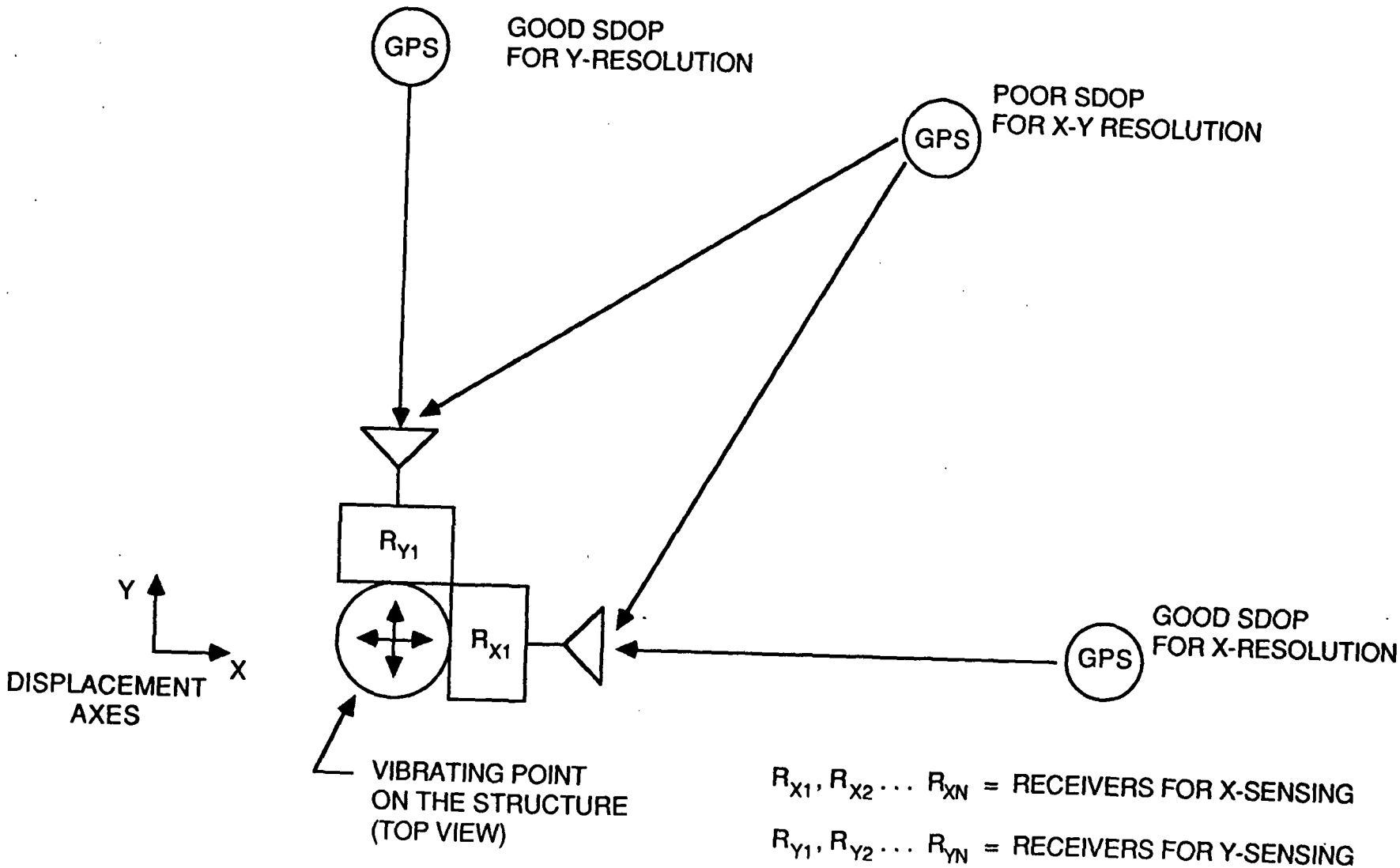

Figure 3.5-2. Good vs. Poor SDOP for Two-Dimensional (x-y) Displacement.

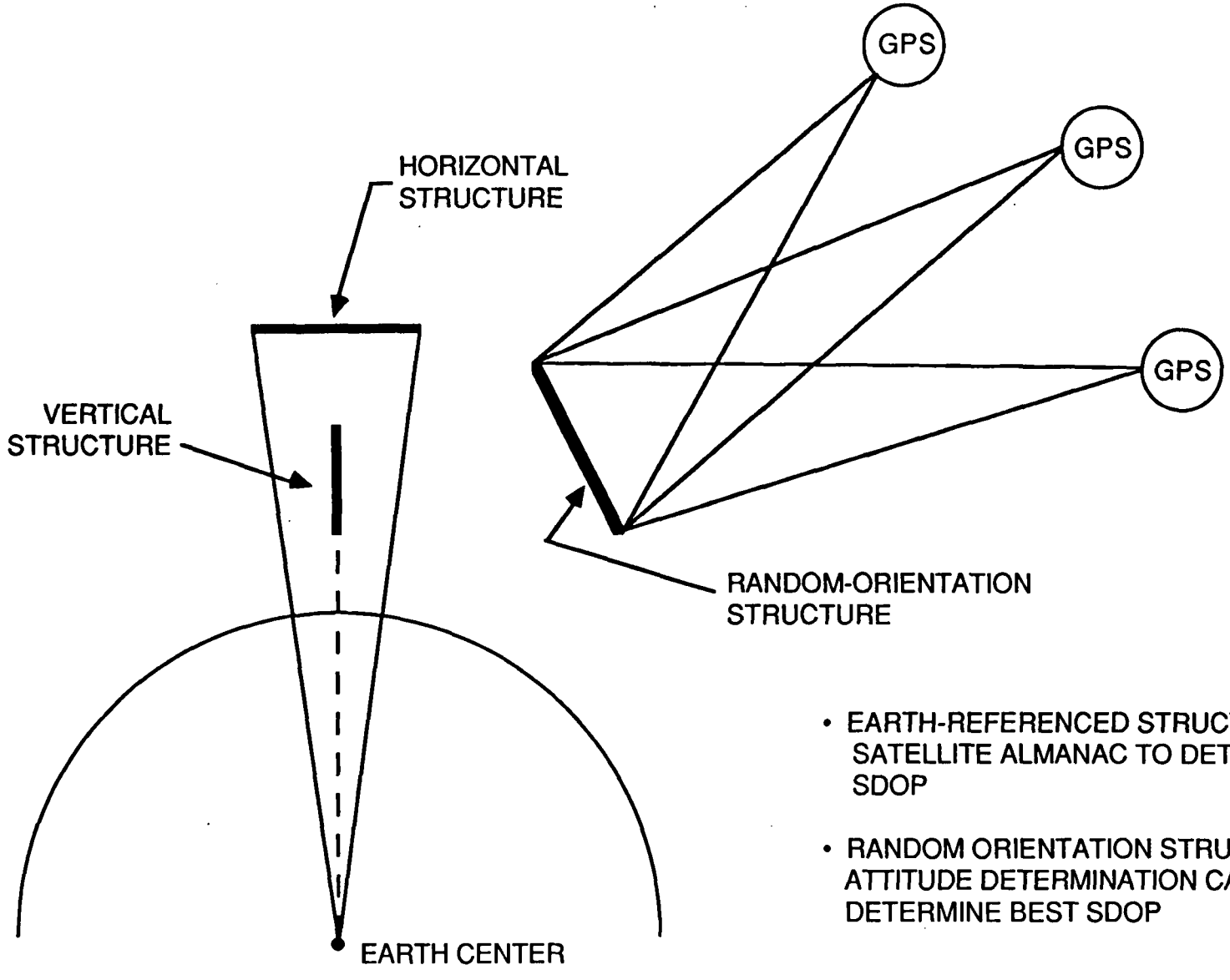

- EARTH-REFERENCED STRUCTURES MAY USE SATELLITE ALMANAC TO DETERMINE BEST SDOP
- RANDOM ORIENTATION STRUCTURES MAY NEED ATTITUDE DETERMINATION CAPABILITY TO DETERMINE BEST SDOP

Figure 3.5-3. Earth-Referenced vs. Random Orientation Structure Attitudes.

3.6 Simulation Results

Figure 3.6-1 shows a result of a simulation program used for structure vibration sensing. Although the frequency and amplitude of the vibration indicated were selected arbitrarily, other parameters represented a relatively close "true life" situation. The purpose of this exercise run was to test the validity of our displacement sensing model described in Section 3.4.

Figure 3.6-2 shows the true displacement for this test run and the associated measurement error introduced by random (thermal) noise and multipath. The statistics associated with error are listed in this figure.

3.7 Comparison with Alternate Approaches (Large Space Structure Control)

An alternate technology for directly monitoring relative structural motion is the laser / retroreflector technology such as represented by Ref 3.7-1. This instrument uses a fully solid state sensor for monitoring the relative dynamic motion of several points in its field of view. Developed for the Solar Array Experiment, the Retroreflector Field Tracker is designed to characterize the motion of large flexible space structures in low orbit. Twenty-three (23) reflective targets are tracked with a Charge Injector Device optical tracker. Accuracy of tracking is limited by the resolution of the sensor with a 19 degree field of view. The accuracy is on the order of a few millimeters for all of the targets.

Table 3.7-1 lists the techniques available for the control of large space structures. Table 3.7-3 provides an evaluation of these alternatives.

3.8 References

[3.7-1] Specification Sheet for Retroreflector Field Tracker, Ball Aerospace Systems Division, Boulder, Colorado.

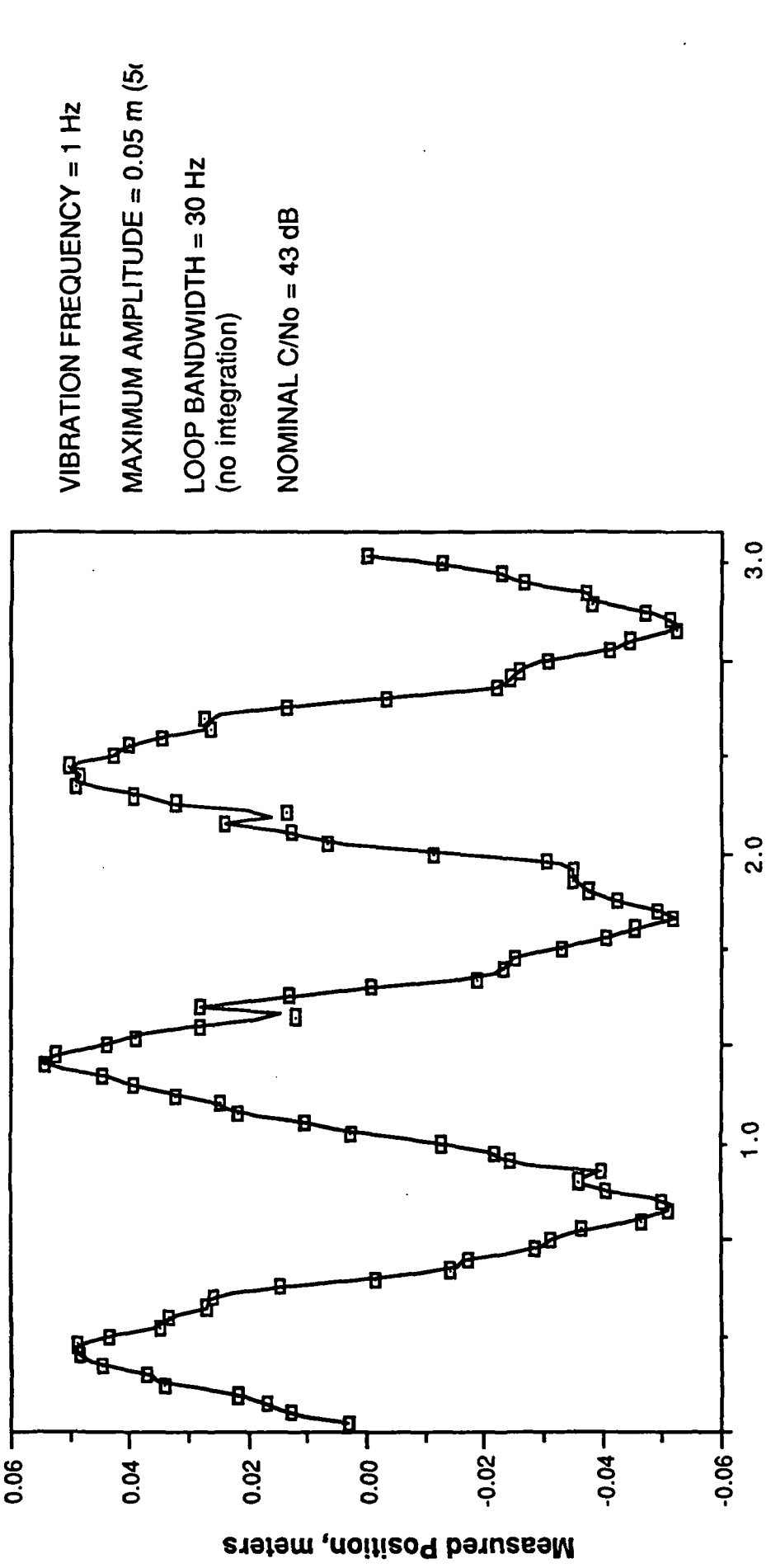

Figure 3.6-1. Structure Vibration Sensing (with Multipath).

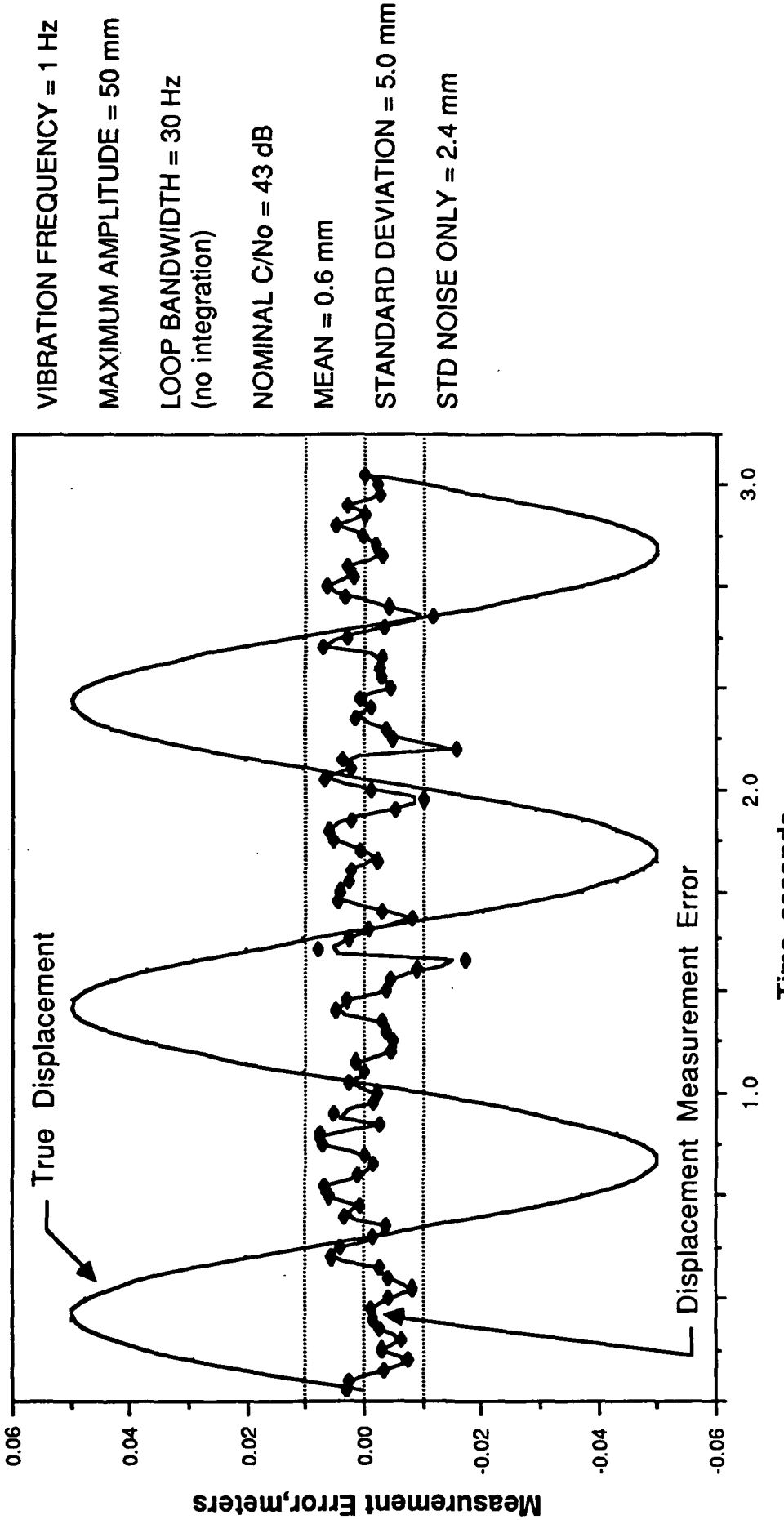

Figure 3.6-2. Structure Vibration Error.

GPS	→	PRECISE RELATIVE PHASE – MULTIPLE ANTENNAS (SIMILAR TO ATTITUDE CONTROL AND TRACKING) MINIMUM BANDWIDTH DEPENDENT ON STRUCTURAL MODE FREQUENCIES
RETRO-REFLECTOR FIELD TRACKER	→	OPTICAL OBSERVATIONS OF RELATIVE FLEXURE
INERTIAL SENSORS	→	ACCELEROMETERS/GRYO

Table 3.7-1. Large Space Structure Control Alternatives.

	PERFORMANCE	COST	RELIABILITY	COMPLEXITY
GPS	HIGH .001 m RELATIVE	HIGH @ $1M	MED	MED
RETRO-REFLECTOR FIELD TRACKER	HIGH	MED	MED	HIGH
INERTIAL RATE SENSORS (IFOG)	HIGH	MED	HIGH	LOW

Table 3.7-2. Technology for Spaceborne Sructure Flexure Measurement.

4.0 RELATIVE GPS NAVIGATION FOR SPACE TRAFFIC CONTROL

The Global Positioning System is perhaps the most accurate and efficient navigation standard available for low earth orbits. It provides four dimensional navigation solutions (position/time and velocity/frequency) directly in earth-centered, earth-fixed coordinates at relatively high rates, precision, and accuracy. The technology to build these receivers for terrestrial applications is becoming mature; programs to carry receivers into space have been conducted successfully (GPSPAC, 1981) or are currently in progress (TOPEX, 1992). As such, it is the leading candidate for tracking and traffic control about the Space Station.

There are three different phases of space traffic control about the Space Station. The first phase, with the weakest requirements, is non-rendezvous orbit and orbits outside 40 km. Autonomous GPS navigation with virtually any GPS receiver configuration is sufficient for space vehicles to maintain the proper clearance for collision avoidance purposes or pre-rendezvous at 40 km from the Space Station. The accuracy of GPS in standalone mode depends on the receiver, but ranges from roughly 10 meters and .02 meter/sec for P-code receivers to 100 meters and .15 meter/sec for the lower accuracy C/A-code. Both receivers will suffice for non-rendezvous orbits.

The second phase of space traffic control, which constituted the focus of this study, is rendezvous control, from roughly 40 km to a hundred meters. The practical accuracy requirement in this phase is to deliver the vehicle to the next phase, berthing or docking, with sufficient accuracy to provide a considerable safety margin in the control of the approaching vehicle (henceforth denoted simply the vehicle, as opposed to the Space Station). Standalone C/A-code accuracy of 100 meters is unacceptable, and even the P-code accuracy of 10 meters or better does not meet the requirements as the vehicle approaches the final phase of rendezvous. Relative GPS, the differencing of the two GPS solutions from the vehicle and the Space Station respectively, is the method proposed here to meet the accuracy requirements.

The third phase of flight brings the vehicle from 100 meters separation to the actual berthing or docking event. Accuracy requirements in this phase are much higher, potentially on the sub-meter level, and the incoming vehicle will be controlled manually. Reaction times are relatively short and the navigation data must be highly reliable. Relative GPS or phase interferometry is a candidate for use in this phase, but as will be explained later, presents a high risk at this stage of development in the Space Station program.

4.1 Relative GPS in Rendezvous Control

The advantage of relative GPS is that the many GPS navigation errors are locally common biases. Specifically, such errors as ionospheric delay error and position/time error of the GPS SVs (Space Vehicles, the orbiting navigation signal transmitters) are perfectly correlated at near distances and decorrelate slowly. Other errors, such as receiver noise and multipath, are unique to the particular receiver. Over the 40 km distances projected for rendezvous control, relative GPS reduces the effect of the locally common bias errors to virtually nil, and, if multipath can be controlled, GPS navigation is extremely accurate.

Improper implementation of the relative GPS can reduce the accuracy improvement considerably. If the satellites used in the two GPS navigators are not the same, the locally common bias errors are not fully canceled. If relative GPS is implemented by subtracting positions and velocities of two independent navigation filters, there can also be problems associated with the response to incorrect measurement models associated with ionospheric effects and satellite switches. These are discussed in more detail in the sections below, as well as distinctions between authorized (P-code) and unauthorized (C/A-code) receivers.

The criterion for judgment in determining the solution to these problems should be twofold; accuracy and reliability is an obvious requirement, but also important is the complexity of the implementation. Many of the possible solutions impose restrictive requirements on the GPS receiver of the vehicle.

4.1.1 Relative GPS Implementations

There are many methods of implementing relative GPS. The design options encompass: whether the relative solution is computed aboard the vehicle or the Space Station; whether filtering occurs before or after differencing the GPS data; and, if the differencing occurs after filtering, i.e., there are two filters, to what extent are the two filters coordinated.

The first issue, where the relative navigation solution is computed, is commonly resolved in terrestrial applications by having a well-tuned high-rate navigation filter onboard the approaching vehicle, that applies GPS ranging "corrections" computed by a static reference station. The corrections have the net effect of causing the vehicle to navigate in the reference station position/time coordinates rather than the GPS coordinates; presumably, the two are fairly close. This system requires precise knowledge of the reference station location; in space, it would require precise knowledge for the orbital dynamics of the Space Station. A one-way datalink, from reference to vehicle, is required, with data rates on the order of one hundred or more bits per second, that broadcast the pseudoranges or computed corrections. If control of the approaching vehicle from the reference station is desired, a two-way data link must be established with the position and velocity computed by the vehicle sent back to the reference station. Data rates on the return link will be determined by the controllability requirements on the vehicle. Although this approach yields good results, the third approach (pseudodata method) is preferred, with basically similar results.

The above system is practical when the differencing is being done before the filtering, and there is a sophisticated navigation filter aboard the vehicle, perhaps with fast-loop inertial measurement units integrated with the GPS. If the differencing occurs after filtering, i.e., solutions from two standalone navigation filters are differenced, the relative navigation technically can be done either aboard the vehicle, then transmitted to the Space Station, or done aboard the Space Station. From the viewpoint of traffic control, the

relative navigation (i.e., differencing) will be done aboard the Space Station. A one-way data link is required in this case to send the position solution from the vehicle to the Space Station, along with satellite constellation information and time tags. A return link may be necessary if coordination of the satellite constellations is desired.

The third approach, denoted the pseudodata method, requires the vehicle to send raw GPS data to the Space Station, where it is processed together with the GPS data from the Space Station receiver to yield a relative navigation solution directly. This approach has many advantages, among them the fact that the dynamics in the relative navigation frame of the two vehicles is much lower than the dynamics of each in the earth-fixed frame that is the natural GPS coordinate system. It is consequently much less sensitive to errors in high-frequency gravity field modeling, allowing a lower-order gravity model than an equally accurate standalone navigation filter, one of the advantages over the first approach described above. Moreover, the dynamics of the vehicle relative to the Space Station can be modeled in a single filter rather than in two separate filters - possibly mismatched in ways that cause bias errors, as explained in Section 4.1.3. The data link can be one-way, transmitting raw GPS data from vehicle to Space Station at a roughly a couple hundred bits per second; a return link may be required to coordinate satellites if the vehicle receiver is not all-in-view, and for communication of the traffic control commands.

The remaining two issues are : whether differencing occurs before the navigation filter (implicit in the third method) or after the navigation filter (as in the second method); and, if the second method is chosen, how closely the filters are coordinated. The juxtaposition of differencing and filtering is a design issue, with potentially no appreciable effect on accuracy provided it is designed properly. The issue of coordination will be discussed in the following two sections, dealing with coordinated choice of GPS navigation satellite constellations and filter models respectively.

4.1.2 Coordinated Constellations

GPS navigation errors occur (and are eliminated) on a satellite-by-satellite basis, so relative GPS navigation only brings full benefit if the Space Station and vehicle are using the same satellite constellation. The possibility exists that the vehicle and the Space Station may be running autonomous navigation filters with differing constellations. One or more of the satellite measurements would be uncorrected, leading to a degradation of accuracy.

To gain a perspective on the possibility of different satellite constellations, a short explanation of the GPS navigation procedure is appropriate. GPS is essentially a ranging system; the GPS SV's are synchronized radiobeacons in known (computable) locations. To fully measure its own position/time coordinates, the receiver must multilaterate using a constellation of at least four satellites. The constellation is chosen from whichever satellites are visible and, depending on time and location, there may be as few as four and as many as ten. Many current receivers can track only four satellites at one time, usually the "best four" according to a criterion that minimizes the geometric dilution of precision. If all receivers use the same algorithm, the choice of satellites for nearby receivers will be the same, but in practice there is no standard for satellite selection. One receiver may switch constellations frequently, tracking the criterion very closely; a different receiver may be optimized to not make constellation switches unless significant accuracy improvement can be made. Some receivers compute the criterion rather infrequently, and constellation switches are usually unsynchronized, even between receivers from the same manufacturer. And, of course, some receivers will be computing overdetermined solutions using more than four satellites.

The solution to this Babel of constellations in terrestrial applications of differential GPS (similar to relative GPS, except one receiver is stationary and surveyed) is for the stationary receiver to track all satellites in view and compute "measurement corrections" for each satellite. The satellite measurements from the mobile receiver are then offset by the appropriate corrections. As long as the mobile receiver constellation is a subset of the

satellites in view at the reference receiver, all of the satellite measurements will be corrected.

In the space environment, similar performance can be achieved if the Space Station is capable of measuring all satellites in view. The Space Station would then be prepared to perform relative navigation on whichever satellites might be chosen by the receiver on the vehicle. This scheme is least restrictive from the viewpoint of designing the receiver in the vehicle. Because of the danger that satellites normally visible to the Space Station are blocked by solar panels or other structures on the Space Station itself, steps should be taken to avoid a mismatch of satellites due to poor visibility at the Space Station. To prevent uncoordinated satellite constellations, the navigation filters must have access to the constellation being tracked at the Space Station. Space Station must also broadcast its available constellation, from which the vehicle can choose a subset as its own constellation; or the vehicle receiver can have more than four channels, preferably all-in-view. The vehicle could then modify its choice of satellites to correspond with a subset of those available at the Space Station.

The advantages of all-in-view satellite receivers extends beyond relative GPS capability. Extra satellites can provide failure detection (at least five) and isolation (at least six) should a satellite signal or channel have errors. Many current receiver designs, commercial as well as military, have at least five channels for continuous reading of satellites; TOPEX, a satellite-borne GPS receiver, has six channels; and some commercial designs are coming with as many as ten or twelve channels, specifically for use as a differential GPS reference station. The cost of extra channels on space-qualified receivers may be a factor in determining the appropriate number.

4.1.3 Coordination of Filters

Beyond coordination of the satellite constellation being used, the filter structures themselves must be coordinated for maximum accuracy. Coordination can occur on many levels: the filters can be jointly tuned; the filters can be identical; measurement "corrections" can be generated on the Space Station and broadcast to the vehicle; or, at the highest level, GPS measurements from both vehicle and Space Station can be entered into a single relative navigation filter that will estimate the relative position and velocity directly without necessarily estimating the absolute position and velocity of the vehicles. Again, using the criterion of minimal impact on the receiver design of the vehicle, this last method (denoted "pseudodata" method) is the leading candidate.

To understand the impact of independently tuned filters, an examination of the low-orbit GPS navigation filter is required. The output of this filter will be very smooth if the GPS receiver measures carrier phase continuously or if the orbital/thrust model is accurate. The former is characteristic of most multi-channel GPS receiver configurations currently being produced, and has been examined in recent orbital studies under the name of non-destruct Doppler measurement. The latter item encompasses the fidelity of the gravity model and how accurately the thrust is measured by accelerometers; poor models will decrease the lag in the vehicle relative to the lag in the Space Station filters, increasing noise and at the same time responsiveness.

4.1.3.1 Continuous (Non-Destruct) Doppler Measurement

Receivers typically measure Doppler by sampling the output of a phase lock loop or Costas loop, differencing with the previous phase reading and dividing by intervening the time interval. This can be converted back to a delta-phase output by multiplying by the time interval and gives an extremely accurate estimate of delta position over the time period. If carrier lock is not lost, the deltarange relative to the satellite over long periods of time can be determined to the accuracy of the ephemeris information. Although absolute range is

impossible to determine from the carrier phase measurement, the very precise delta ranging from the carrier combined with the absolute ranging from code combine to average noise from the filter solution very quickly, inversely proportional to the square root of averaging time.

The system would be quite ideal except for two issues: there are two phenomena for which carrier behavior does not match code behavior. The first is multipath; from a navigation point of view, multipath has a lesser effect on carrier than code, so designing the filter to weight the carrier heavily (as a continuous Doppler model will do) actually improves performance. The net effect of continuous Doppler is to average through multipath error in the code, which without the damping effect of the carrier exhibits roughly sinusoidal behavior with periods of tens to upwards of a hundred seconds and amplitudes of a few meters.

The second phenomenon is ionospheric delay, and in this area reliance on continuous Doppler can degrade navigation. This has not been a serious problem in terrestrial navigation, but in space the effect is worse because the ionosphere in view changes so rapidly in ninety minute orbits. The major effect of ionosphere, due to total electron content (TEC) along the ray path, is a delay in the code and an apparent advance in the phase. Thus, as observed ionosphere becomes heavier (TEC grows) the ionospheric delay increases but the carrier phase "delay" decreases. This effect is observable in terrestrial locations, especially with static stations observing low elevation (rising or setting) satellites. If a filter blindly models deltarange as measured by the carrier to be equal to the deltarange as measured by the noisier code, the filtered pseudorange will be biased from the true value as demonstrated in Figure 4.1.3.1-1. The solution to this problem exists already in GPS. The ionospheric effect in this portion of the spectrum is inversely proportional to the square of the frequency, and the GPS navigation signal is broadcast synchronously on two frequencies. By comparing the relative delay between the two signals, the absolute delay can be calculated. The advance on the carrier is equal and

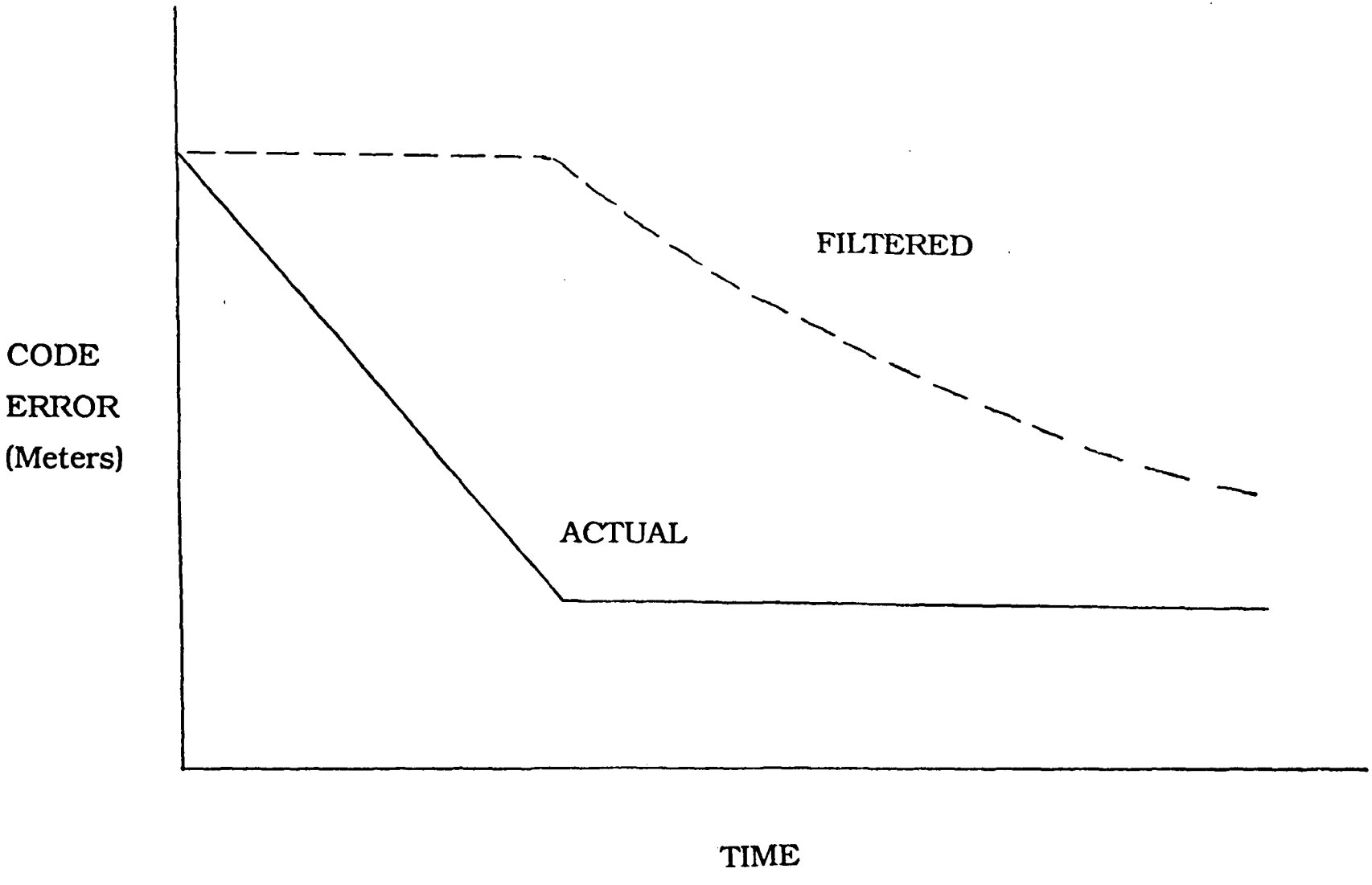

Figure 4.1.3.1-1. Filter Mismodeling of Ionospheric Effect on Code and Carrier.

opposite to the delay on the code, so a similar operation on the carrier removes the phase advance as well. In accordance with military policy, the code on the second frequency is not generally available to unauthorized receivers, the so-called C/A only receivers available to commercial users. The authorized receivers have two drawbacks: first, they are classified hardware, but it is assumed that precautions on the Space Station will allow their use; and secondly, they are in general more expensive because the P-code signal is ten times faster than the C/A-code signal. If the Space Station and all berthing space vehicles are not equipped with authorized receivers, the effect of ionosphere can be damaging under a certain set of circumstances. These include high ionospheric density, such as might be due to sunspot activity and low elevation satellites; single frequency receivers; and relative navigation accomplished by differencing positions from highly damped, independent navigation filters. This last is added because the position bias due to ionospheric effect will depend upon the filter damping constants and the time at which each satellite comes into the constellation at each receiver. The methods of resolving the problem of ionospheric bias are can be listed as one or more of the following:

- Use of a two frequency receiver. This can be either an authorized dual frequency (P) code and carrier P-code receiver, or unauthorized single (C/A) code with dual frequency carrier measurement. The latter are now commercially available as geodetic survey receivers and allow compensation of the carrier to match the effect of ionosphere on code.

- Change in the form of the navigation filters. This would entail either addition of an ionospheric rate bias state or increase the process noise in the filter. In highly damped form, the filter process noise matrix is rank four; expansion to rank eight will loosen up the filter considerably.

- Strictly coordinating the navigation filters. This is unduly restrictive on the navigation filter design of the vehicle.

- Real-time navigation by pseudodata. The effects on the raw code and carrier data are virtually identical for vehicle and Space Station; it disappears when the measurements are differenced, before they enter the relative navigation filter. This approach has the least impact on receiver design.

4.1.3.2 Independently Tuned Filters

The GPS navigation filter is subject to a number of error sources in standalone mode that do not significantly affect performance on the 5-10 meter level. Typical of these is a switch between satellite constellations. If the navigation filter is heavily damped, the satellite switch does not cause an abrupt change in position but rather a smooth transition over a long period of time. If the navigation filter is loosely tuned, the satellite switch may cause an abrupt change in position. The abrupt change adjusts very quickly to the new constellation, the damped response maintains a bias for a considerable period of time. The Space Station navigation filter, to maintain maximum accuracy, must match the bias.

To illustrate the difficulty in defining a Space Station relative GPS navigation system, consider two potential vehicles approaching the Space Station. The first has a lightweight, inexpensive, sequential C/A-code receiver without continuous Doppler; the second has a multichannel, C/A-code receiver with continuous Doppler. The response of the two navigation filters to satellite switches and ionospheric effects will be completely different. Compared to the latter, more sophisticated receiver, the former will be noisy but will respond very quickly to satellite switches and probably have no appreciable effect due to ionospheric mismodeling of the measurements. The latter will have a much less noisy position history, and will have a damped impulse response to the ranging biases when satellite constellations are switched; it will also have an ionospheric bias for newly risen satellites. The accuracy requirements for approach and berthing or docking will be the same for the two configurations, and clearly the Space Station must be able to handle both navigation configurations. If relative navigation is achieved by differencing the state

vectors, the Space Station navigation filter must match the vehicle's navigation filter in real-time so that the characteristic biases, especially those in the latter configuration, will difference out. The alternative is to perform the relative navigation on the measurement level through the pseudodata formulation. This alternative is much less restrictive in terms of design than trying to match the two independent filters.

4.1.4 Authorized Versus Unauthorized Receivers

In order to secure the system against unauthorized use of positioning for military purposes, the receivers have been divided into two classes: unauthorized receivers, able to track only C/A-code on a single frequency; and authorized receivers, able to track P-code on two frequencies. The unauthorized receivers are thus subject to ionospheric modeling errors, since ionospheric delay cannot be resolved as using a real-time empirical dual frequency algorithm. The Department of defense has found it necessary to deny accuracy to C/A-code users by threatening degradation of the signal to a relatively high level, by adding random, time varying biases of up to a hundred or more meters to the C/A ranging signal.

Differential GPS is used in terrestrial applications to defeat these error sources for geometries similar to the relative GPS navigation zone surrounding the Space Station. Differential GPS commonly performs its ranging corrections directly on the measurements, similar to the pseudodata method. Experience has shown that differential C/A-code using continuous Doppler yields virtually the same accuracy as differential P-code using continuous Doppler over distances ranging a few tens of kilometers.

A difference does occur in relative navigation using differenced C/A-code position solutions, however. This effect becomes evident unless the filters are carefully coordinated, and stems from two sources. The first is the reaction of the two navigation filters to large impulses, on the order of a hundred meters, caused by constellation

switches. The second is the biases caused when the two receivers are navigating from two separate constellations, again with a hundred meters of bias.

4.1.5 Dual Frequency Receivers

Ionospheric effects were discussed in section 4.1.3.1. Dual frequency GPS transmissions are implemented solely to measure these effects in real time. In differential GPS, however, single frequency corrections are the exception rather than the rule. This is for two reasons: first, the mismodeling effect of group advance/phase delay is minor in the relatively slow-moving ionospheric conditions of terrestrial users; and second, two-frequency corrections are slightly noisier. In space, the ionosphere moves much more quickly. To lessen error due to the ionosphere, one of the following three design options should be taken: dual frequency receivers; carefully coordinated, tuned navigation filters; or pseudodata corrections.

4.2 Phase Interferometry

Phase interferometry has been used in geodetic surveys to obtain centimeter-level accuracy from differential GPS. Theoretically the same technique can be applied to relative GPS. The object of phase interferometry is to measure relative carrier phase between the two receivers – which can be done accurate to a few millimeters - and infer the unknown integral number of wavelengths between the receivers by other means. In the case of GPS, this is done by the technique of accumulated deltarange as measured by the carrier tracking loops. This currently requires about twenty minutes of static data collection for terrestrial survey applications, the time needed to gain observability through the change in satellite geometry. In low orbits, the satellite geometry changes roughly eight times faster than it does on the surface of the earth (ninety minute receiver orbits as opposed to twelve hour GPS transmitter orbits), so the resolution of the integer wavelength ambiguity for phase interferometry can be achieved much faster in space.

This is all dependent on hyper-accurate relative motion models. In the geodetic survey case, for instance, the relative motion model of the two points is well-known - they are both bolted to the earth. In space, the relative motion depends upon whether the reaction control system is operating, and if so how accurately the acceleration of the thrust can be measured, and how accurately the relative gravitational field between the two vehicles is modeled.

Once the integer ambiguity is resolved, relative GPS can track the relative motion of the object using only the carrier tracking loops. Practically speaking, this system would require the approaching vehicle and the Space Station to enter a special, well modeled phase ambiguity acquisition mode at a separation of a kilometer or less for two to five minutes, and then maintain carrier lock until docking.

Phase interferometry is, however, not reliable and robust enough to perform as the docking positioning system in the Space Station environment. Its reliability depends on clear view of the satellites, which is not guaranteed by the Space Station location of antennas and docking procedures. It is also subject to multipath error; the Space Station has many reflective surfaces that can create damaging multipath at both Space Station and vehicle receivers. Lastly, the technology has not been developed to the point where it can provide the inputs to a real-time control system. Although successfully used in commercial surveying, GPS phase interferometry is currently limited to post-processing. Real-time failure detection techniques are non-existent; in docking, with short reaction times, failures of the navigation system must be identified immediately and with a reliability approaching 100%.

It is doubtful, given the current state of technology, that the accuracy of phase interferometry can be used in docking procedures of the Space Station. The GPS code is necessary to perform relative positioning reliably and robustly in space. Although reliance on carrier (continuous Doppler) makes this method very precise, relative ranging still carries with it small receiver-to-receiver code biases that prevent accuracies of much better

than a meter. If the GPS receiver and antenna design is sufficiently multipath protected or if multipath detection techniques are developed from dual frequency comparisons, if clear view can be obtained for the Space Station and vehicle GPS antennas, and if a reliable backup is provided, then phase interferometry might be available as the primary sensor.

4.3 Results

Simulation runs were performed using a TAU GPS Monte Carlo simulation modified to accept low orbit trajectories. A single rendezvous trajectory was analyzed. The range-to-go as a function of time is shown in Figure 4.3-1. Accuracy is roughly equivalent (within the capabilities of GPS) for the methods of differencing carefully coordinated navigation filters and the pseudodata method; this is because differencing, as a linear operation, is commutative with the linear navigation filter. Accuracies degrade when the filters are badly mismatched or the measurements are not coordinated.

The results presented here were taken from runs performed using identical eight state filters on both Space Station and vehicle. The results are shown to highlight the possible errors that arise from uncoordinated satellite selection with severe satellite bias errors, as might occur if a GPS transmitter clock is in a degraded state or an unauthorized receiver is used in Selective Availability conditions.

Four runs were performed. The results from each run are encapsulated in three figures: a three dimensional relative navigation position error plot in ECEF coordinates; a plot comparing RSS position error in conventional and relative navigation; and a plot comparing RSS velocity error, conventional and relative.

The first run (Figures 4.3-2 through 4.3-4) used the pseudodata approach with C/A-code receivers subject to Selective Availability errors of roughly sixty meters RSS. Accuracy is in the two meter range, well within the requirements for rendezvous approach.

The second run (Figures 4.3-5 through 4.3-7) used differenced navigation solutions from well-matched navigation filters and P-code receivers. As expected, due to

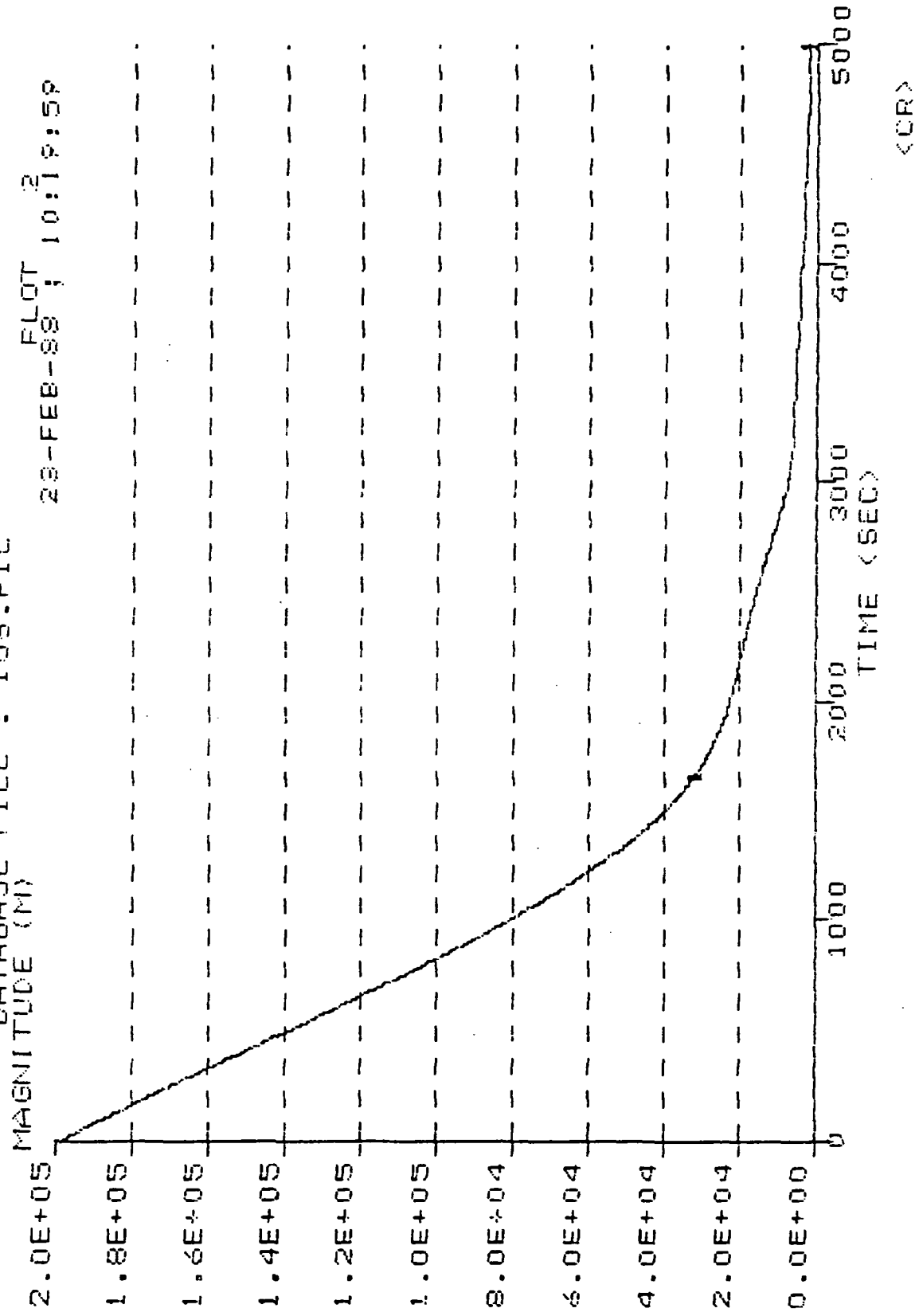

Figure 4.3-1. Range Between Vehicle and Space Station.

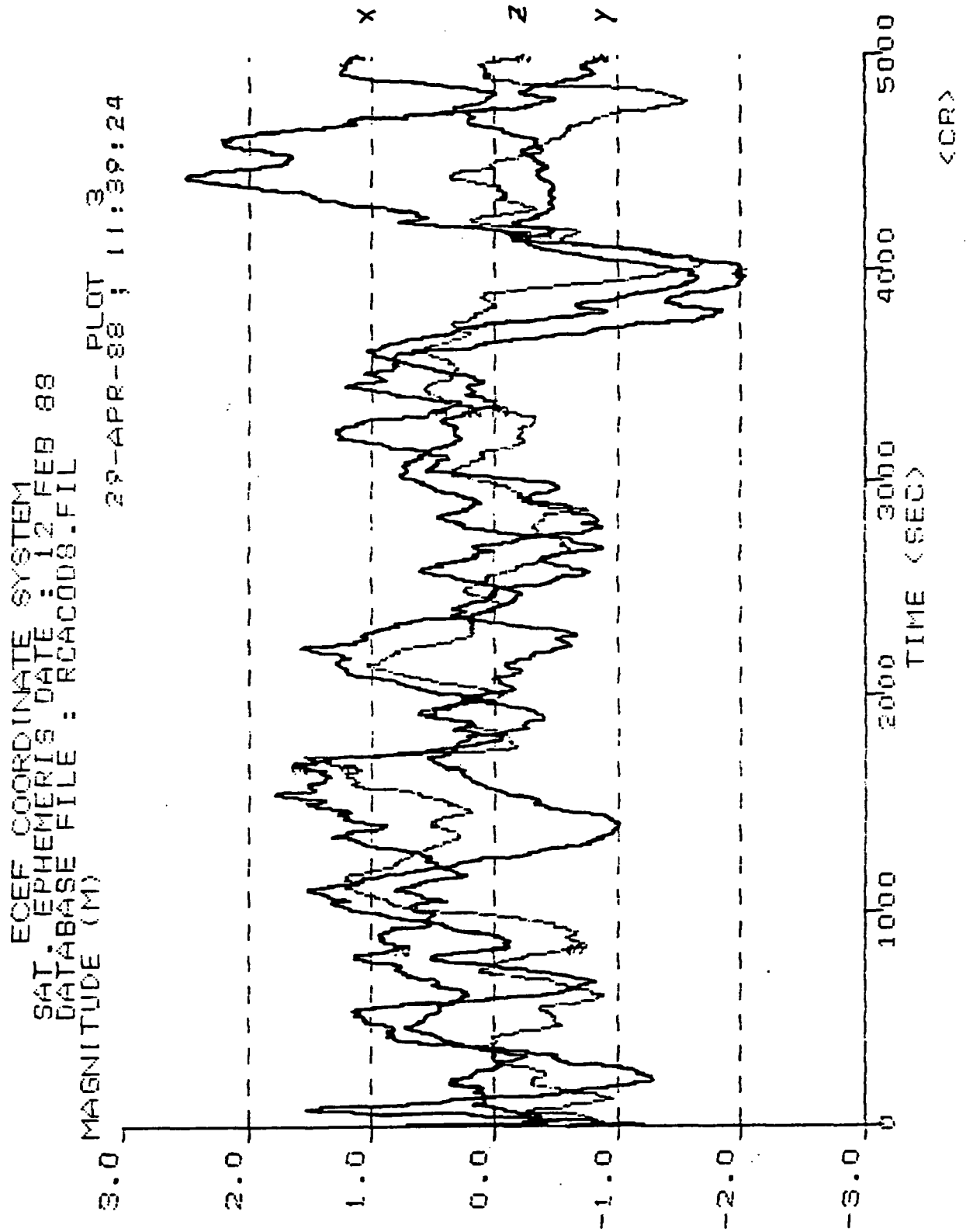

Figure 4.3-2. Relative Position Error, Pseudodata.

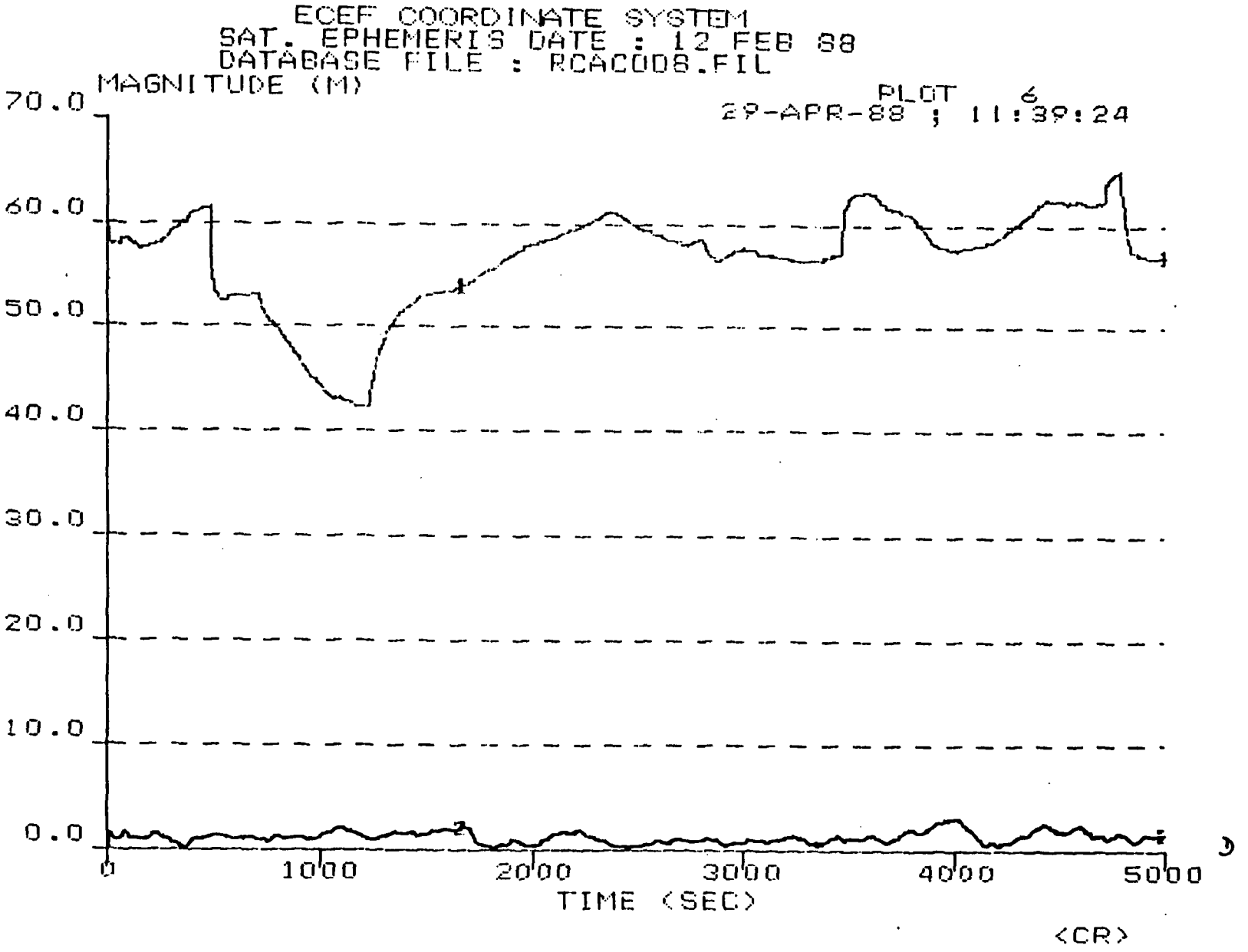

Figure 4.3-3. Standalone v. Relative Position Error, Pseudodata.

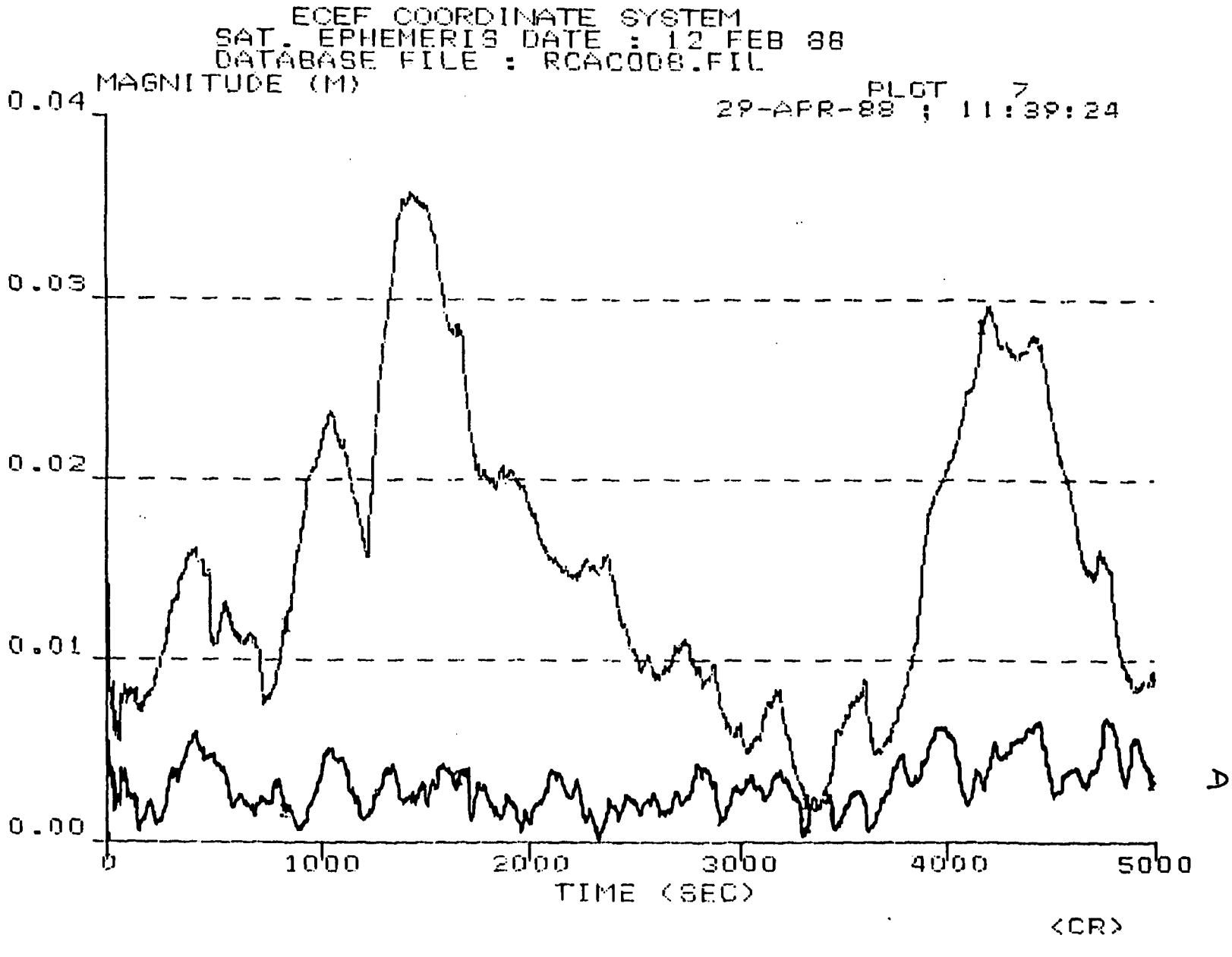

Figure 4.3-4. Standalone v. Relative Velocity Error, Pseudodata.

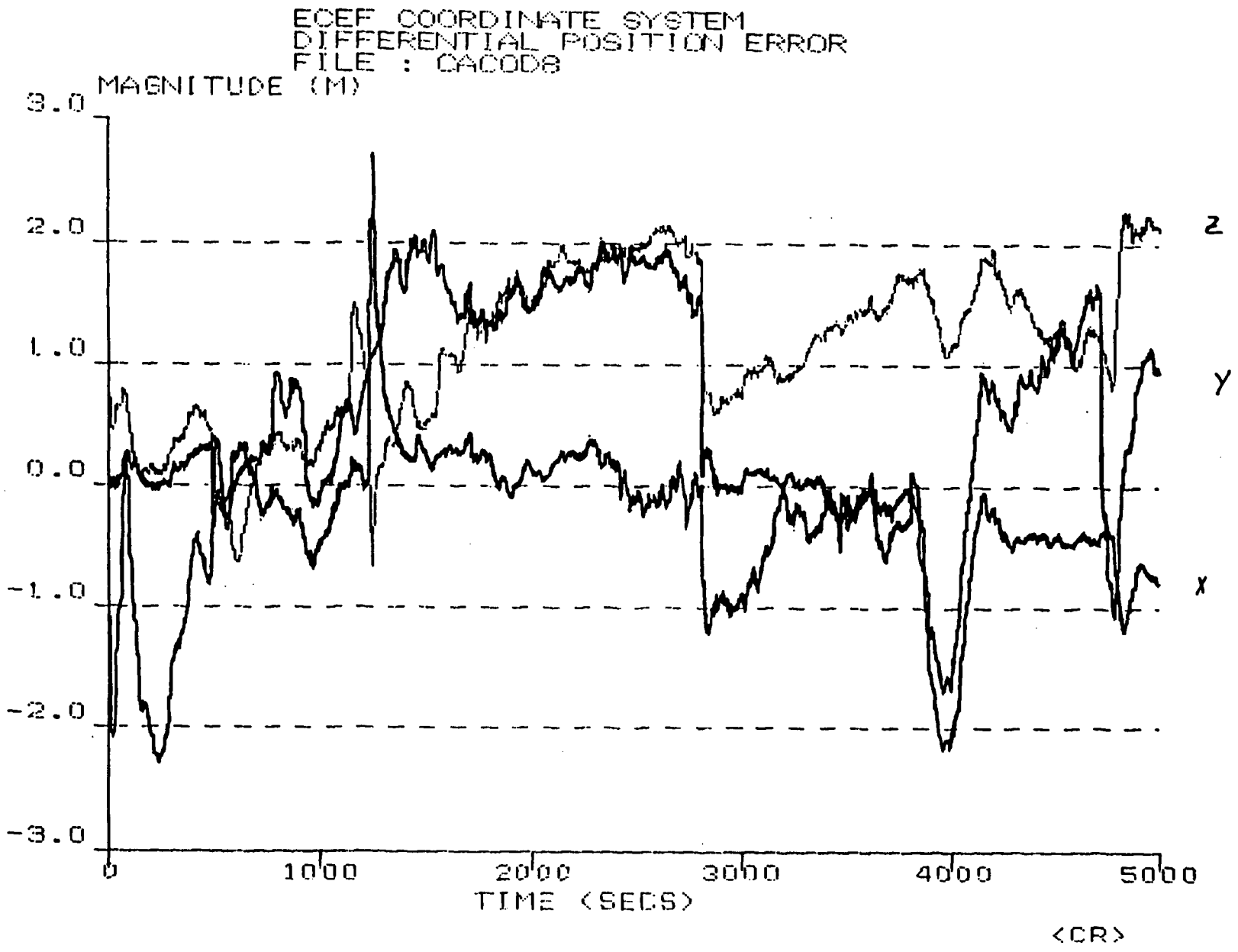

Figure 4.3-5. Relative Position Error, State Vector Difference.

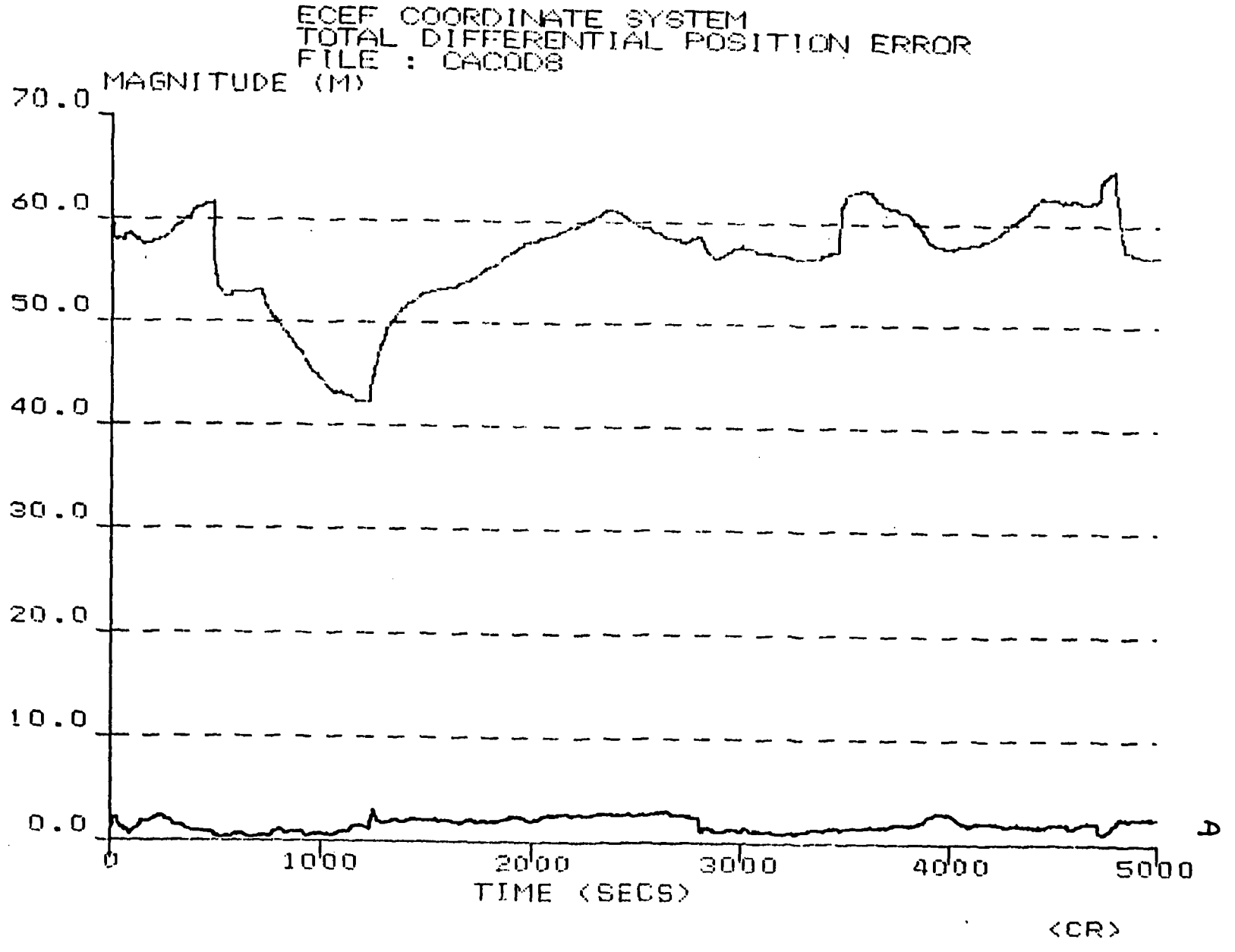

Figure 4.3-6. Standalone v. Relative Position Error, State Vector Difference.

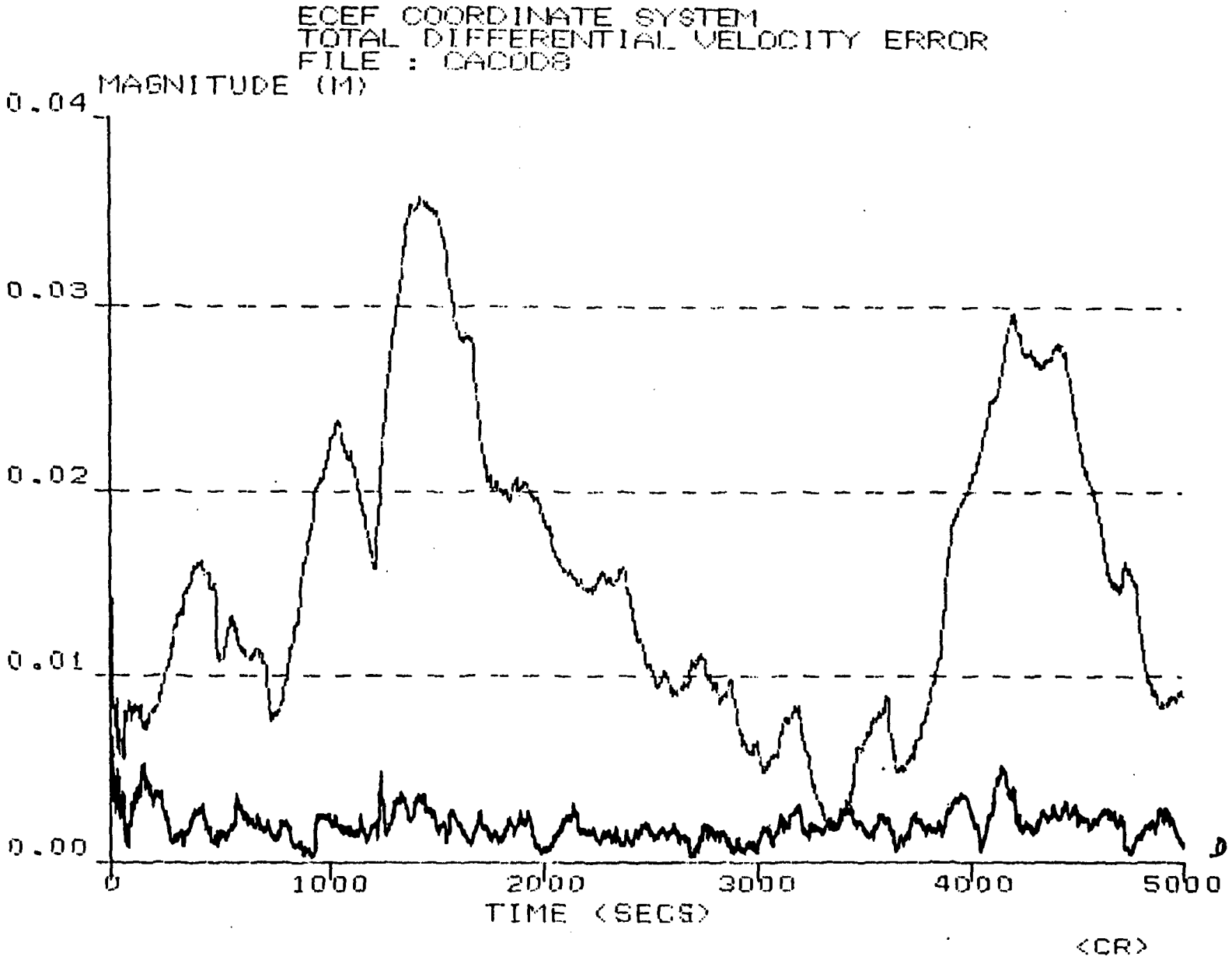

Figure 4.3-7. Standalone v. Relative Velocity Error, State Vector Difference.

the commutativity of filter and differencing, there is little difference between this and the first method in terms of accuracy.

The third run (Figures 4.3-8 through 4.3-11) illustrates the potential for damage when the filters are severely mismatched. In this case, pseudodata corrections were passed through a heavily damped filter before combination with the vehicle measurements (both using P-code receivers). This emulates the behavior of relative navigation between a heavily damped Space Station navigation filter and a lightly damped vehicle navigation filter; position errors are significantly higher than with the previous two runs, and marginal as to whether the accuracy levels of rendezvous approach are being met.

The last run (Figures 4.3-12 through 4.3-13) highlights the effect of uncoordinated satellite constellations. Each receiver in this case was a C/A-code receiver, capable of the same relative navigation accuracy over these distances a P-code receiver; Selective Availability was invoked, adding a random bias of hundred meter standard deviation. During the last five hundred seconds, a desirable satellite was removed from the view of the Space Station but the approaching vehicle was not informed, resulting in a mismatch of GPS constellations. Position error rose to an unacceptable level.

4.4 Summary

Relative navigation produces accuracy levels on the order of two meters provided that the following conditions are met:

1. satellite constellations are coordinated; at any one time, navigation is performed using at least four common GPS navigation satellites;
2. either
   a. the pseudodata approach is implemented;
   b. if differencing navigation filter position solutions is implemented, the filters are matched to prevent biases due to unmatched damping of

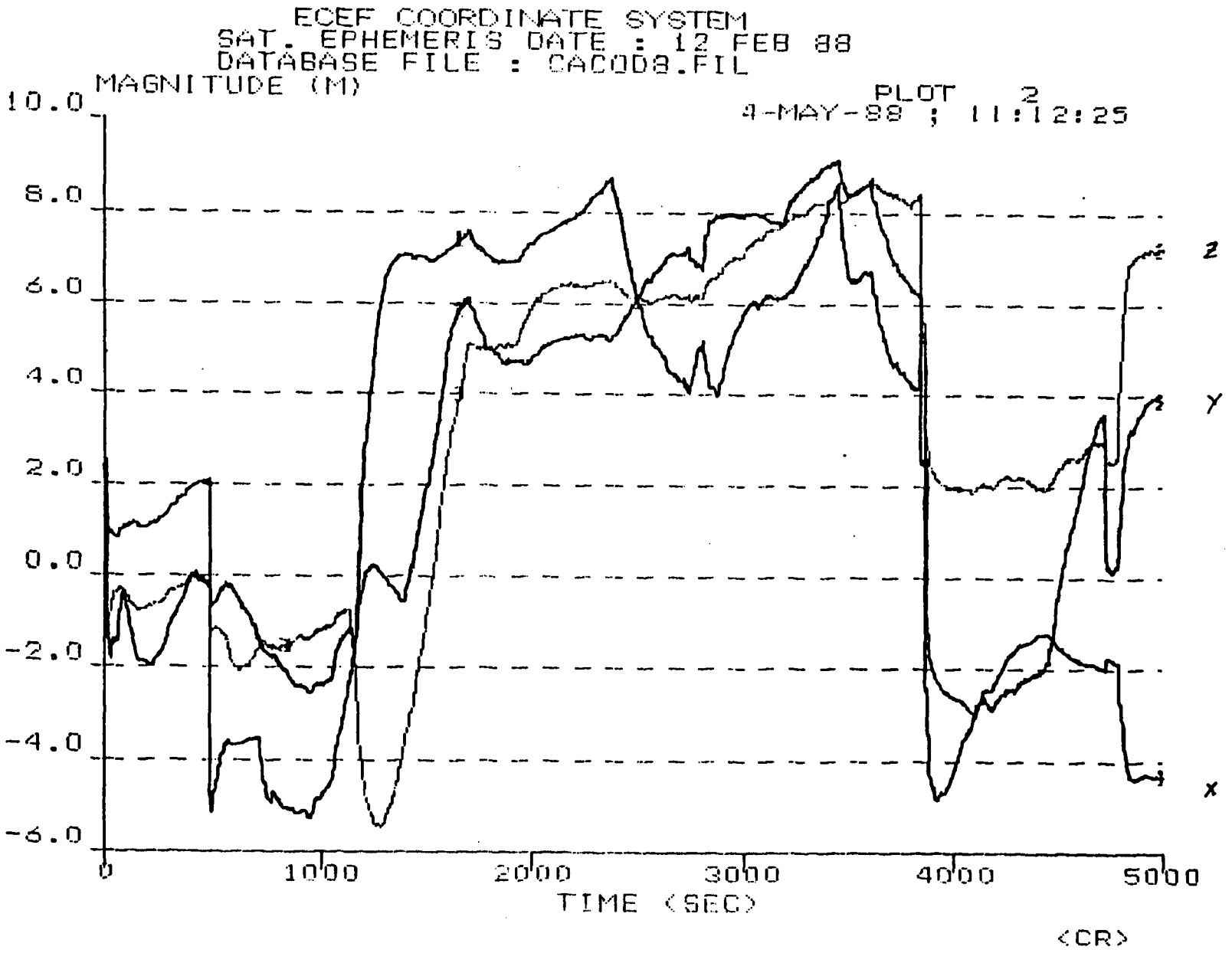

Figure 4.3-8. Relative Position Error, Unmatched Filters.

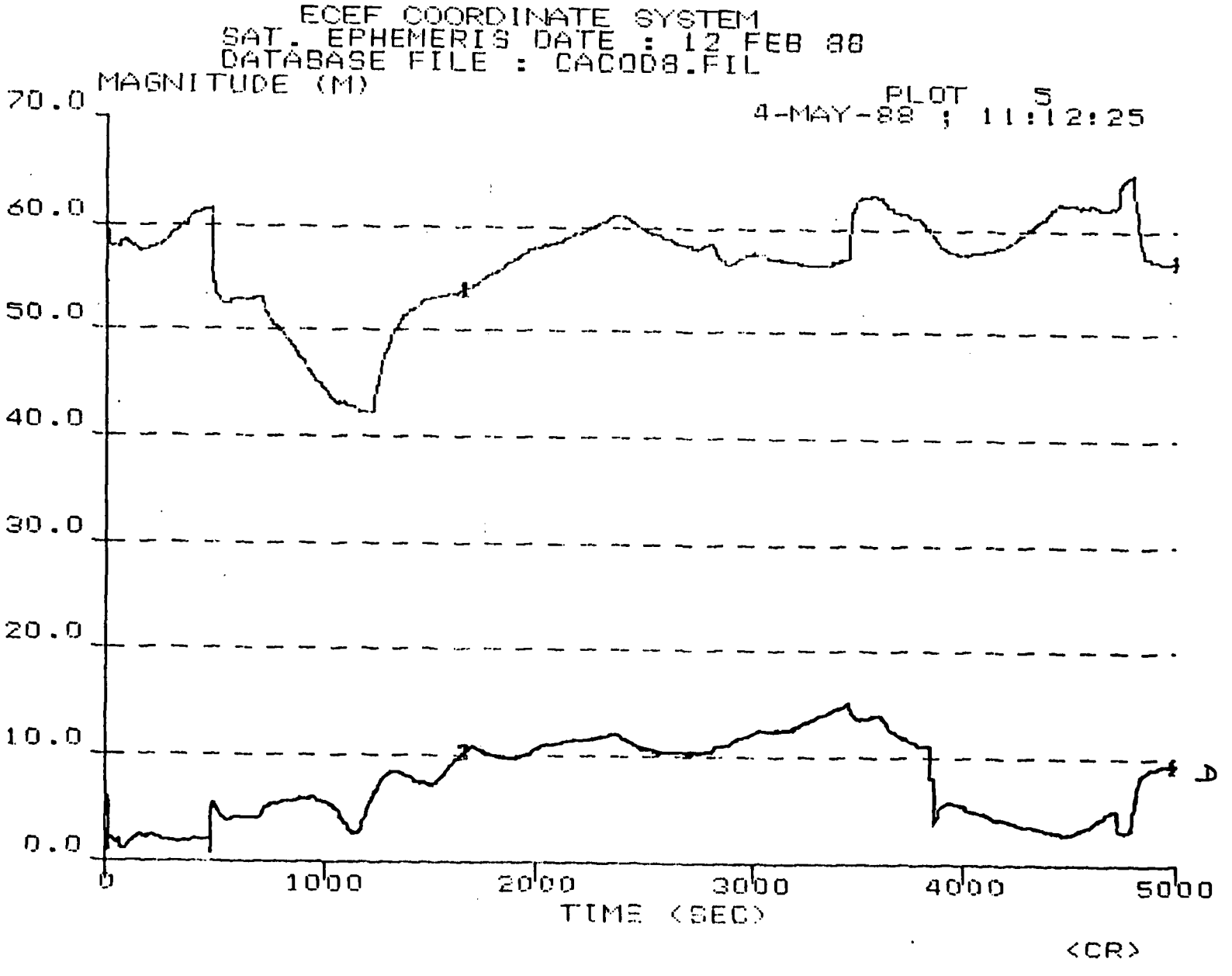

Figure 4.3-9. Standalone v. Relative Position Error, Unmatched Filters.

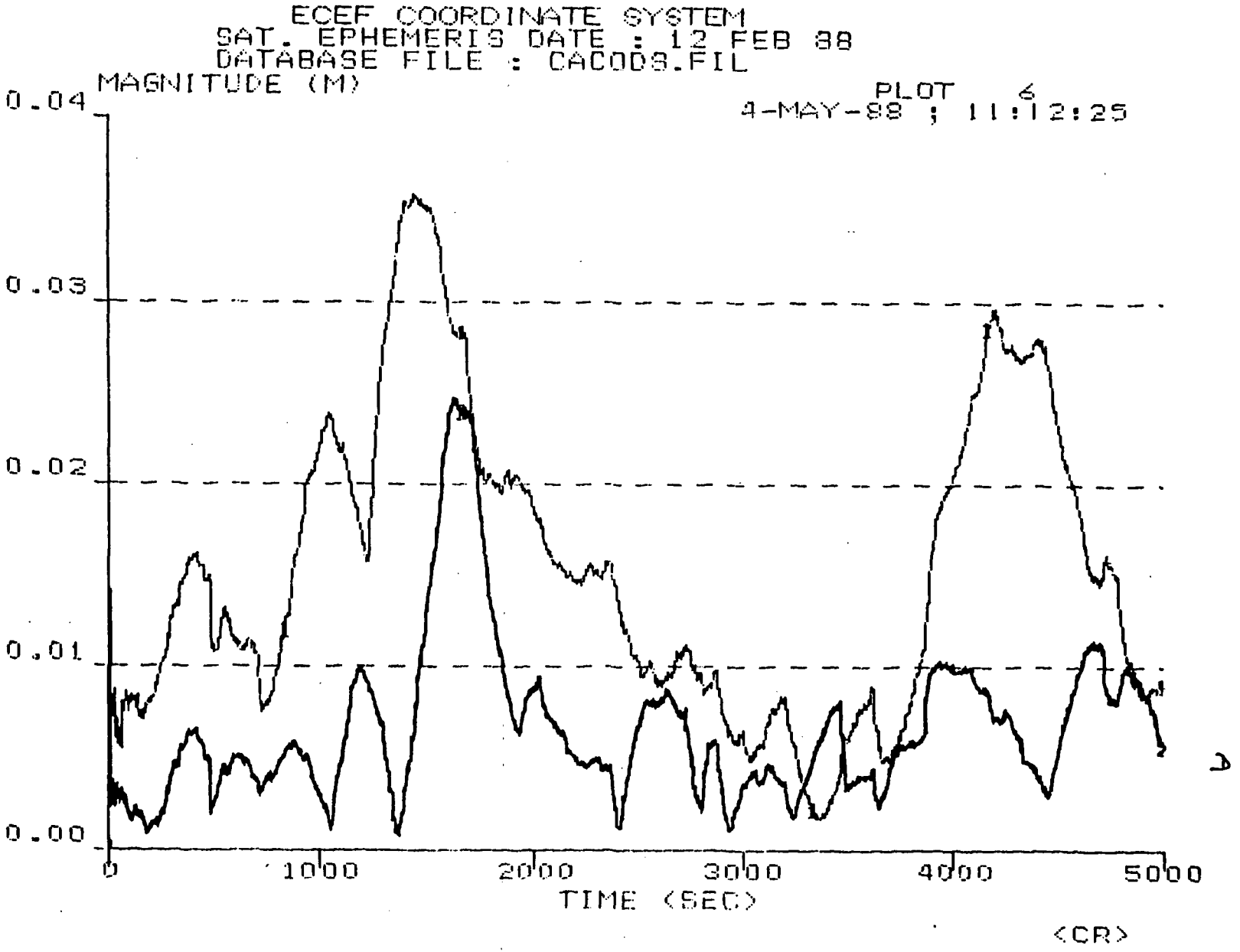

Figure 4.3-10. Standalone v. Relative Velocity Error, Unmatched Filters.

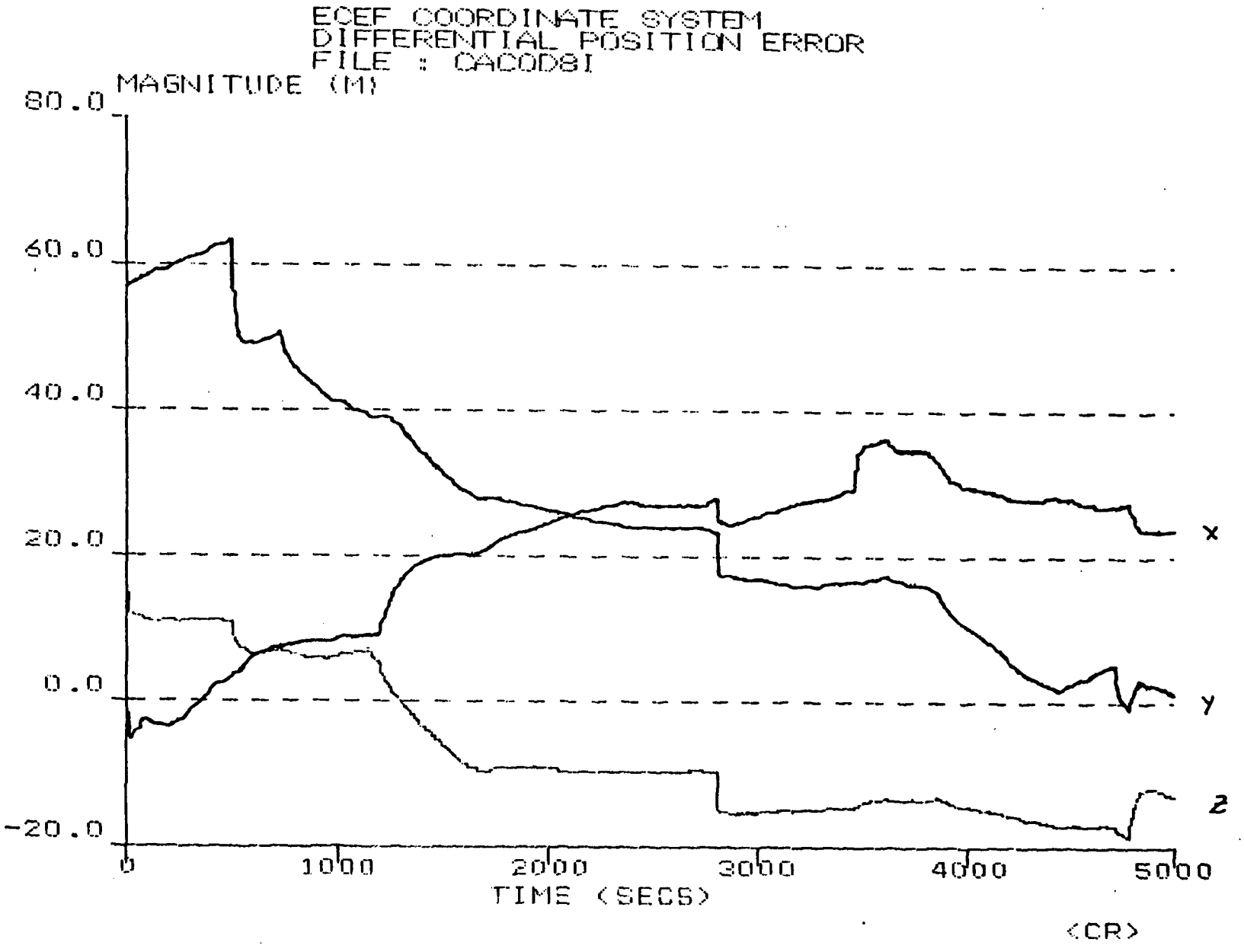

Figure 4.3-11. Relative Position Error, Uncoordinated GPS Constellations.

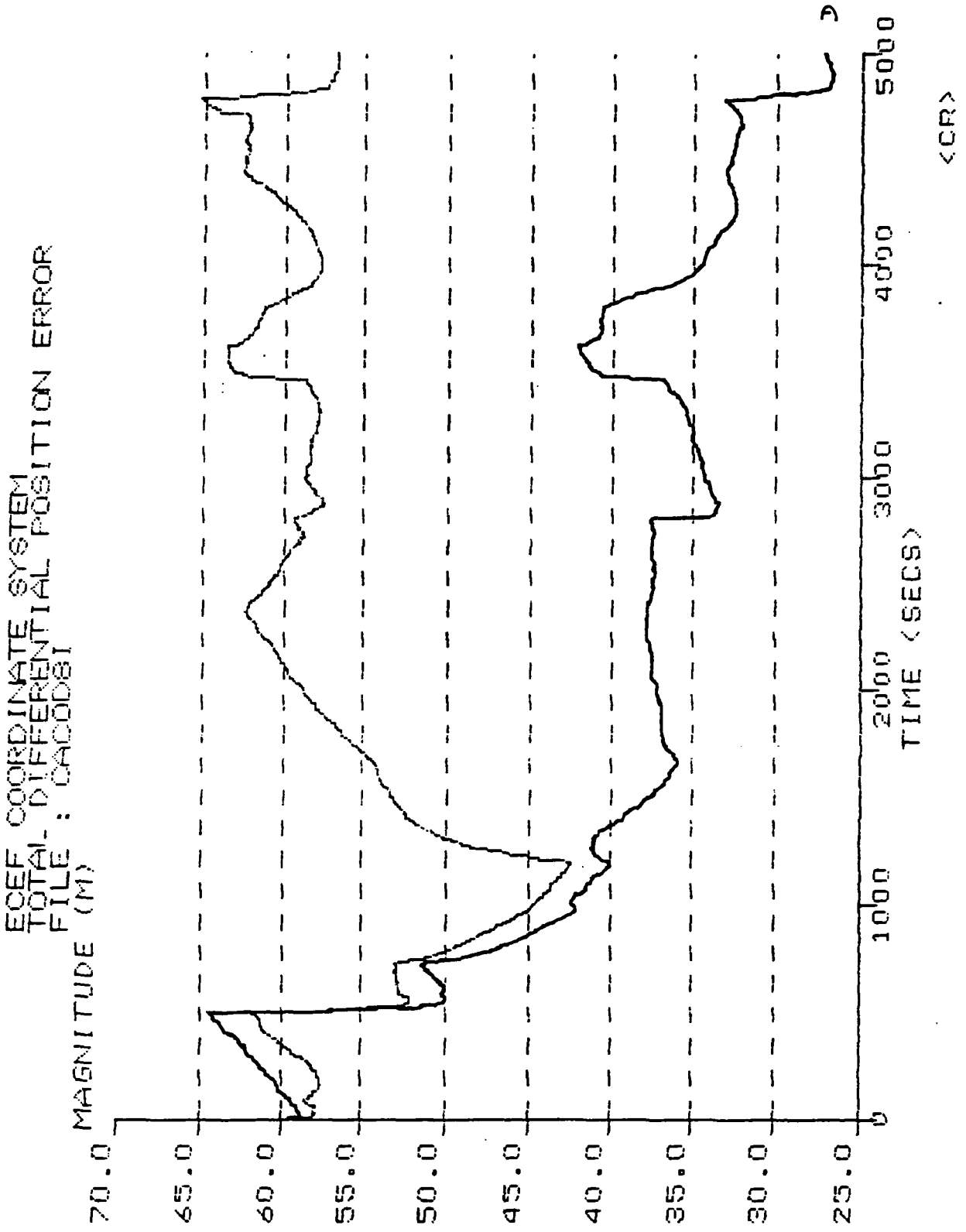

Figure 4.3-12. Standalone v. Relative Position Error, Uncoordinated GPS Constellations.

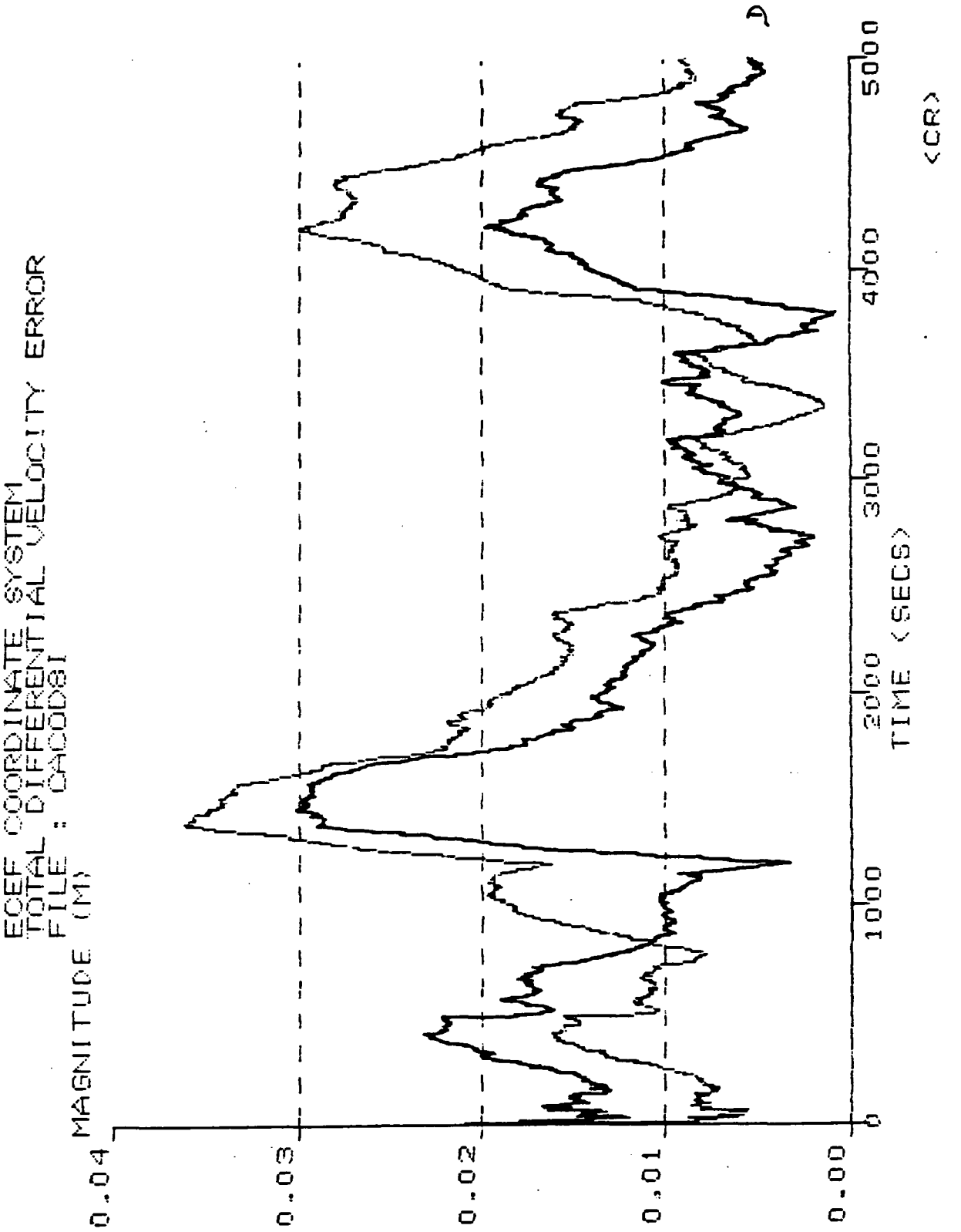

Figure 4.3-13. Standalone v. Relative Velocity Error, Uncoordinated GPS Constellations.

ionospheric effects and step function ranging errors due to constellation switches.

Because ionospheric effects and Selective Availability do not affect P-code receivers, the importance of filter tuning is not as great with P-code receivers. However, accuracy can degrade to a marginal level even with P-code if the mismatch is serious.

Data link loading is roughly equivalent between the various implementations. The deciding factor among them is the ease of implementation. In examining the implementations for minimal impact in terms of the design of the receiver on the approaching vehicle, the pseudodata approach, requiring only a code and carrier measurement output port on the vehicle receiver, represents a relatively painless solution. Furthermore, the pseudodata approach would be better adaptable to the many configurations of vehicle receiver that may be encountered, from slow sequencing single channel C/A-code to multichannel P-code. The pseudodata approach invokes a separate, special purpose resident on the Space Station that does not interfere with nor place restrictions on the autonomous navigation filter of the approaching vehicle.

4.5 Comparison with Other Techniques (Spaceborne Traffic Control)

The alternate technology that is appropriate for spaceborne traffic control is a rendezvous radar. A primary advantage of the radar is that it would accommodate the requirements of noncooperative tracking. Accuracies sufficient for the OMV mission, i.e., 20 ft. (or 2% of range) and 0.4 ft. per second could be achieved with a GPS differential system. However, such a system would require that both target and host vehicle carry GPS receivers and that a data link communicate data between vehicles.

The autonomy of a radar makes it a viable consideration for the Space Station in view of possible broad requirements for tracking noncooperative targets in a very busy "Air Traffic Control" environment of the low altitude orbiting Space Station. However, the size of the Space Station may prohibit any evasive action that would result from knowledge of an impending collision with a noncooperative target.

Table 4.5-1 lists the techniques applicable for traffic control in space. Table 4.5-2 provides the comparison of these alternatives.

GPS ⟶ (DIFFERENTIAL) – SEVERAL ADVANCED SYSTEMS AVAILABLE

C/A CODE + PHASE ⟶ < 1 METER ACCURACY

RADAR ⟶ RANGE / ANGLE MEASUREMENT – X-BAND; KU-BAND

INERTIAL
REFERNCE SYSTEMS

Table 4.5-1. Traffic Control Alternatives.

	PERFORMANCE	COST	RELIABILITY	COMPLEXITY
GPS	HIGH	MED	MED	MED
RADAR	MED	MED (NATURE)	MED	MED
INTERTIAL REFERENCE SYSTEMS	MED	MED (NATURE)	MED	MED

Table 4.5-2. Technology for Spaceborne Traffic Control.

5.0 TIME BASE – TIME TRANSFER

5.1 Overview

The potential for precise interpretation of electromagnetic radiation in space is greatly enhanced with precise timebase information. The GPS system provides a mean for achieving such synchronization on board the Space Station. Precise time synchronization accuracy through GPS is dependent on differential performance. Although the timebase for the GPS satellites is maintained to the accuracy level of 1 microsecond, the potential for differential time accuracy based on two observers deriving their time from the same set of GPS satellites is on the order of a few nanoseconds. The primary mode of navigation using GPS involves the solution of 3 coordinates of position and time bias, using pseudorange measurements from at least 4 appropriately selected satellites from the GPS constellation. Thus, the precision of time determination is commensurate with the position uncertainty divided by the speed of light.

Spaceborne time synchronization using atomic clocks is used by GPS. Thus, the GPS high performance system is in effect servicing all the users with a common set of very high accuracy clocks. Quartz crystal, Rubidium, and Cesium beam clocks have been successfully flown in space. The quartz crystal clock is the least expensive and most reliable clock and is in greatest use in many aerospace applications. The Rubidium oscillator exhibits sensitivity to temperature and must be compensated with temperature – controlled baseplate to achieve the best accuracy. NAVSTAR-8 uses a Rubidium clock and its performance is reported in Ref. [5.1-1]. The cesium beam clock has also been flown in space on NAVSTAR-9. Both of these clocks provide long-term accuracies at the level of one part in 10^{11} or better.

5.2 Technology Considerations

As part of our team's long involvement with the GPS program, we have kept abreast of the development of the Time Transfer application. The choice here is between high quality frequency standards and a GPS time transfer system. Satellite frequency standards have progressed from the quartz oscillators, used in the Navy Satellite System (NSS) satellites and early TIMATION launches, to rubidium clocks used in the NTS-1 of NAVSTAR GPS to cesium clocks in NTS-2 and to hydrogen maser clocks projected in NTS-3. Quartz oscillators typically have an accuracy of one part in 10^9 with a "short term" stability of one part in 10^{11} for several minutes. The quartz oscillators used for the TIMATION I launches had an accuracy of 3 parts in 10^{11} per day, while those used for the TIMATION II launches had an accuracy of 1 part 10^{11} per day. Rubidium clocks have an accuracy of 5 to 10 parts in 10^{13} per day, while cesium clocks used in NTS-2 achieved 1 to 2 parts in 10^{13} per day and hydrogen maser 1 part in 10^{14} per day. Cesium clocks require frequency updating to maintain a specified accuracy. Since hydrogen maser clocks are more accurate, they would maintain an accuracy equivalent or better than cesium clocks over larger periods of time without updates. The previous discussion is addressed in more depth in Reference [5.2-1]

The concept of using GPS as an accurate source of time information has been discussed extensively in the literature. The principles involved in the Time Transfer process using GPS are addressed by Van Dierendonck and Melton [5.2-2] and Yakos and Hirt [5.2-3]. McLean and Hua [5.2-4] described such a time transfer system, the TTS-502, developed by Stanford Telecommunications, Inc., and currently available on the market.

Other systems have been developed and are currently available, e.g., the TRIMBLE 5000 A and the OSBORNE-TTR-5

In its basic mode of operation, the GPS provides a suitably equipped user listening to four satellites, with position, velocity and time information with accuracies of 16 m,

0.1m/sec and 100 nanoseconds, respectively. In the case of a stationary user, or of a user whose position is known as function of time, only one satellite is required to solve for time. Since the position of the GPS satellite is known as a function of time from the received navigation message, the distance (as a function of time) from the GPS satellite to the user can be computed.

The propagation delay to cover this distance at the speed of light is calculated next (including ionospheric and tropospheric delays). The time of transmission is determined by synchronizing the received code with a locally generated code and determining the slewing required for the synchronization to occur. The GPS time is then determined by adding the transmission time to the transmission delay. The calculation of the propagation delay includes ionospheric and tropospheric delays, if applicable, as well as calibrated hardware delays. In addition, since the GPS satellite clock is not exactly synchronized with GPS time, the transmission time is further corrected by using the clock correction parameters including in the satellite navigation message.

The time transfer operation just described requires only 1 channel, can be performed using the C/A -code and provides an accuracy better than 100 nsec. The 100 nsec limitation is due to several inherent errors including those in ionospheric and tropospheric delays estimates, as well as the ability to measure the pseudoranges (i.e., the ability to pinpoint the maximum correlation between the transmitted and received codes). The latter is limited by the "edges slope" of the C/A code chip (C/A has a frequency of 1.023 MHz). The smaller the slope, the larger the uncertainty. If a better accuracy is required, a more complex receiver, using the more precise P-code (10.23 MHz) can be utilized. The use of the P-code allows tracking on both L1 and L2 frequencies, providing for a better means of ionospheric delay corrections.

Yet another mode of operation is the so-called "common-mode- common view" method, in which two receivers track the same satellite at the same time. One of the receivers is a reference station where an additional high precision clock is available (e.g.,

National Bureau of Standards). Both receivers provide error estimates of their internal clocks. The reference receiver estimated clock error is compared to the actual clock error as determined from the high precision clock. This error in estimation is attributed to several GPS inherent error sources including mis-modeled ionospheric delays, hardware delays and GPS satellite ephemeris and clock errors. These errors are assumed common for both receivers and the estimation error in the reference receiver is then applied to the user receiver clock error estimate so that a better estimate is achieved.

As briefly mentioned earlier, some of the issues specific to the satellite application include satellite altitude, ionospheric modeling, remote control and monitoring of the GPS receiver, accuracy achievable, and cost. The GPS satellites transmit data towards the earth. They are in 6-quasi-circular orbits at approximately 20,000 km altitude, and have a period of 12 h. It is clear that all space vehicles at higher altitudes than the GPS satellites will not be able to use the system (the broadcast signals are directional). Also, the distances between the user and the GPS satellites can vary considerably. It is also possible that in one case no tropospheric delays and a single ionospheric delay computation will be required and that in another both the tropospheric and ionospheric delays are to be accounted. In this case ionospheric and tropospheric delays need further study. Another issue is that of monitoring and control of the GPS receiver. Obviously, remote capabilities have to be devised in conjunction with more autonomous set operation as compared to an "accessible" GPS receiver.

On the issue of accuracy, performance results were presented in Reference [5.2-1] for several of the methods discussed above. They are provided in Table 5.2-1. A Time Dilution of Precision (TDOP) of 1.68 was selected and multiplied by the R.S.S. of all error sources (excluding the position error).

Table 5.2-1. GPS Time Transfer Performance for Non-Coordinated Users.

Error Source		Time Transfer Equipment and Accuracy (in nanoseconds)					
		C/A-L1 Only		P-L1 Only		P-L1/L2	
		Raw Measurements	Smoothed Measurements	Raw Measurements	Smoothed Measurements	Raw Measurements	Smoothed Measurements
Satellite Ephemeris and Clock		20	20	20	20	20	20
Atmospheric Delay		5 – 40	5 – 40	5 – 40	5 – 40	3	3
Receiver Noise		10	1.5	1	0.15	3	0.45
Quantization Noise		15	2.5	1.5	0.25	4.5	0.75
Position Error		5 – 15	5 – 15	5 – 15	5 – 15	5 – 15	5 – 15
RSS	Position Known	28 – 50.5	21.5 – 47.2	21.3 – 47.2	21.2 – 47.2	21.5 – 25.8	20.9 – 25.2
	Unknown Location	46 – 81	35 – 75.3	34.8 – 75.2	34.6 – 75.1	35.2	34

5.3 Comparison with other Techniques (Time Base – Time Transfer)

Table 5.3-1 shows several time synchronization alternatives, GPS being one of them. Table 5.3-2 shows the evaluation of these alternatives. As indicated in that table, the GPS provides a medium cost and moderate complexity alternative with performance accuracies of 1×10^{-12}.

5.4 References

[5.1-1] McCaskill, Thomas B. and James A. Buisson, "On-Orbit Frequency Stability Analysis of Navstar GPS Clocks and the Importance of Frequency Stability to Precise Positioning," Presented at PLANS 86.

[5.2-1] Bartholomew, C. A., "Satellite Frequency Standards", Journal of the Institute of Navigation, Special GPS issue, Volume I.

[5.2-2] Van Dierendonck, A.J. and W.C. Melton, "Applications of Time Transfer Using NAVSTAR GPS", Journal of the Institute of Navigation, Volume 30, No. 2, Summer 1983.

[5.2-3] Yakos, M.D. and E.H. Hirt, "Time Dissemination Using NAVSTAR Global Positioning System (GPS) Phase IIB User Equipment," Rockwell International/Collins Division.

[5.2-4] McLean, R. and O.D. Hua, "An Advanced Microprocessor-Controlled GPS Time Transfer System," Stanford Telecommunications, Inc.

GPS	→	WORLD REFERENCE SYSTEM – 18 TIME STANDARDS HIGH SYSTEM INTEGRITY
RUBIDIUM OSCILLATORS	→	USED FOR GPS SATELLITES
		3×10^{-11} FOR SHORT TERM
		$< 10^{-11}$ FOR 1 HR → ∞
QUARTZ CRYSTAL	→	SUITABLE FOR SHORT TERM
		10^{-11} FOR SHORT TERM
		10^{-10} FOR 1 HR
CESIUM		
HYDROGEN MASER		

Table 5.3-1. Time Synchronization Alternatives.

	PERFORMANCE	COST	RELIABILITY	COMPLEXITY
GPS	$1:10^{12}$	MED	SYSTEM DEPENDENT (HIGH)	MODERATE
RUBIDIUM OSCILLATOR	$1:10^{12}$ SENS PRESS MAG. FIELD	HIGH	MED	LOW
QUARTZ CRYSTAL OSCILLATOR	$1:10^{9}$ SENSITIVE TEMP.	LOW	HIGH	LOW
CESIUM BEAM	HIGH	HIGH	?	LARGE
HYDROGEN MASER	HIGH	HIGH	?	LARGE

Table 5.3-2. Technology for Spaceborne Time Synchronization.

6.0 CONCLUSIONS

The results of this study lead to the following conclusions:

- The primary application of GPS on the Space Station or other space vehicles is for traffic control and time synchronization. For cooperative vehicles, differential GPS is an attractive alternative to radar. Although requirements for tracking noncooperative vehicles may suggest an active radar sensor, it may not be practical to avoid a finite probability of collision, even with radar tracking information on a non cooperative target.

- GPS provides an excellent method for distribution of a precise time base that would be useful in bi-static radar applications.

- Attitude determination and structural monitoring using GPS would be technologically attractive if costs could be reduced and if the effects of multipath could be mitigated. However, current projections suggest that optical and optical/inertial technologies are competitive for spaceborne attitude determination and structural monitoring.

APPENDIX A

HARDWARE COMPARISONS OF GPS AND OTHER TECHNIQUES

SPACECRAFT APPLICATIONS OF ADVANCED GLOBAL POSITIONING SYSTEMS TECHNOLOGY

by

I. Newton Durboraw, III

Final Report
May, 1988

Prepared for:

Axiomatix Corporation

and

NASA Johnson Space Center

MOTOROLA INC.
Strategic Electronics Division
2501 S. Price Rd.
Chandler, AZ 85248-2899

SPACECRAFT APPLICATIONS OF ADVANCED GLOBAL POSITIONING SYSTEM TECHNOLOGY

I. Newton Durboraw, III

Motorola Inc.

This report summarizes the conclusions of a study by Motorola as part of a joint study for NASA Johnson Space Center with Axiomatix and Tau Corporation. This portion of the study performed under subcontract to Axiomatix (MOT 8707) addresses hardware related issues concerning the application of GPS technology and provides comparisons with alternative instrumentation methods for specific functions required for an advanced low earth orbit spacecraft.

The functions that have been identified for potential GPS instrumentation are:

1) Attitude control and tracking.

2) Structural Control

3) Traffic Control

4) Time Base Definition (synchronization)

Each of these issues are addressed in the following section. Each GPS approach will be briefly described along with a discussion of hardware constraints related to fundamental GPS measurements as well as the alternative techniques and their limitations.

1.0 ATTITUDE TRACKING CONTROL:

Attitude measurement via GPS involves the precise determination of baseline vectors between 3 or more spatially diverse L band GPS antennas. The basic measurement to be exploited is the carrier phase. Measurement of relative carrier phase between multiple antennas can be used in an interferometric sense to derive attitude information. Since the position of each of the GPS satellites is precisely known to the user and the satellites are at a significant distance (ie. >20,000 Km.), the direction to each of the satellites is precisely defined. Thus, a relative phase measurement may be related to the orientation of the baseline with respect to the vector pointing to the GPS satellite.

The direct measurement of the relative phase between antennas is limited by uncertainties of signal propagation within the hardware as well as basic environmental factors such as the multipath effect. Hetrodyning of the GPS signal to IF requires a distribution of a reference signal phase to each of the antenna elements. Therefore, the variation of this reference signal phase with temperature of the spacecraft is a factor that must be reckoned with when considering methods to resolve the carrier cycle ambiguity. A technical approach to the problem involves the use of simultaneous observations of the carrier phase from multiple satellites at each of the antennas over some period of time, during which the motion of the platform must be precisely modeled. In essence, the reduction of signals to determine the attitude of an array of antennas is equivalent to the determination of the baselines between each of the antennas, based on relative Doppler information contained in each of observed satellite difference signatures derived from each antenna respectively. Although this method is practical for precise determination of baseline vectors in a terrestrial environment, it is required to collect data over an extended period to achieve the relative Doppler level of accuracy that is required to resolve the carrier cycle ambiguity. The primary limitation of this method is that the relative motion of the antennas must be accurately modeled during an extended observation period of several tens of minutes.

Determination of baseline vectors in a stationary environment has yielded accuracies that are 1 cm under favorable conditions, using observation periods of 1 hour. At this level of accuracy, however, the influence of multipath distortion of the signal becomes a dominant factor and is difficult to circumvent due to the fact that the effect is dependent on the relatively slowly changing geometry of the satellites relative to the antenna environment. With careful selection of antenna design, the error can be further reduced to levels approaching the 1 mm level. However, for terrestrial platforms, the effects of multipath are likely to limit the performance at this level. Space applications are somewhat differently affected by multipath because of the changing geometry. However, on a space platform, the time available for continuous observation will necessarily be shorter because of the platform movement in orbit.

The alternative method of attitude determination is to use a star tracker such as represented by Ref 1. Such instruments have been proven for space applications and can achieve accuracies that are 2 order of magnitude better than those projected for schemes using the GPS signals. This cost of a

star tracker is also competitive with projected costs for multiple spaceborne GPS receivers to observe attitude.

2.0 STRUCTURAL CONTROL:

Large space stations involving extendable panels, sections, and modules are highly flexible and will likely exhibit very low frequency and very lightly damped relative bending motion. It is, therefore, desired to monitor the relative motion so that active controls can be employed to damp the bending motion. GPS relative phase measurements could be used to monitor relative motion of distinct elements of the structure. By placing antennas on those elements likely to exhibit bending mode response, the bending flexure could be inferred from the phase data. Since the measurements will generally be harmonic, constant phase biases can be solved for and will be of less importance in determining appropriate damping control action. However, a slowly changing bias over the time of 1 cycle of the bending motion cannot be separated from the measurement of the bending mode and will limit the ability to make the desired measurement.

An alternate technology for directly monitoring relative structural motion is the laser/retro reflector technology such as represented by Ref 2. This instrument uses a fully solid state sensor for monitoring the relative dynamic motion of several points in its field of view. Developed for the Solar Array Experiment, the Retroreflector Field Tracker is designed to characterize the motion of large flexible space structures in low orbit. Twenty-three (23) reflective targets are tracked with a Charge Injector Device optical tracker. Accuracy of tracking is limited by the resolution of the sensor and with a 19 degree field of view, the accuracy is on the order of a few millimeters for all of the targets.

3.0 TRAFFIC CONTROL:

The space station is expected to interface with many platforms. Control of the rendezvous and docking phase is critical. This area of the study includes an assessment of technology that is associated with the navigation and control of these platforms during the rendezvous and docking maneuvers.

Differential GPS is a natural for spaceborne rendezvous and docking. The requirements for power are reduced since no active transmissions are required other than a low data rate communication of the GPS state vector as reported by GPS to the user. In terrestrial tests, GPS has been established as

a proven technology for differential as well as autonomous navigation. Commercial receivers such as the Motorola Eagle (Ref 3) have demonstrated differential performance on the order of 2-5 meters and less in a dynamic environment as well as static. Under favorable conditions, the errors can be under 1 meter. In a spaceborne mission, with appropriate considerations of satellite visibility and multipath, comparable performance levels may be expected.

The key to high performance in a differential GPS system is the control of 'non-common' error sources. Common errors are those errors that affect both receivers equally. By using measurements of pseudorange from 4 or more satellites simultaneously, the position of a user can be established with high precision relative the constellation that is being tracked at the given time. However, the absolute position is influenced by several error sources, among which are uncertainties in the satellite orbit itself. If all users are coordinated to track the same set of satellites, then the non-common errors are greatly reduced and only those errors associated with the receiver itself remain. Through the use of carrier aiding such as employed by Motorola Eagle and the TOPEX GPSDR receivers, the receiver-dependent errors are largely eliminated.

The alternate technology that is appropriate for spaceborne traffic control is a rendevous radar. A primary advantage of the radar is that it would accommodate the requirements of noncooperative tracking. Accuracies sufficient for the OMV mission ie. 20 ft. 36 (or 2% of range) and 0.1 ft. per second could be achieved with a GPS differential system. However, such a system would require that both target and host vehicle carry GPS receivers and that a data link communicate data between vehicles. The autonomy of a radar makes it a viable consideration for the space station in view of possible broad requirements for tracking non cooperative targets in a very busy "Air Traffic Control" environment of the low altitude orbiting space station. However, the size of the space station may prohibit any evasive action that would result from knowledge of an impending collision with a non cooperative target.

4.0 TIMEBASE:

The potential for precise interpretation of electromagnetic radiation in space is greatly enhanced with precise timebase information. The GPS system provides a means for achieving such synchronization on board the space station. Precise time synchronization accuracy through GPS is dependent on differential performance. Although the timebase for the GPS satellites is maintained to the accuracy level of 1 microsecond, the potential for differential time accuracy

based on two observers deriving their time from the same set of GPS satellites is on the order of a few nanoseconds. The primary mode of navigation using GPS involves the solution of 3 coordinates of position and time bias, using pseudorange measurements from at least 4 appropriately selected satellites from the GPS constellation. Thus the precision of time determination is commensurate with the position uncertainty divided by the speed of light.

Spaceborne time synchronization using Atomic clocks is used by GPS. Thus the GPS high performance system is in effect servicing all the users with a common set of very high accuracy clocks. Quartz crystal, Rubidium, and Cesium beam clocks have been successfully flown in space. The quartz crystal clock is the least expensive and most reliable clock and is in greatest use in many aerospace applications. The Rubidium oscillator exhibits sensitivity to temperature and must be compensated with a temperature- controlled baseplate to achieve the best accuracy. NAVSTAR-8 uses a Rubidium clock and its' performance is reported in Ref 4. The Cesium beam clock has also been flown in space on NAVSTAR-9. Both of these clocks provide long-term accuracies at the level of 1:10^11 or better.

CONCLUSIONS:

The primary application of GPS on the Space Station is for traffic control and time synchronization. For cooperative vehicles, differential GPS is an attractive alternative to radar. Although requirements for tracking non cooperative vehicles may suggest an active radar sensor, it may not be practical to avoid a finite probability of collision, even with radar tracking information on a non cooperative target. GPS provides an excellent method for distribution of a precise time base that would be useful in bi-static radar applications. Attitude determination and structural monitoring using GPS would be technologically attractive if costs could be reduced and if the effects of multipath could be mitigated. However, current projections suggest that optical and optical/inertial technologies are competitive for spaceborne attitude determination and structural monitoring.

References

1) Specification Sheet for Large Field of View Star Tracker - CT-411 Ball Aerospace Systems Division, Boulder, Colorado.

2) Specification Sheet for Retroreflector Field Tracker, Ball Aerospace Systems Division, Boulder, Colorado.

3) Durboraw, I. Newton, Thomas P. Gilb, and Michael King, 'The Motorola Eagle' - A High Quality - Low Cost GPS Receiver., Presented at the Fall Meeting of the Institute of Navigation, Colorado Springs, Colorado, September 24, 1987.

4) McCaskill, Thomas B. and James A Buisson 'On-Orbit Frequency Stability Analysis of Navstar GPS Clocks and the Importance of Frequency Stability to Precise Positioning.', presented at PLANS 86.

APPENDIX

Final Report

Slide Presentation

April 26, 1988

The Application of GPS technology is of interest for spacecraft planned for the 1990's. It is of particular interest to examine the feasibility of 4 applications of GPS technology. For this study, the primary factors for consideration are performance, cost, reliability, and complexity. Particular emphasis is to be given to competing technologies an hardware limitations that apply to the techniques.

The 4 applications include

1) Attitude Control
2) Large space structure control
3) Traffic Control
4) Timebase alternatives

Attitude control is motivated by high accuracy geodetic baseline results that have been obtained on stationary platforms and depends on being able to successfully resolve the carrier cycle ambiguity in GPS phase observations. Primary limitations of such technology include the effect of multipath caused by scattering of the GPS signals from objects on the spacecraft. The effect of multipath on code tracking is more severe than the effect on the carrier tracking, however because of the extreme phase accuracy that is generally required for attitude control, the effect will be significant. Phase center stability on the antenna is related to multipath and in fact difficult to consider as a separate issue since it will depend on the entire antenna environment of multipath reflectors. The effect of satellite clock variations can be mitigated with the use of synchronous sampling of the GPS observables and an algorithm that recognizes the distortion of the observables due to satellite clock variation. Of course, phase jitter of the receiver due to thermal noise is important but can be minimized with good receiver design.

Star trackers provide the best alternative to GPS for attitude monitoring and control. A typical instrument, a Large Field of View Star Tracker built by Ball Aerospace Systems Division for the space shuttle orbiter has a 10 x 10 field of view and an accuracy of 1 arc minute and is estimated to cost about $1 meg.

Related to attitude control is the need for stabilization which can be accommodated using accurate inertial rate sensors such as those which have been developed by Honeywell. The Interferometric Fiber Optic Gyro (IFOG) technology is particularly interesting as a candidate for space application because of it's high potential for reliability as well as accuracy in a package that is very small, light weight and uses very little power. A significant factor in comparison of this technology with the ring laser gyro technology is that the IFOG does not have any mechanical moving parts. Another important factor for this technology is it's projected low cost.

Large Structure Control can also be addressed by GPS. Precise Relative Phase measurements would be obtained from a system with multiple antennas. The problem is similar to attitude control and tracking in the sense that the ultimate measurement is a vector baseline between the antennas. A minimum bandwidth required is dictated by the structural modal frequencies which are expected to be very low. Star trackers can again be used for this application and the retroreflector field tracker is particularly suited to this application. On board instrumentation consists of a single active device as compared with a GPS approach which would require at the minimum, multiple antenna elements distributed over the structure to monitor the mode of flexure of the structure. Finally, since the primary requirement for structure control is for damping oscillatory motion, it may be feasible to consider inertial sensors that would measure relative rates at various points on the structure and compare these rates to define effective control law for damping the oscillatory motion.

In comparing the technologies for Structural Flexure measurement, the primary factor that is noted is the cost advantage of the IFOG technology. The retroreflector is also less expensive and less complex than the GPS and is probably the most practical technology for addressing this problem.

Traffic control can be addressed using either GPS or a Radar system. The primary advantage of Radar is the application to non cooperative vehicle tracking. Using GPS in a differential mode provides the best accuracies but requires sensors in all space craft and cooperation between the space craft, with state vectors to be transmitted over a radio link. Accuracies of a differential GPS system can be insensitive to planned methods of Selective Availability and are expected to be in the range of 2-5 meters or better.

Time synchronization of spacecraft may be important for certain missions and can be accommodated using the GPS system if all spacecraft synchronize their time to GPS time. The GPS system uses high accuracy rubidium clocks. The major consideration in the use of GPS for spacecraft time synchronization is that it will provide a high level of accuracy with only a modest increase

in the cost of a GPS receiver that will likely be on board the spacecraft for positioning.

In conclusion, GPS is best suited for traffic control and time syncronization in the early 1990's. Attitude control to the level of 1 mrad may be feasible technologically, but at a cost penalty due to the fact that multiple antennas with associated electronics must be included at a cost that will be substantially more than the cost of alternative technology to perform the same function. The same is true for structure flexure monitoring which appears to be more practical using optical techniques.

SPACECRAFT APPLICATIONS

OF

ADVANCED GLOBAL POSITIONING

SYSTEMS TECHNOLOGY

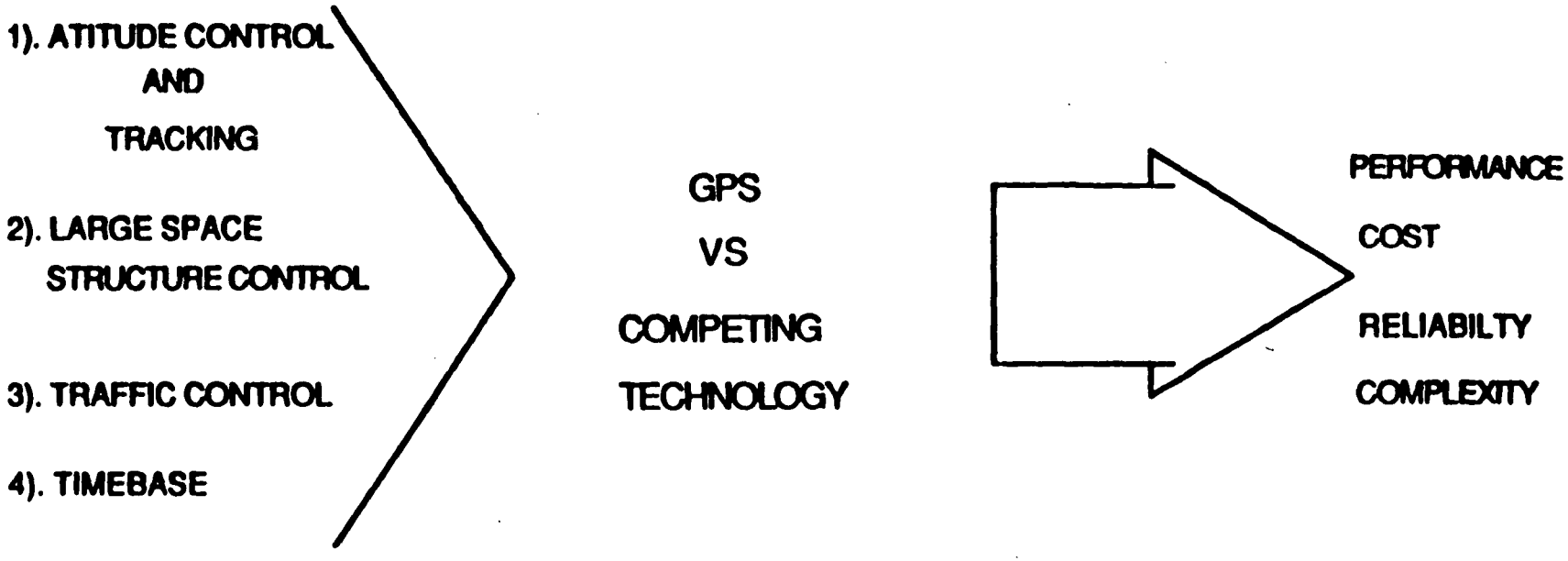
1). ATITUDE CONTROL
AND
TRACKING
2). LARGE SPACE
STRUCTURE CONTROL
3). TRAFFIC CONTROL
4). TIMEBASE
GPS
VS
COMPETING
TECHNOLOGY
PERFORMANCE
COST
RELIABILTY
COMPLEXITY

ATTITUDE CONTROL AND TRACKING

GPS → PRECISE RELATIVE PHASE - MULTIPLE ANTENNA

a) RELATIVE PHASE BETWEEN ANTENNAS

b) RELATIVE BASELINE BETWEEN ANTENNAS

- MULTIPATH / PHASE CENTER STABILITY
- REFERENCE PHASE DELAY
- SATELLITE CLOCK VARIATIONS
- PHASE

STARTRACKERS → STAR FIELD TRACKING

a) ABSOLUTE ATTITUDE MEASUREMENT

b) PROVEN TECHNOLOGY

IFOG → INERTIAL ATTITUDE SENSING - NEEDS ABSOLUTE REFERENCE

a) RELATIVE ATTITUDE SENSING

b) MATURING TECHNOLOGY

	PERFORMANCE	COST	RELIABILITY	COMPLEXITY
GPS	1 mrad	$ 3M	MED (3-5 YR LIFE)	MED 6 CHANNEL 1500 PARTS
STAR TRACKERS	.05 mrad	$ 1M	MED	MED
INTER-FEROMETRIC FIBEROPTIC GRYO	0.34 $\frac{\text{mrad}}{\text{hr}}$	$.035 $\frac{\text{M}}{\text{axis}}$	HIGH	LOW

TECHNOLOGY FOR SPACEBORNE ATTITUDE CONTROL AND TRACKING

LARGE SPACE STRUCTURE CONTROL

GPS ⟶ PRECISE RELATIVE PHASE - MULTIPLE ANTENNAS
(SIMILAR TO ATTITUDE CONTROL AND TRACKING)

MINIMUM BANDWIDTH DEPENDENT ON STRUCTURAL MODE FREQUENCIES

STARTRACKERS ⟶ OPTICAL OBSERVATIONS OF RELATIVE FLEXURE

INERTIAL SENSORS ⟶ ACCELEROMETERS / GRYO

	PERFORMANCE	COST	RELIABILITY	COMPLEXITY
GPS	HIGH .001 m RELATIVE	HIGH @ $ 1M	MED	MED
RETRO-REFLECTOR FIELD TRACKER	HIGH	MED	MED	HIGH
INERTIAL RATE SENSORS (IFOG)	HIGH	LOW	HIGH	LOW

TECHNOLOGY FOR SPACEBORNE STRUCTURE FLEXURE MEASUREMENT

TRAFFIC CONTROL

GPS ⟶ (DIFFERENTIAL) - SEVERAL ADVANCED SYSTEMS AVAILABLE

C/A CODE + PHASE ⟶ < 1 METER ACCURACY

RADAR ⟶ RANGE/ANGLE MEASUREMENT - X-BAND; Ku BAND

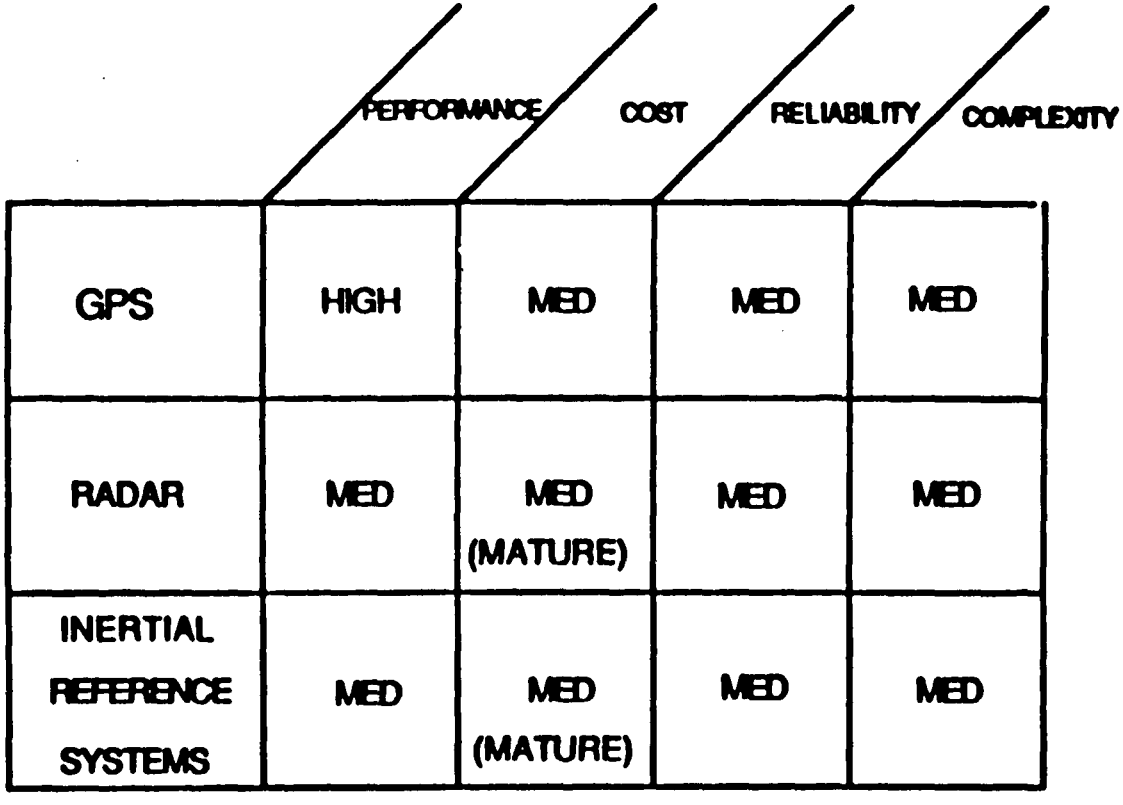

TECHNOLOGY FOR SPACEBORNE TRAFFIC CONTROL

TIME SYNCRONIZATION

GPS → WORLD REFERENCE SYSTEM - 18 TIME STANDARDS
HIGH SYSTEM INTEGRITY

RUBIDIUM OSCILLATORS → USED FOR GPS SATELLITES
3×10^{-11} FOR SHORT TERM,
$< 10^{-11}$ FOR 1 hr → ∞

QUARTZ CRYSTAL → SUITABLE FOR SHORT TERM
10^{-11} FOR SHORT TERM
10^{-10} FOR 1 hr

CESIUM

HYDROGEN MASER

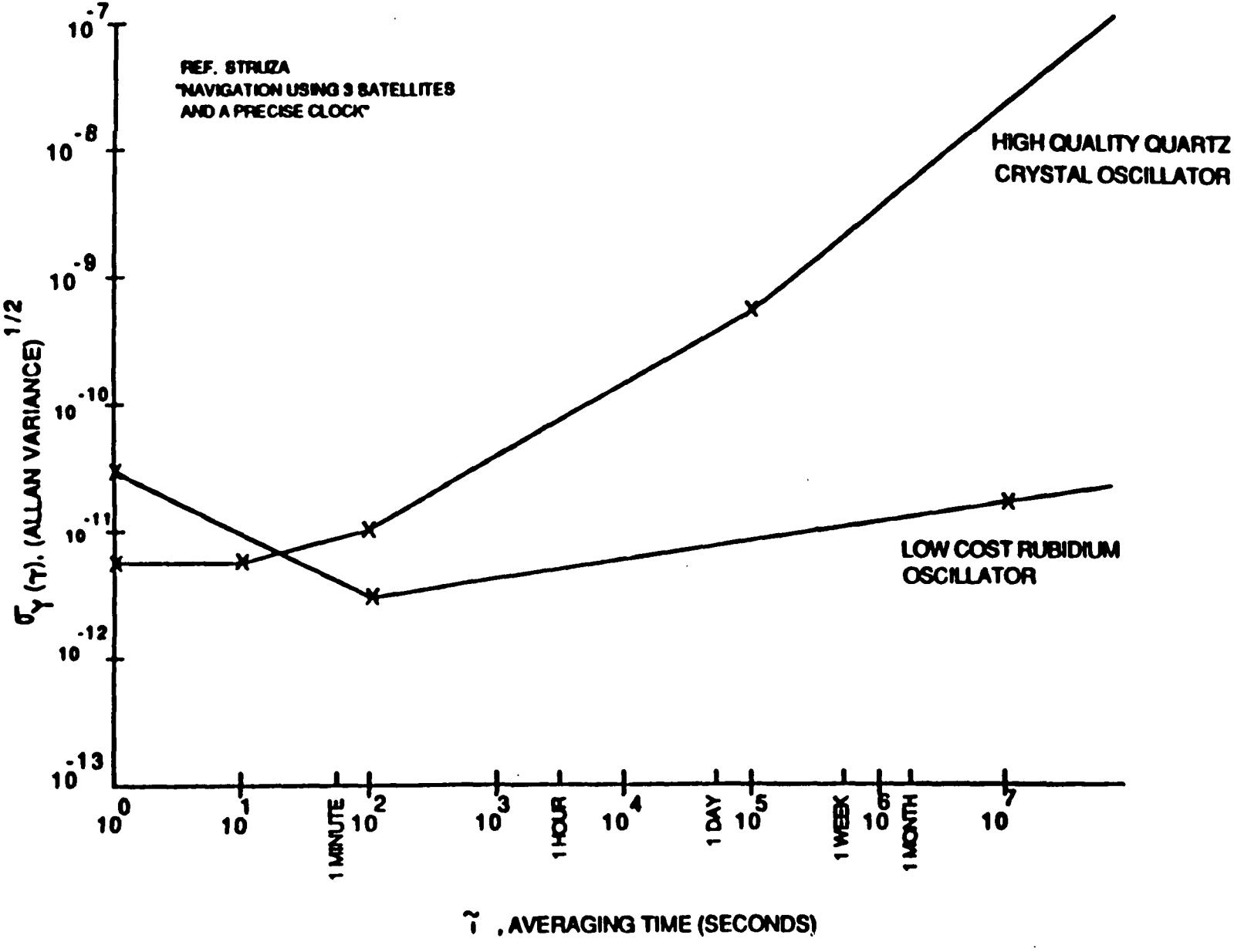
REF. STRUZA
"NAVIGATION USING 3 SATELLITES
AND A PRECISE CLOCK"
HIGH QUALITY QUARTZ
CRYSTAL OSCILLATOR
LOW COST RUBIDIUM
OSCILLATOR
$\sigma_y(\tau)$, (ALLAN VARIANCE)$^{1/2}$
10^{-7}
10^{-8}
10^{-9}
10^{-10}
10^{-11}
10^{-12}
10^{-13}
10^{0}
10^{1}
10^{2}
10^{3}
10^{4}
10^{5}
10^{6}
10^{7}
1 MINUTE
1 HOUR
1 DAY
1 WEEK
1 MONTH
τ, AVERAGING TIME (SECONDS)

	PERFORMANCE	COST	RELIABILITY	COMPLEXITY
GPS	1: 10^{12}	MED	SYSTEM DEPENDENT (4 1 6 11)	MODERATE
RUBIDIUM OSCILLATOR	1: 10^{12} SENS PRESS MAG. FIELD	HIGH	MED	LOW
QUARTZ CRYSTAL OSCILLATOR	1: 10^{9} SENSITIVE TEMP	LOW	HIGH	LOW
CESIUM BEAM	HIGH	HIGH	?	LARGE
HYDROGEN MASER	HIGH	HIGH	?	LARGE

TECHNOLOGY FOR SPACEBORNE TIME SYNCRONIZATION

CONCLUSIONS

- GPS BEST SUITED FOR TRAFFIC CONTROL AND TIME SYNCRONIZATION IN EARLY 1990's
- ATTITUDE TRACKING WITH GPS MAY BE FEASIBLE TO LEVEL OF 1 mr ⟶ COST ?
- STRUCTURE FLEXURE MONITORING VIA OPTICAL TECHNOLOGY APPEARS TO BE COST EFFECTIVE

APPENDIX B

SUPPORTING ANALYSIS FOR DERIVATION OF CONE INTERSECTION

APPENDIX B

SUPPORTING ANALYSIS FOR DERIVATION OF CONE INTERSECTION

1.0 DERIVATION OF GPS/BASELINE CONE INTERSECTION

1.1 Introduction

The attitude of a baseline referenced to three GPS satellites can be derived by solving for the intersections of three cones. Each cone represents the surface generated by rotating the baseline through an angle defined by the phase difference of a GPS signal between two points on the baseline, as described in a prior section. This section presents the derivation of the equation of a vector defined by the intersection of two cones. Solution of a quadratic equation is involved, which is not unexpected, since the cones will generally intersect at two vectors as shown in Figure 1.1-1. Solution involves using the three vector equations given in Figure 1.1-1 to solve for the three unknown direction cosines of the desired unit vector $\hat{v}$.

1.2 Derivation of Cone Intersection

The solution for the unit vector $\hat{v}$ is based on the three vector equations $\hat{v} \cdot \hat{G} = \cos \alpha_1$, $\hat{v} \cdot \hat{H} = \cos \alpha_2$, and $\hat{v} \cdot \hat{v} = 1$. The first two equations represent the two cones of half angle α_1 and α_2, respectively, and the third defines $\hat{v}$ as a unit vector. If we break $\hat{v} \cdot \hat{G}_1 = \cos \alpha_1$, down into its components, we have:

$$v_1 g_1 + v_2 g_2 + v_3 g_3 = \cos \alpha_1. \tag{1}$$

Similarly,

$$v_1 h_1 + v_2 h_2 + v_3 h_3 = \cos \alpha_2, \quad \text{and} \tag{2}$$

$$v_1^2 + v_2^2 + v_3^2 = 1 \tag{3}$$

Equation (1) and (2) can be solved to eliminate v_1, which gives:

$$\hat{v}_1 \cdot \hat{G} = \cos \alpha_1 \quad \text{(cone 1)}$$

$$\hat{v}_2 \cdot \hat{H} = \cos \alpha_2 \quad \text{(cone 2)}$$

$$\hat{v}_1 \cdot \hat{v}_1 = \hat{v}_2 \cdot \hat{v}_2 = 1 \text{ (unit vector)}$$

$$\hat{v} : \hat{v} \cdot \hat{v} = 1$$

$$\hat{v} \cdot \hat{G} = \cos \alpha_1$$

$$\hat{v} \cdot \hat{H} = \cos \alpha_1$$

$$\hat{G} = g_1 \hat{x} + g_2 \hat{y} + g_3 \hat{z}$$

$$\hat{H} = h_1 \hat{x} + h_2 \hat{y} + h_3 \hat{z}$$

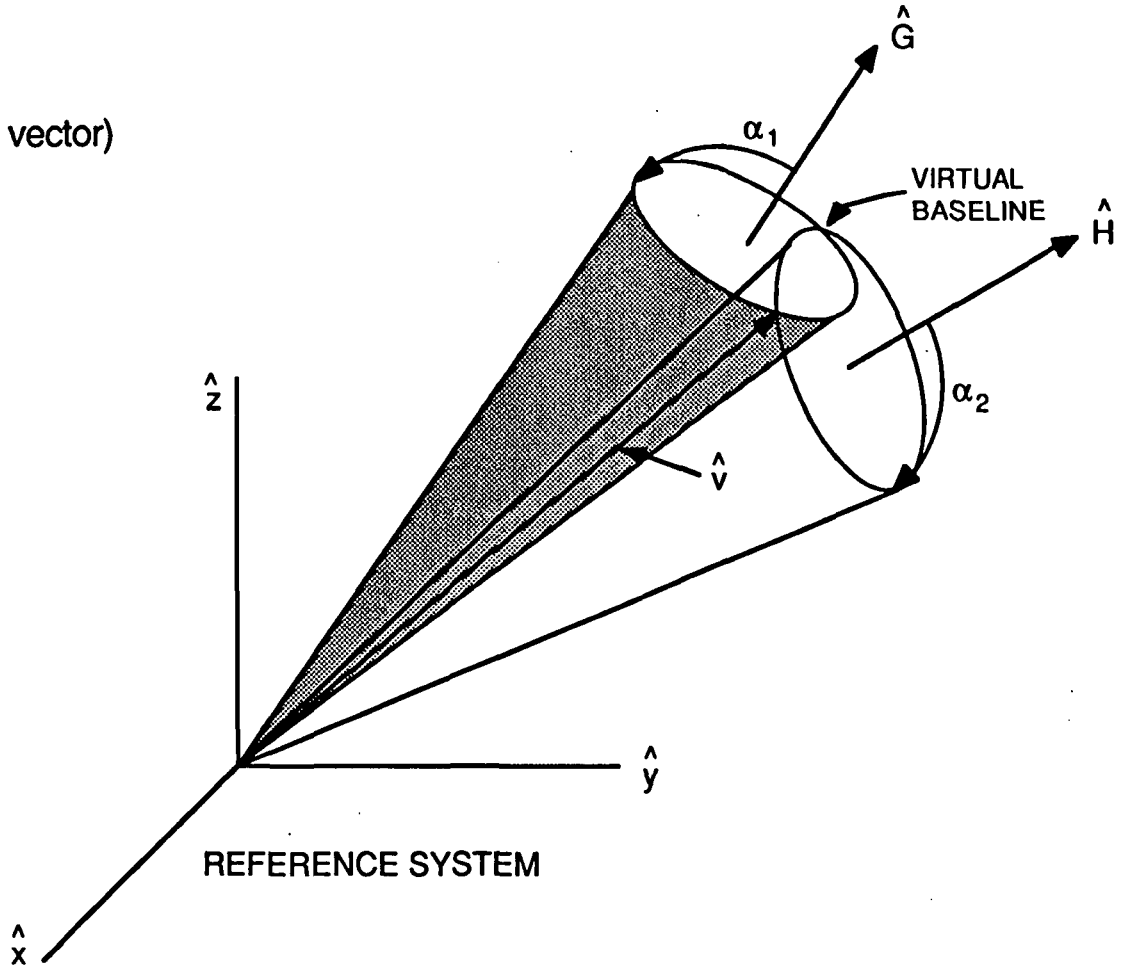

Figure 1.1-1. Definition of Baseline unit Vector $\hat{v}$.

$$v_2(g_2h_1 - g_1h_2) + v_3(g_3h_1 - g_1h_3) = \cos\alpha_1 h_1 - \cos\alpha_2\, g_1 \tag{4}$$

Let $A = \cos\alpha_1 h_1 - \cos\alpha_2 g_1$,

$B = g_3h_1 - g_1h_3$, and

$C = g_2h_1 - g_1h_2$.

Then we can define v_2 in terms of v_3 as

$$v_2 = \frac{A - B\, v_3}{C} . \tag{5}$$

This will be used in a subsequent substitution.

Equation (1) can be rewritten as

$$v_1 = \frac{1}{g_1}(\cos\alpha_1 - v_2g_2 - v_3g_3), \tag{6}$$

and Equation (3) can be rewritten as

$$v_1 = (1 - v_2^2 - v_3^2)^{1/2} .$$

Eliminating v_1 and collecting terms, we have

$$1 - v_2^2 - v_3^2 = \frac{1}{g_1^2}\left\{(\cos^2\alpha_1 - 2v_2g_2\cos\alpha_1 - 2v_3g_3\cos\alpha_1 + v_2g_2v_3g_3 + 2v_2^2g_2^2 + v_3^2g_3^2\right\} \tag{7}$$

The next step is to substitute equation 5, linear in v_2 and v_3, into the quadratic equation (7). Collecting terms of v_3^2, and v_3, we get a quadratic of the form

$$AAv_3^2 + BBv_3 + CC = 0. \tag{8}$$

This notation is consistent with the variables as defined in the FORTRAN implementation. The constants are defined as follows:

$$AA = (Bg_2/C)^2 + (B^2 + C^2)\,(g_1/C)^2$$

$$BB = 2(Bg_2/C - g_3)\,(\cos\alpha_1 - Ag_2/C) - 2AB(g_1/C)^2$$

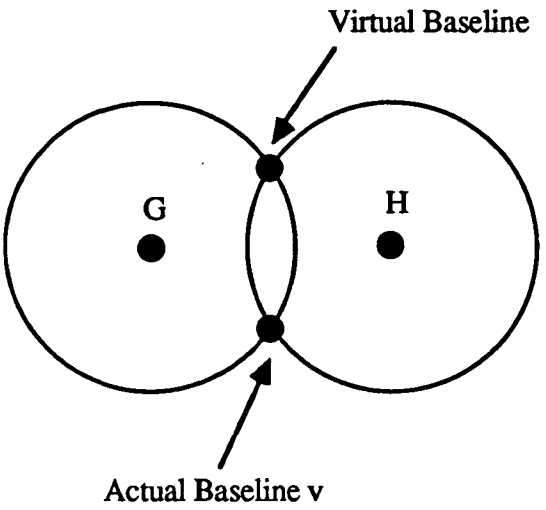

Figure 1.3-1a. G-H Cones Intersecting at Two Points.

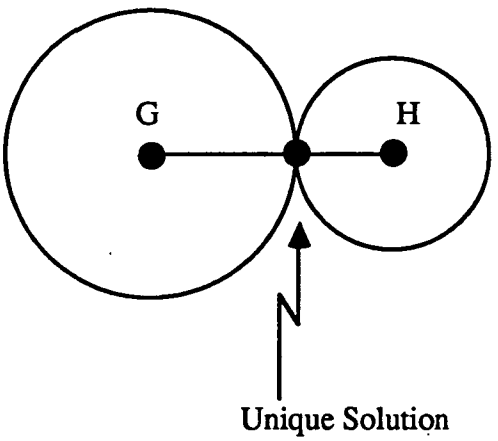

Figure 1.3-1b. G-H cones Intersecting at One Point.

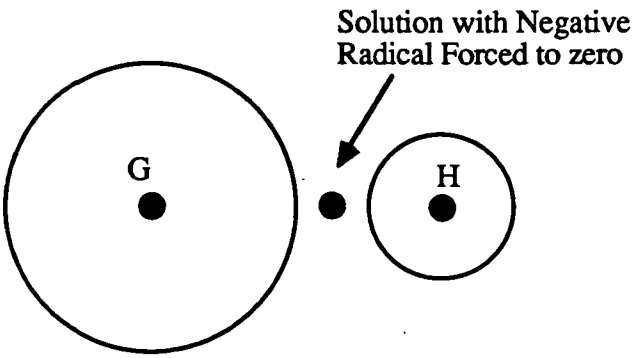

Figure 1.3-1c. Disjoint G-H Cones.

$$CC = \cos\alpha_1^2 + (Ag_2/C)^2 - 2Ag_2(\cos\alpha_1)/C - g_1^2 + (Ag_1/C)^2 \ ,$$

with A, B, C as in equation (5).

After solving this quadratic for v_3 using the standard form, equation (5) is used to solve for v_2, and equation (6) is solved to obtain v_1.

The two solutions from the quadratic are stored for later comparison with the other two pairs of solutions. The simulation picks the three closest solutions to form an average estimate of the baseline attitude.

1.3 Degenerate Solutions

The normal solution for the cone intersection provides a pair of vectors representing a true baseline and a pseudo, or virtual baseline. These are depicted in Figure 1.3-1a. Mathematically, these are given by the alternate signs of the radical in the standard solution of a quadratic, $v_3 = (-BB \pm (BB^2 - 4AACC)^{1/2})/2AA$. However, in the pathological case having the baseline vector coplanar with the two vectors to the GPS satellites, the radical will be zero, and there will be a single unique solution. This is depicted in Figure 1.3-1b. A problem can arise in the presence of noise. If the baseline vector is close to, or on, the plane defined by the two GPS vectors $\hat{G}$ and $\hat{H}$, the noisy determination of α_1 and α_2 can result in two cones which don't intersect, as shown in Figure 1.3-1c. In this case, the argument of the radical is negative and a real solution does not exist. We have chosen to treat this case by setting the radical to zero if the argument is negative. The effect of this substitution is minimal, since the argument of the radical is extremely small in these cases.